THE PROCEEDINGS OF
THE PHYSICAL SOCIETY

Section A

VOL. 64, PART 11 1 November 1951 No. 383 A

On the Quantum Theory of Reciprocal Fields and the Correspondence Principle

BY J. RAYSKI
Department of Physics, Nicolas Copernicus University, Torun, Poland

Communicated by M. Born; *MS. received* 18*th May* 1951

ABSTRACT. A method of quantization of non-local fields whose interaction is expressible by means of integral equations is given. The S-matrix is constructed by Yang's method. The non-local field theory is free of the usual convergence difficulties. It is possible to satisfy generally either the postulate of reciprocity or the postulate of correspondence, but it seems impossible to satisfy both principles simultaneously.

§ 1. GENERAL INTRODUCTION AND SUMMARY

THE ideas of non-localizability and reciprocity (originated by Born (Born and Peng 1944, Born and Green 1949) and developed further by Yukawa (1950)) are very attractive for the following reasons: The assumption that the wave function depends not only upon the operator of position but also upon the displacement operator constitutes a vast generalization. Some of the classical numbers have been replaced by operators, so that the evolution of quantum mechanics is seen as a natural continuation from classical theory. On the other hand, the postulate of reciprocity introduces a new symmetry into the fundamental laws of nature, similar to that introduced by restricted relativity: as relativity takes account of the velocity of light and quantum mechanics of Planck's constant, so reciprocity introduces, in a very elegant way, a third fundamental constant, i.e. the universal length λ. It is to be expected that the non-localizability will remove the usual convergence difficulties.

The basic ideas seem very promising, but the theory is not yet sufficiently developed, and the decisive problems which need solution are: (i) how to interpret the non-local fields; (ii) how to take account of interaction between non-local fields; (iii) how the non-local field should be quantized; (iv) whether it is possible to secure a reciprocity of interaction; (v) whether it is possible to secure correspondence with the local field theory.

In order to avoid complications we investigate the above-mentioned problems on the simplest possible field model: a complex scalar field ψ with a scalar interaction with a real scalar field ϕ. In the frame of the traditional field theory these fields obey the equations

$$(\Box - m^2)\psi = -g\phi\psi, \quad \ldots\ldots(1) \qquad (\Box - \kappa^2)\phi = -g\psi^*\psi, \quad \ldots\ldots(2)$$

where g is the coupling constant assumed small compared with unity (weak coupling). The equations (1) and (2) should be generalized for the case of a non-local field ψ. The real field ϕ is assumed as localizable for simplicity.

We shall investigate first the non-local field ψ *in vacuo*. A correspondence rule will enable us to set up expressions which may be interpreted as densities. The quantization of the field *in vacuo* is performed by assuming suitable commutation relations in conformity with the postulate of reciprocity. It will be shown that, apart from a slight difference in densities, this theory of the non-local and reciprocal field is fully equivalent to the usual quantum theory of a local scalar field *in vacuo*.

In § 3 we shall set up some integral field equations in order to take account of a non-local interaction. In this way we avoid the infinitesimal point of view intimately connected with differential equations. The integral equations in question constitute a straightforward generalization of the equations of Yang and Feldman (1950) adopted for the case of scalar fields, and may be written either in terms of 'retarded' or 'advanced' potentials. The form of the generalized $\bar{\Delta}$ function appearing in the integral field equations need not be specified for the purposes of § 3. The perturbed fields may be quantized by a method called here a 'direct quantization', avoiding completely the Hamiltonian formalism and the Schrödinger equation. The method of direct quantization consists simply in the assumption that the ingoing and outgoing waves obey the reciprocal commutation relations for the case of fields without interaction. The commutation relations for the perturbed waves then follow automatically from the field equations which may be solved by iteration. The S-matrix may be computed by means of the method of Yang and Feldman. General rules for an immediate transcription of the traditional S-matrix elements into the non-local form are inferred. The existence of an S-matrix proves the compatibility of the field equations and the consistency of the whole scheme.

In §§ 4 and 5 two alternative assumptions for the generalized $\bar{\Delta}$ function are investigated. The first alternative provides us with a formalism satisfying generally the principle of correspondence: the formalism goes over into the usual one in the limit $\lambda \to 0$. However, the postulate of reciprocity is then violated (i.e. restricted to the case of a field *in vacuo*). On the other hand, the second alternative secures the reciprocity of interaction but violates the principle of correspondence in orders of approximation higher than g^2. The fundamental discrepancy between the traditional field theory (or a theory standing in a full correspondence to the local theory) and the completely reciprocal field theory manifests itself in the extremely relativistic region, but is without influence upon effects whose main contributions lie in the non-relativistic region (as, for example, the Lamb shift). The non-local field theory is free from the usual convergence difficulties.

§ 2. THE RECIPROCAL SCALAR FIELD *IN VACUO*

In conformity with Born's (Born and Peng 1944, Born and Green 1949) and Yukawa's (1950) ideas of non-localizability and reciprocity, we assume that the wave function ψ depends not only upon the operator of position x_μ but also on the displacement operator d_μ:

$$\psi = \psi(\mathbf{x}, \mathbf{d}), \quad \text{where} \quad [\mathbf{x}_\mu, \mathbf{d}_\nu] = \delta_{\mu\nu}, \qquad \ldots\ldots(3)$$

We postulate the following reciprocal commutation relations:

$$[\mathbf{x}_\mu, [\mathbf{x}_\mu, \psi]] = \lambda^4 [\mathbf{d}_\mu, [\mathbf{d}_\mu, \psi]], \quad \ldots\ldots(4)$$

$$[\mathbf{d}_\mu, [\mathbf{x}_\mu, \psi]] = 0 \quad \ldots\ldots(5), \qquad [\mathbf{d}_\mu, [\mathbf{d}_\mu, \psi]] = m^2\psi. \quad \ldots\ldots(6)$$

The relation (6) is reciprocal, due to (4). Equations (4), (5) and (6) are equivalent to the equations of Yukawa (1950), with the only difference that his λ has been replaced by our $m\lambda^2$.

Following Yukawa, we use a representation in which $\mathbf{x}_\mu$ are represented by diagonal matrices. In this representation ψ is a matrix $\langle x' | \psi | x'' \rangle$ which may be written also as a function of two variables,

$$\psi = \psi(x, r), \quad \text{where} \quad x = \tfrac{1}{2}(x' + x''), \quad r = x' - x''. \quad \ldots\ldots(7)$$

In this representation our equations (4), (5) and (6) assume the form

$$r_\mu^2 \psi(x, r) = \lambda^4 \Box_x \psi(x, r) \quad \ldots\ldots(4')$$

$$r_\mu \frac{\partial}{\partial x_\mu} \psi(x, r) = 0, \quad \ldots\ldots(5'), \qquad (\Box_x - m^2)\psi(x, r) = 0. \quad \ldots\ldots(6')$$

Let us apply Fourier analysis to the wave function $\psi(x, r)$. Its Fourier transform must be of the form

$$\psi(p, r) = N(p)\psi(p)\delta(r_\mu p_\mu)\delta(r_\mu^2 + p_\mu^2\lambda^4) \quad \ldots\ldots(8)$$

in order to satisfy (4′) and (5′). $N(p)$ is a normalizing factor extracted from $\psi(p)$ for convenience. Equation (8) could still contain an arbitrary, though regular, function of r_μ but we purposely drop this factor in order to avoid higher spin values. As has been shown by Bloch (1950), this may be consistently achieved by means of a supplementary condition. If $\psi(x, r)$ also satisfies (6′) then the Fourier transform $\psi(p)$ contains a third delta function $\delta(p_\mu^2 + m^2)$, and the function $\delta(r_\mu^2 + p_\mu^2\lambda^4)$ in (8) may be replaced by $\delta(r_\mu^2 - m^2\lambda^4)$.

In order to establish a correspondence and an interpretation of the non-local formalism we postulated in a previous paper (Rayski 1950) that for any gauge invariant polynomial $a(x, r)$ of wave functions and their derivatives the observable quantity is

$$a(x) = \int d^4r\, a(x, r). \quad \ldots\ldots(9)$$

The same postulate has been proposed independently by Møller (see Bloch 1950). By putting

$$N(p) = \left\{ \int d^4r \delta(p_\mu r_\mu)\delta(r_\mu^2 + p_\mu^2\lambda^4) \right\}^{-1} \quad \ldots\ldots(10)$$

we get from (8)

$$\psi(p) = \int d^4r \psi(p, r), \quad \ldots\ldots(11)$$

which is of the same form as (9).

With the aid of (9) we form the scalar density corresponding to

$$v(x) = \psi^*(x)\psi(x). \quad \ldots\ldots(12)$$

Remembering that the wave functions are actually matrices, we have

$$v(x) = \int d^4r\, v(x, r) = \int d^4r \langle x' | \psi^* \psi | x'' \rangle$$

$$= \int\int d^4r\, d^4x''' \langle x' | \psi^* | x''' \rangle \langle x''' | \psi | x'' \rangle, \quad \ldots\ldots(13)$$

which may be also written as follows:

$$v(x) = \int\int d^4r\, d^4s\, \psi^*(x - \tfrac{1}{2}r, s)\psi(x - \tfrac{1}{2}s, r). \quad \ldots\ldots(14)$$

Since

$$\psi(x + Cr, r) \equiv \psi(x, r), \quad \ldots\ldots(15)$$

where C is an arbitrary constant, the density (14) may be written also in the form

$$v(x)=\int\int d^4r\, d^4s\psi^*(y,s)\psi(y,r) \qquad \ldots\ldots(16)$$

with

$$y=x-\tfrac{1}{2}(r+s). \qquad \ldots\ldots(17)$$

Thus the rule for constructing an observable scalar density at the point x is: multiply $\psi(x,r)$ by $\psi^*(x,s)$, translate the point x to y and then integrate over $d^4r\, d^4s$. The same rule may be easily generalized for other densities, for instance the current density. The above considerations enable us to write immediately an equation corresponding to (2) in the case of a non-local field ψ: we have only to replace the product appearing on the right-hand side of (2) by the expression (16).

Quantization

We quantize the non-local field *in vacuo* by assuming the following commutation relations:

$$\left.\begin{aligned}&[\psi(x,r),\ \psi^*(x',s)]=i\Delta(x-x',r,s),\\&[\psi(x,r),\ \psi(x',r')]=[\psi^*(x,s),\psi^*(x',s')]=0.\end{aligned}\right\} \qquad \ldots\ldots(18)$$

The generalized Δ function is defined in the following way:

$$\Delta(x,r,s)=\frac{1}{(2\pi)^4}\int d^4p\exp(ip_\mu x_\mu)\Delta(p,r,s), \qquad \ldots\ldots(19)$$

the Fourier transform being

$$\Delta(p,r,s)=\Delta(p)\rho(p,r)\rho(p,s), \qquad \ldots\ldots(20)$$

where $\Delta(p)$ is the Fourier transform of the usual $\Delta(x)$ function, well known from the theory of Schwinger (1949):

$$\Delta(p)=-2\pi i\delta(p_\mu^2+m^2)\operatorname{sgn}p_0, \qquad \ldots\ldots(21)$$

while $\rho(p,r)$ is written for

$$\rho(p,r)=N(p)\delta(p_\mu r_\mu)\delta(r_\mu^2+\lambda^4p_\mu^2) \qquad \ldots\ldots(22)$$

with $N(p)$ given by (10).

Since

$$\int d^4r\rho(p,r)=1, \qquad \ldots\ldots(23)$$

we have

$$\int\int d^4r\, d^4s\Delta(x,r,s)=\Delta(x). \qquad \ldots\ldots(24)$$

We notice the following properties of the generalized Jordan–Pauli function:

$$\Box_x\Delta(x,r,s)\equiv\lambda^{-4}r_\mu^2\Delta(x,r,s)\equiv\lambda^{-4}s_\mu^2\Delta(x,r,s), \qquad \ldots\ldots(25')$$

$$r_\mu\frac{\partial}{\partial x_\mu}\Delta(x,r,s)\equiv s_\mu\frac{\partial}{\partial x_\mu}\Delta(x,r,s)=0, \qquad \ldots\ldots(25'')$$

$$(\Box_x-m^2)\Delta(x,r,s)=0, \qquad \ldots\ldots(25''')$$

which show that the $\Delta(x,\ r,s)$ function is a reciprocal concept and that the commutation relations (18) are compatible with the field equations (4′), (5′) and (6′). We notice that Δ is an odd function of x_μ,

$$\Delta(-x,r,s)=-\Delta(x,r,s), \qquad \ldots\ldots(26)$$

as usual, but it should be stressed that the generalized Δ function is neither antisymmetric in x_0 nor vanishes outside the light cone, in contradistinction to local field theory. This new property is a characteristic feature of non-local fields and is closely connected with the finite dimensions of particles. Due to the

existence of the delta functions $\delta(p_\mu^2+m^2)$, $\delta(p_\mu r_\mu)$, $\delta(r_\mu^2+p_\mu^2\lambda^4)$, etc., in the generalized Δ function the four-vectors r_μ and s_μ are space-like and their components tend (separately) to zero for $\lambda\to 0$. In this case the generalized Δ function goes over into the traditional one, so that the correspondence with the local field theory is fully taken into account. The non-commutability of wave functions at points x_μ and x_μ' lying outside each other's light cones is appreciable only for distances comparable with the absolute length λ.

The wave functions satisfying the commutation relations (18) are of the form (8), where $\psi(p)$ are now matrices identical with those used in the local theory of a complex scalar field *in vacuo*.

Applying the rule (9) we may introduce the charge and current density, energy density, etc., quite analogous to the scalar density (16). It may be easily shown that such densities obey the continuity equations, and it may be verified that, although the densities differ from the traditional ones, the total charge, energy and momentum operators (obtained by integrating the corresponding densities over three-dimensional space) are identical with the traditional ones. Thus, except for a slight difference in densities, this theory of a non-local and reciprocal field *in vacuo* is fully equivalent to the usual local field theory and may be written in a canonical form.

§ 3. THE RECIPROCAL FIELD, INCLUDING INTERACTION

We have to determine the proper form of the field equations in the case of interaction and to quantize the perturbed field ψ. The considerations of the foregoing section led us already to the plausible assumption for the generalized equation (2) describing the influence of the non-local field ψ upon the local field ϕ,

$$(\Box-\kappa^2)\phi(x)=-gv(x), \qquad \ldots\ldots(27)$$

where $v(x)$ is given by (16) and (17). The problem of a generalization of the equation (1) describing the influence of the field ϕ upon the non-local ψ is more difficult. It is obvious, from the very outset, that we have to avoid the infinitesimal point of view to take full account of the non-local character of fields and their interaction. The integral equations, avoiding completely the infinitesimal approach, constitute the most natural form for the description of a non-local interaction; therefore we look rather for integral than differential field equations. First of all we may replace (27) by the equivalent integral equation written either by means of retarded or advanced potentials,

$$\phi(x)=\overset{\text{in}}{\phi}{}^{\text{out}}(x)+\tfrac{1}{2}g\int dP'\overset{\text{ret}}{\Delta}{}^{\text{adv}}(x-x')\{\psi^*(y',s'),\psi(y',r')\}, \qquad \ldots\ldots(28)$$

where the product of the non-local wave functions has been written in a symmetrized form. The symbol $\int dP'$ stands for

$$\int dP'\equiv\iiint d^4x'\,d^4r'\,d^4s'\equiv\iiint d^4y'\,d^4r'\,d^4s', \qquad \ldots\ldots(2^0)$$

where

$$x'=y'+\tfrac{1}{2}(r'+s'), \qquad \ldots\ldots(17')$$

while

$$\overset{\text{ret}}{\Delta}{}^{\text{adv}}(x)=\overline{\Delta}(x)\mp\tfrac{1}{2}\Delta(x). \qquad \ldots\ldots(30)$$

The $\Delta(x)$ functions involve the mass constant κ of the real field ϕ, but this cannot introduce any confusion with the delta functions $\Delta(x,r,s)$ connected with the non-local field and involving the mass constant m.

The ingoing and outgoing waves ϕ^{in}, ϕ^{out} obey the Schrödinger–Gordon equation *in vacuo*,

$$(\Box-\kappa^2)\overset{\text{in}}{\phi}{}^{\text{out}}=0. \qquad \ldots\ldots(31)$$

Denoting half the sum of the ingoing and outgoing waves by the superscript (0), we have also

$$\phi(x)=\phi^{(0)}(x)+\tfrac{1}{2}g\int dP'\bar{\Delta}(x-x')\{\psi^*(y',s'),\psi(y',r')\}. \qquad \ldots\ldots(32)$$

Now we may postulate analogous integral equations accounting for the influence of the local field $\phi(x)$ upon the non-local $\psi(x,r)$. We suppose that there exists a generalized $\bar{\Delta}(x,r,s)$ function constituting a counterpart of the local $\bar{\Delta}(x)$, so that we may introduce the 'retarded' and 'advanced' functions

$$\overset{\text{ret}}{\Delta}{}^{\text{adv}}(x,r,s)=\bar{\Delta}(x,r,s)\mp\tfrac{1}{2}\Delta(x,r,s). \qquad \ldots\ldots(33)$$

The form of the generalized $\bar{\Delta}(x,r,s)$ need not be specified for the purpose of this section. At any rate, the application of the operator $\Box_x-m^2$ to the generalized $\bar{\Delta}(x,r,s)$ must not yield a (minus) Dirac delta function which was characteristic for the local theory. With the aid of the generalized $\bar{\Delta}(x,r,s)$ function we assume the following equation:

$$\psi(y,r)=\psi^{(0)}(y,r)+\tfrac{1}{2}g\int dP'\bar{\Delta}(y-y',r,s')\{\psi(y',r'),\phi(x')\} \qquad \ldots\ldots(34)$$

and similar equations written in terms of advanced or retarded potentials which need not be written down explicitly. The ingoing and outgoing waves are assumed to obey the reciprocal equations *in vacuo*, i.e. the equations (4′), (5′) and (6′). The form of the equation (34), and similar equations for the retarded and advanced potentials, is suggested by analogy with (32). In particular, it should be noticed that we have had to use the translated variables y (instead of x) in order to obtain the corresponding density (16) at the point x. Since the application of the operator $\Box-m^2$ to the generalized $\bar{\Delta}$ function is not supposed to yield a Dirac delta function, equation (34) is not reducible to a pure differential equation, in contradistinction to (32) which reduces to (27) due to the local character of the field ϕ.

Quantization

The usual Hamiltonian formalism and the Schrödinger equation (which are typical for an infinitesimal point of view) are not adequate for the quantization of fields with a non-local interaction. On the other hand it is possible to quantize directly the fundamental integral equations written in terms of retarded or advanced potentials by assuming the interaction-free commutation relations for the ingoing and outgoing waves. The same relations hold for $\psi^{(0)}$ and $\phi^{(0)}$. The commutation relations between the perturbed wave functions then follow automatically from the field equations and may be computed by iteration. In such a direct method of field quantization the role of the Heisenberg picture is predominant. It seems doubtful whether, in the case of non-local fields, it will be possible to go over to the Schrödinger picture or to the intermediate picture of Tomonaga and to restore a Schrödinger equation.

By subtracting the equations with advanced potentials from those with retarded potentials we get

$$\psi^{\text{in}}(y,r)-\psi^{\text{out}}(y,r)=\tfrac{1}{2}g\int dP'\Delta(y-y',r,s')\{\psi(y',r'),\phi(x')\}, \qquad \ldots\ldots(35)$$

$$\phi^{\text{in}}(x)-\phi^{\text{out}}(x)=\tfrac{1}{2}g\int dP'\Delta(x-x')\{\psi^*(y',s'),\psi(y',r')\}. \qquad \ldots\ldots(36)$$

By applying the method described by Yang and Feldman we may construct the S-matrix for the non-local field theory. Since the ingoing and outgoing waves satisfy the same commutation relations, there should exist a unitary matrix transforming simultaneously the ingoing into the outgoing waves

$$\psi^{\text{out}} = S^{-1}\psi^{\text{in}}S, \qquad \phi^{\text{out}} = S^{-1}\phi^{\text{in}}S \qquad \ldots\ldots(37)$$

with the same S, provided our equations are compatible with each other. From (35), (36) and (37) we have

$$[\psi^{(0)}(y,r), S] = -\tfrac{1}{2}g\left\{S, \int dP'\Delta(y-y',r,s')\{\psi(y',r'), \phi(x')\}\right\}, \quad \ldots\ldots(38)$$

$$[\phi^{(0)}(x), S] = -\tfrac{1}{2}g\left\{S, \int dP'\Delta(x-x')\{\psi^*(y',s'), \psi(y',r')\}\right\}. \quad \ldots\ldots(39)$$

From (32), (34), (38) and (39) the S-matrix may be computed as a power series in the coupling constant g. But we may immediately guess the result: the reciprocal S-matrix elements may be obtained simply from the traditional ones by exactly the same substitutions which convert the corresponding field equations of the local theory into our (32), (34), (38) and (39). Thus, in order to obtain the new S-matrix elements we have to replace in the traditional S-matrix elements every $\psi^{(0)}(x)$ and $\psi^{*(0)}(x)$ by $\psi^{(0)}(y,r)$ and $\psi^{*(0)}(y,s)$, every $\bar{\Delta}(x'-x'')$ and $\Delta(x'-x'')$ involving the mass constant m by $\bar{\Delta}(y'-y'', r', s'')$ and $\Delta(y'-y'', r', s'')$ while the local $\phi^{(0)}(x)$ and its Δ functions remain unchanged. Moreover, the integrals $\int d^4x'd^4x''\ldots$ have to be replaced by the threefold integrals $\int dP'\,dP''\ldots$ given by (29).† Thus we have proved the existence of the S-matrix by construction. The existence of an S-matrix constitutes, at the same time, a proof of the compatibility of our quantized equations and of the consistency of the whole scheme. It offers at the same time a possibility of confirming the formalism by experiment.

§ 4. THE CASE OF FULL CORRESPONDENCE AND RESTRICTED RECIPROCITY

Our next task is to determine the form of the non-local substitute for the traditional $\bar{\Delta}$ function. We cannot take over literally the usual expression of Schwinger of the $\bar{\Delta}$ function

$$\bar{\Delta}(x) = -\tfrac{1}{2}\operatorname{sgn} x_0 \,.\, \Delta(x) \qquad \ldots\ldots(40)$$

and replace in it the $\Delta(x)$ function by its non-local counterpart given by equations (19) to (22) since the non-local $\Delta(x,r,s)$ does not vanish outside the light cone, in which case (40) is not invariant. One of the possibilities of introducing a generalized $\bar{\Delta}(x,r,s)$ may be accomplished by the following procedure: we may first replace $\operatorname{sgn} x_0$ by the invariant function $\eta(x)$, which is unity in the future light cone, minus unity in the past light cone and zero outside the light cone,

$$\eta(x) = \left\{\begin{array}{l} 1 \text{ for } x_\mu^2 \leqslant 0,\ x_0 > 0 \\ 0 \text{ for } x_\mu^2 > 0 \\ -1 \text{ for } x_\mu^2 \leqslant 0,\ x_0 < 0, \end{array}\right\} \qquad \ldots\ldots(41)$$

and write in the case of a local field

$$\bar{\Delta}(x) = -\tfrac{1}{2}\eta(x)\Delta(x), \qquad \ldots\ldots(42)$$

† This procedure of constructing an S-matrix has been applied by the author in a previous paper (Rayski 1951).

which is completely equivalent to (40) owing to the fact that the local $\Delta(x)$ vanishes outside the light cone. Now we may postulate a covariant non-local Δ function,

$$\bar{\Delta}(x,r,s) = -\tfrac{1}{2}\eta(x)\Delta(x,r,s). \qquad \ldots\ldots(43)$$

From (33) and (43) we easily see that the function $\Delta^{\text{ret}}(x,r,s)$ yields contributions not only from the past light cone, where it is equal to $-\Delta(x,r,s)$, but also from the domain outside the light cone, where it is equal to $-\frac{1}{2}\Delta(x,r,s)$. Thus the superscript 'ret' is now justified merely by the fact that no contributions come from the future light cone. The contributions coming from outside the light cone mean an action propagating with higher velocity than that of light, but this does not contradict relativity since such actions cannot be used for sending signals. Such effects are limited to distances comparable with the length λ, and thus are only a consequence of the finite dimensions of elementary particles in the interior of which we cannot possibly trace causality.

Let us consider an S-matrix element. The variables $r', r'', \ldots s', s'' \ldots$ appearing in it are connected either with the unperturbed $\psi^{(0)}$ functions or with the generalized $\Delta(x,r,s)$ functions. Since their Fourier transforms $\psi^{(0)}(p,r)$ or $\Delta(p,r,s)$ contain time-like p_μ: $p_\mu{}^2 = -m^2$, the four-vectors r_μ and s_μ are space-like and their components tend to zero for λ tending to 0. Therefore any S-matrix element goes over into the local one in the limit $\lambda = 0$*. Thus there exists a complete correspondence between this formalism and the local field theory. On the other hand, it is the unperturbed field $\psi^{(0)}(x,r)$ only that satisfies the reciprocal equations (4') and (5'), but not the perturbed field $\psi(x,r)$ (given by (34)). In this formulation the postulate of reciprocity is restricted to non-local fields *in vacuo*.

§ 5. THE CASE OF A FULL RECIPROCITY AND RESTRICTED CORRESPONDENCE

In this section we show that it is possible to guarantee the reciprocity of the perturbed wave function ψ, but, as we shall see later, in this case the postulate of correspondence cannot be satisfied in higher orders of approximation. The complete reciprocity may be achieved by means of an alternative definition of the generalized $\bar{\Delta}$ function. Instead of introducing the generalized Δ function into (42) we may directly generalize the local $\bar{\Delta}(x)$ function on the same lines as we have generalized the Δ function by means of equations (19) to (22). We assume that the generalized $\bar{\Delta}$ is

$$\bar{\Delta}(x,r,s) = \frac{1}{(2\pi)^4}\int d^4p\,\bar{\Delta}(p,r,s)\exp(ip_\mu x_\mu), \qquad \ldots\ldots(44)$$

where the Fourier transform may be written in the form

$$\bar{\Delta}(p,r,s) = \bar{\Delta}(p)\rho(p,r)\rho(p,s), \qquad \ldots\ldots(45)$$

$\bar{\Delta}(p)$ being the Fourier transform of the usual $\bar{\Delta}(x)$ function, well known from the theory of Schwinger,

$$\bar{\Delta}(p) = Pv/(p_\mu{}^2 + m^2), \qquad \ldots\ldots(46)$$

* Born and Yang have informed the author that they have convinced themselves by a direct, though lengthy, calculation that the equations (38) and (39), which define S in the non-local theory, go over, for $\lambda \to 0$, into the corresponding equations of the local theory.

while $\rho(p,r)$ is given by (22). Owing to the delta functions $\delta(r_\mu{}^2+p_\mu{}^2\lambda^4)$, $\delta(p_\mu r_\mu),\ldots$ in the Fourier transforms (45), the new $\bar{\Delta}(x,r,s)$ satisfies the equations (4′) and (5′):

$$(r_\mu{}^2-\lambda^4\Box_x)\bar{\Delta}(x,r,s)=(s_\mu{}^2-\lambda^4\Box_x)\bar{\Delta}(x,r,s)=0, \qquad \ldots\ldots(47)$$

$$r_\mu\frac{\partial}{\partial x_\mu}\bar{\Delta}(x,r,s)=s_\mu\frac{\partial}{\partial x_\mu}\bar{\Delta}(x,r,s)=0, \qquad \ldots\ldots(48)$$

which show that the generalized $\bar{\Delta}$ function is a reciprocal concept. It should be noted that the application of the operator $\Box_x-m^2$ to the generalized $\bar{\Delta}$ does not yield a Dirac delta function, in contradistinction to the local field theory, whence the equation (34) is not reducible to a pure differential equation.

The unperturbed function $\psi^{(0)}(y,r)$ appearing in (34) is assumed to obey (4′), (5′) and (6′), while the new $\bar{\Delta}$ function obeys (4′) and (5′). Therefore the application of the operators $r_\mu{}^2-\lambda^4\Box_y$ or $r_\mu(\partial/\partial y_\mu)$ on the right-hand side of (34) yields identically zero, whence the left-hand side yields zero also. In this way it is proved that not only $\psi^{(0)}(x,r)$ but even the perturbed wave function $\psi(x,r)$ satisfies the reciprocal equations (4′) and (5′). By applying to (34) the operator $\Box_y-m^2$, using (47), and changing the variables, we get an integro-differential equation

$$(\Box_x-m^2)\psi(x,r)=f(x,r), \qquad \ldots\ldots(49)$$

where $f(x,r)$ is the following function of ψ and ϕ:

$$f(x,r)=\tfrac{1}{4}g\int dP'(\Box_x+r_\mu{}^2\lambda^{-4}-2m)\bar{\Delta}(x-x',r,s')\{\psi(x',r),\ \phi[x'+\tfrac{1}{2}(r'+s')]\}. \qquad \ldots\ldots(50)$$

Equation (49) is reciprocal since $\psi(x,r)$ obeys (4′) and (5′) and $f(x,r)$ is self-reciprocal. Thus the perturbed wave function $\psi(x,r)$ satisfies the reciprocal equations (4′), (5′) and (49). In this way the non-local field theory, including interaction, is put into a completely reciprocal form.

We mentioned above that this completely reciprocal formulation violates, to a certain extent, the principle of correspondence. This is due to the circumstance that the Fourier components of the $\bar{\Delta}(x,r,s)$ function are not restricted to $p_\mu{}^2=-m^2$, but $p_\mu{}^2$ may assume any value, even positive. For space-like p_μ the variables r and s (which are connected with p_μ through the delta functions $\delta(p_\mu r_\mu)$ and $\delta(r_\mu{}^2+p_\mu{}^2\lambda^4)$, etc.) may be time-like and their components do not vanish in the limit $\lambda\to 0$, in contradistinction to the case investigated in § 4.

Let us discuss the results of the above displayed formalism. It may be easily seen that the new S-matrix elements yield non-vanishing probabilities only for processes in which the total energy and momentum are conserved. But the probability amplitudes differ from the traditional ones by a set of factors of the type

$$J(p,q)=\int d^4r\exp(\tfrac{1}{2}iq_\nu r_\nu)\rho(p,r), \qquad \ldots\ldots(51)$$

where p_μ and q_μ are energy and momentum four-vectors for real or virtual states of the non-local particles. By introducing the notation

$$N^{-1}(p,q)=\int d^4r\exp(\tfrac{1}{2}iq_\nu r_\nu)\delta(p_\mu r_\mu)\delta(r_\mu{}^2+p_\mu{}^2\lambda^4) \qquad \ldots\ldots(52)$$

the factors (51) may be written, from (22), as

$$J(p,q)=N(p)N^{-1}(p,q). \qquad \ldots\ldots(53)$$

The computation of the integral (52) yields the following result: $N(p,q)$ is a function of the argument, invariant and symmetrical in p and q,

$$a=\tfrac{1}{4}\lambda^4[(p,q_\nu)^2-p_\mu{}^2q_\nu{}^2], \qquad \ldots\ldots(54)$$

of the form

$$N(p,q)=\frac{\pm 1}{2\pi\lambda^2}\frac{\sqrt{a}}{\sin\sqrt{a}} \quad \text{for} \quad a\geqslant 0,\ p_\mu{}^2\begin{cases}<0\\>0\end{cases}, \qquad \ldots\ldots(55')$$

$$N(p,q)=\frac{1}{2\pi\lambda^2}\sqrt{-a}\exp(\sqrt{-a}) \quad \text{for} \quad a<0. \qquad \ldots\ldots(55'')$$

If we compute directly the normalizing factor $N(p)$ from (10) then we get simply

$$N(p)=\pm 1/2\pi\lambda^2 \quad \text{for} \quad p_\mu{}^2\begin{cases}<0\\>0\end{cases}. \qquad \ldots\ldots(56)$$

Hence the factor (53) becomes

$$J(p,q)=\frac{1}{\sqrt{a}}\sin\sqrt{a} \qquad \text{for} \quad a\geqslant 0, \qquad \ldots\ldots(57')$$

$$J(p,q)=\frac{1}{\sqrt{-a}}\exp(-\sqrt{-a}) \quad \text{for} \quad a<0. \qquad \ldots\ldots(57'')$$

Thus $J(p,q)$ is a convergence factor strongly diminishing the interaction for $|a|\to\infty$. In consequence of the existence of the factors $J(p,q)$ the formalisms discussed here are free of the usual convergence difficulties.

The case $a\geqslant 0$ occurs always when at least one of the four-vectors p_μ, q_ν is not space-like. (This is always the case for the formulation given in §4, where p_μ is always time-like.) In this case the convergence factor tends to unity for $\lambda\to 0$, as it should do in a theory obeying the principle of correspondence. The case $a<0$ is rather exceptional and may occur only for virtual processes in higher orders of approximation than g^2, where both p_μ and q_μ may be space-like simultaneously. In such cases we get a strange result violating the principle of correspondence: $J(p,q)\to\infty$ for $\lambda\to 0$. For λ finite, but such p_μ and q_μ that $a\to -0$, the convergence factor $J(p,q)$ tends also to infinity, so that we encounter an unexpected case of resonance. The question whether this singularity does, or does not, introduce new divergences needs a special investigation.

This strange feature of the reciprocal interaction may be partly removed by the following device: The normalizing factor $N(p)$ given by (10) is identical with $N(p,p)$ as defined by (52) and may be regarded as a limit

$$N(p)=\lim_{q\to p}N(p,q). \qquad \ldots\ldots(58)$$

This limit transition is, however, ambiguous. If we perform the transition to the limit from the domain $a\geqslant 0$ we get, from (55'),

$$N(p)=\lim_{\substack{q\to p\\ a\to +0}}N(p,q)=\frac{1}{2\pi\lambda^2}; \qquad \ldots\ldots(59')$$

but if we let $q\to p$ so that $a<0$, then we get, from (55''),

$$N(p)=\lim_{\substack{q\to p\\ a\to -0}}N(p,q)=0. \qquad \ldots\ldots(59'')$$

In view of the above ambiguity we may define $N(p)$ appearing in (53) according to whether p and q appearing in (53) yield $a \geqslant 0$ or $a<0$. Now the convergence factor becomes

$$J(p,q) = \begin{cases} \dfrac{\sin\sqrt{a}}{\sqrt{a}} & \text{for } a \geqslant 0, \\ 0 & \text{for } a<0. \end{cases} \qquad \ldots\ldots(60)$$

Consequently, any virtual transition between two states characterized by space-like four-vectors of energy and momentum of virtual particles is made impossible and the formalism is free from any resonance for $a \to 0$ and from the usual divergences.

The higher order corrections to scattering processes will be sensitive to the irregular behaviour of the S-matrix elements for $a<0$ which may constitute a possibility of experimental check of the reciprocal formalism. At any rate, all the effects restricting the principle of correspondence lie in the relativistic region (since small perturbations cannot change the time-like character of the four-vector of energy and momentum of the (virtual) particle). Thus the correspondence principle is still valid in the non-relativistic limit.

§6. CONCLUSION

We have seen that it is possible to formulate a quantum theory of non-local scalar fields in full agreement either with the postulate of correspondence with the local quantum field theory or with Born's postulate of reciprocity, but it seems impossible to satisfy both postulates simultaneously. If the reciprocity is quite generally taken into account then the correspondence is restricted, and vice versa.

Finally we have to examine whether it is possible to apply similar ideas to more complicated fields and interactions, above all to quantum electrodynamics. It is difficult to decide if, in case of a spinor field *in vacuo*, we should retain equations (4) and (5) and replace (6) by the Dirac equation, or whether we should look for a suitable equation of the first order to replace (4) and to secure full reciprocity with the Dirac equation. The first alternative spoiling some of the reciprocal aspects is simpler, and it seems questionable whether a general reciprocity should be maintained also in the case of spinning particles, as the reciprocity establishes a symmetry between the operators of position and displacement but not between position and the rotational degrees of freedom.

The extension of the above-described formalism (without the replacement of (4) by an equation similar to the Dirac equation) lies at hand. However, some of the traditional features of quantum electrodynamics will be lost in consequence of the non-localizability. The continuity equation for the (perturbed) current formed with the aid of the correspondence principle (9) cannot be maintained and the gauge invariance of the second kind will also be violated. In the opinion of the author the lack of gauge invariance and of the continuity equations for the perturbed current do not disqualify such a formalism of quantum electrodynamics. We should remember that the introduction of new universal constants is necessarily accompanied by some renunciations. The inclusion of the finite velocity of light necessitated the sacrifice of the notion of absolute time, the introduction of Planck's constant, the sacrifice of the traditional concept of state and measurability. It seems quite natural that the incorporation of a fundamental length will necessitate also a renunciation of some of the notions which we were accustomed to and liked

so much. It seems that this time we have to abandon the details of kinematics of densities resulting in the continuity equations, as it is obviously impossible to trace the currents inside the charged particles.

In spite of the lack of a continuity equation, the integral charge conservation law is guaranteed simply by the gauge invariance of the first kind. On the other hand, the gauge invariance of the second kind is by no means a necessary condition for the vanishing of the rest mass of the photon. The value zero for the photon rest mass may be secured by other devices, e.g. by a realistic compensation by means of charged bosons or by a formal mass renormalization which, in the frame of a convergent formalism, becomes a mathematically correct procedure. In this respect the new formalism does not constitute any drawback in comparison with the traditional quantum electrodynamics which was gauge invariant only formally, so that we were also obliged to renormalize the (infinite!) self mass of the photon.

ACKNOWLEDGMENT

The author is indebted to Professor M. Born for his kind interest in this work and for a stimulating discussion.

REFERENCES

BLOCH, C., 1950, *K. Danske Vidensk. Selsk. Mat.-fys. Medd.*, **26**, 1.
BORN, M., and GREEN, H. S., 1949, *Proc. Roy. Soc. Edinb.* A, **92**, 470.
BORN, M., and PENG, H. W., 1944, *Proc. Roy. Soc. Edinb.* A, **62**, 40.
RAYSKI, J., 1950, *Acta Phys. Polon.*, **10**, 103 ; 1951, *Proc. Roy. Soc.* A, in the press.
SCHWINGER, J., 1949, *Phys. Rev.*, **75**, 651.
YANG, C. N., and FELDMAN, D., 1950, *Phys. Rev.*, **79**, 972 (see also KALLEN, G., 1950, *Ark. Fys.*, **2**, 371.)
YUKAWA, H., 1950, *Phys. Rev.*, **77**, 651.

Ferromagnetic Resonance and the Internal Field in Ferromagnetic Materials

BY J. R. MACDONALD*
Clarendon Laboratory, Oxford

Communicated by J. H. E. Griffiths; *MS. received* 20*th February* 1951, *and in amended form* 22*nd June* 1951

ABSTRACT. A classical treatment of the domain energy terms of a homogeneous ferromagnetic solid leads to a formula for the internal field contributions from these terms. With this result, modifications in the resonance condition of ferromagnetic resonance arising from self energy, exchange energy, magnetocrystalline anisotropy, and applied or intrinsic stress are obtained and are applied to various crystalline anisotropy and stress conditions of interest in ferromagnetic resonance experiments. Finally, the bearing of the results on the anomalous g-values obtained in resonance experiments is considered.

§1. INTRODUCTION

THIS paper is chiefly concerned with the forces which influence the direction of the magnetization vector **I** of a ferromagnetic substance in an external magnetic field and with the effects of these forces upon some of the phenomena of ferromagnetic resonance. A macroscopic viewpoint is adopted

* Now at Armour Research Foundation, Chicago, Illinois, U.S.A.

throughout, and all microscopic interactions are replaced by formulae for the magnetic potential energy density of the material which involve the macroscopic magnetization vector.

The usual case considered in calculating theoretical magnetization curves is that of an ellipsoidal ferromagnetic specimen in a static magnetic field (Stoner and Wohlfarth 1948); in this case the magnetization is uniform throughout the specimen and is time-independent. In ferromagnetic resonance experiments, however, a very small high-frequency oscillating magnetic field is applied to the ellipsoidal specimen, as well as a large static field oriented at right angles to the oscillating field. The magnetization of the body may then be neither space nor time independent, although, because of the relative magnitudes of the static and oscillating applied fields, variation of the magnetization vector with time and position will be small. One of the principal problems of ferromagnetic resonance, however, is the determination of this small space-and-time dependence of the direction and magnitude of the magnetization vector. In the purely static case the direction of the magnetization vector is determined from the general condition that the total magnetic potential energy of the body be a minimum. Because the magnetization is here uniform throughout the specimen, minimization of the expression for the magnetic energy density with respect to angle variables allows the direction of the magnetization vector to be uniquely specified.

In the present work the assumption will be made that the same general condition of minimum total magnetic potential energy can be applied to the oscillating field case when the magnetization of the body is homogeneous to yield the direction of the magnetization vector to a good order of approximation. When this minimization procedure is valid, the direction of the magnetization vector which is found is its instantaneous equilibrium direction $\mathbf{I}_{eq}$ defined as the direction in which the magnetization vector would remain or reach quickly if the time variation of the oscillating field were suddenly halted at the instant under consideration (and if retarded fields were of negligible importance).

If the oscillating field is of very high frequency, the actual instantaneous direction of the magnetization vector $\mathbf{I}$ may not coincide with the instantaneous equilibrium direction. The actual instantaneous direction and magnitude of the magnetization at a given point may be found, however, from the solution of the differential equation of motion satisfied by the magnetization vector; this equation involves the instantaneous internal, or local, field $\mathbf{H}^i$ at the point in the body considered. The instantaneous equilibrium magnetization vector is, by definition, parallel to the instantaneous internal field, since minimum magnetic energy of the specimen results when the magnetization vector lies along the internal field at every point in the body.

In §2 the variational principle is applied to the total magnetic potential energy of a homogeneous non-conducting ellipsoidal ferromagnetic body to yield a general method for calculating the internal-field vector when an external magnetic field is applied, and it is shown how the instantaneous direction of the magnetization vector may be determined. The contributions to the internal magnetic field from the various magnetic potential energy terms present in a ferromagnetic specimen are evaluated in §3. In §§4–6 the influence on the ferromagnetic resonance condition of the various energy terms is discussed in detail for macroscopic single crystals and for polycrystalline aggregates. Finally, in §7 the bearing of the results of the paper upon the anomalous Landé g-factors found in resonance experiments is considered.

§2. CALCULATION OF THE INTERNAL FIELD

Before deriving a general expression for the internal field $\mathbf{H}^{\mathrm{i}}$ in terms of the magnetic potential energy density, it is desirable to define further quantities and to consider the dependence of these quantities upon space and time. Since the externally applied field $\mathbf{H}$ is the sum of a static component $\mathbf{H}_0$ and a high-frequency oscillating component $\mathbf{h}$, the internal field $\mathbf{H}^{\mathrm{i}}$ will be a corresponding sum of $\mathbf{H}_0^{\mathrm{i}}$ and $\mathbf{h}^{\mathrm{i}}$, where h/H_0 and $h^{\mathrm{i}}/H_0^{\mathrm{i}}$ are very much smaller than unity. $\mathbf{H}_0$ and $\mathbf{h}$ will be independent of position within the body providing it is a non-conducting ellipsoid; if the ellipsoid is electrically conducting, h will decay with penetration depth because of the skin effect. Similarly, the magnetization vector $\mathbf{I}$ will be a sum of a static component $\mathbf{I}_0$ and an oscillating part $\mathbf{i}$. Because of the smallness of the oscillating field $\mathbf{h}$ compared with the static field, the oscillating component of the resulting magnetization will likewise be far smaller than the static component even at resonance, when the oscillating component is a maximum.

Finally, it is easy to show that the magnitude of the total magnetization vector is very nearly independent of time. The vector differential equation of motion of $\mathbf{I}$, at a given point in the body, is

$$\frac{1}{\gamma}\frac{\partial \mathbf{I}}{\partial t} = \mathbf{I} \times \mathbf{H}^{\mathrm{i}}, \qquad \ldots\ldots(1)$$

where $\gamma = ge/2mc = g\mu_{\mathrm{B}}/\hbar$ is the magnetomechanical ratio, g the Landé splitting factor, and μ_{B} the Bohr magneton. Note that the g-factor is assumed, subject to experimental verification, to be a constant independent of field orientation, body shape, etc. Equation (1) is just an expression for the rate of change of angular momentum per unit volume of the system. It shows that $\mathbf{I}.\partial \mathbf{I}/\partial t = 0$ at all points in the magnetic body, and that therefore I is time-independent. However, a small additional term should be added to equation (1) in order to account for damping caused by interactions between spins in the magnetic material and between the spin system and the crystalline lattice (Kittel 1948, Bloembergen 1950). Such damping may destroy the time-independence of I, but since damping is usually found experimentally to be small, I still remains nearly time-independent; therefore the effect of damping will be neglected in the present treatment. It will now be shown how an expression for the internal field may be derived by extending a method used by Landau and Lifshitz (1935).

There are several contributions to the total magnetic potential energy density which may influence the direction of the magnetization vector in a ferromagnetic body. The following will be considered here: (*a*) the magnetic potential energy density of the body in the external magnetic field, (*b*) the potential energy density arising from the magnetic self-energy of the body associated with its shape, (*c*) the Heisenberg exchange, or Weiss, energy density, (*d*) the magneto-crystalline anisotropy energy density, which is thought mainly to arise from spin–orbit coupling between neighbouring atoms, and (*e*) the strain magnetic energy density connected with magnetostriction and dependent upon the state of strain of the body.

It should be noted that domain wall energy need not be explicitly considered in the present treatment because the static external magnetic field will always be taken sufficiently large for the specimen to be considered a single domain. The domain wall energies and thicknesses for zero applied fields have recently been considered by Lilley (1950) and by Kittel (1949 b).

The magnetic potential energy density of a uniformly magnetized magnetic body (non-conducting ellipsoid) may usefully be considered as a function of the following variables*: $E=E(\mathbf{I}, X_i, \partial\mathbf{I}/\partial X_i)$, where X_i represents the three rectangular coordinates. Hence the total potential energy of the body will be

$$\int_V E\left(\mathbf{I}, X_i, \frac{\partial \mathbf{I}}{\partial X_i}\right) dV.$$

Applying the condition that the total magnetic potential energy of the body must be stationary with respect to small variations of the magnetization vector $\mathbf{I}$, one obtains

$$\int_V \delta E\left(\mathbf{I}, X_i, \frac{\partial \mathbf{I}}{\partial X_i}\right) dV = \int_V \left\{\frac{\partial E}{\partial \mathbf{I}} - \sum_i \frac{\partial}{\partial X_i}\left[\frac{\partial E}{\partial(\partial \mathbf{I}/\partial X_i)}\right]\right\} \cdot \mathbf{I}\, dV = 0.$$

Now the magnitude of $\mathbf{I}$ has been assumed to be a constant independent of time. Therefore the variation $\delta\mathbf{I}$ is not completely arbitrary but must lie in the plane perpendicular to $\mathbf{I}_{eq}$. This is because the variation consists of small changes in the direction of $\mathbf{I}$ from the instantaneous equilibrium direction $\mathbf{I}_{eq}$. Since the variation is otherwise arbitrary in magnitude and direction, however, the integrand of the above integral must itself be zero. One thus obtains

$$(\mathfrak{P}E) \cdot (\delta \mathbf{I}_{eq}) = 0, \qquad \ldots\ldots(2)$$

where $\mathfrak{P}$ is the differential vector operator

$$\left\{-\frac{\partial}{\partial \mathbf{I}} + \sum \frac{\partial}{\partial X_i}\left[\frac{\partial}{\partial(\partial \mathbf{I}/\partial X_i)}\right]\right\}.$$

Equation (2) can only be satisfied if the vector $\mathfrak{P}E$ is parallel or antiparallel to $\mathbf{I}_{eq}$ or is zero, since $\delta\mathbf{I}_{eq}$ is perpendicular to $\mathbf{I}_{eq}$. However, $\mathfrak{P}E$ cannot, in general, be zero as long as an external field is applied. Further, by definition, $\mathbf{I}_{eq}$ is always parallel to the internal field $\mathbf{H}^i$. Therefore $(\mathfrak{P}E)$ must be equal to $\mathbf{H}^i$ apart from a proportionality factor. This factor can be shown to be unity by applying the operator $\mathfrak{P}$ to an energy density term for which the corresponding contribution to the internal field is already known. Hence

$$\mathbf{H}^i = (\mathfrak{P}E) \qquad \ldots\ldots(3)$$

and the instantaneous equilibrium direction of the magnetization vector at any point in the body may be determined from the condition that

$$\mathbf{I}_{eq} \times \mathbf{H}^i = 0. \qquad \ldots\ldots(4)$$

Since $\mathbf{H}^i$ itself will usually be a function of $\mathbf{I}$ and its individual components, equation (4) must be used to determine the actual equilibrium direction of $\mathbf{I}$. A help in solving this vector equation is the auxiliary equation $\mathbf{I}_0 \times \mathbf{H}_0{}^i = 0$, which expresses the fact that the static component of the magnetization lies in the direction of the static component of the internal field. Equation (3) will be used later to compute some of the contributions of the different energy densities to the internal field.

When the applied frequency is very high, the instantaneous direction of the magnetization vector will not coincide with its instantaneous equilibrium direction. The actual instantaneous direction may be found using the equation of motion (equation (1)), which may be rewritten as

$$\frac{1}{\gamma}\frac{\partial \mathbf{I}}{\partial t} = \frac{1}{\gamma}\frac{\partial \mathbf{i}}{\partial t} = \mathbf{I} \times \mathbf{H}^i = (\mathbf{I}_0 + \mathbf{i}) \times (\mathbf{H}_0{}^i + \mathbf{h}^i) \simeq \mathbf{I}_0 \times \mathbf{h}^i + \mathbf{i} \times \mathbf{H}_0{}^i \qquad \ldots\ldots(5)$$

* The index here and in all further equations takes on values from 1 to 3.

since $\mathbf{i}\times\mathbf{h}^{\mathrm{i}}$ is a very small second-order term and may be neglected. Because $\gamma = 1{\cdot}7\times10^{7}$ cycles/sec/oersted, the left side of equation (5) is very small unless the applied frequency is high. When the frequency is low $\mathbf{I}\times\mathbf{H}^{\mathrm{i}}\simeq 0$, and the instantaneous equilibrium and actual directions of the magnetization vector are always effectively the same. But when the frequency is high this is no longer the case, and the direction of $\mathbf{i}$ must be found by solving equation (5). Since $\mathbf{I}_0$ is effectively the saturation value of the magnetization and its direction is fixed by the relation $\mathbf{I}_0\times\mathbf{H}_0^{\mathrm{i}}=0$, the instantaneous direction of the total magnetization vector $\mathbf{I}=\mathbf{I}_0+\mathbf{i}$ may then be found.

§ 3. INTERNAL FIELD CONTRIBUTIONS

In this section the individual contributions to the total internal field from the five potential energy densities mentioned in § 2 will be calculated using equation (3). The five energy density terms may be written as functions of the magnetization vector as follows:

(*a*) External-field energy density: $E_{\mathrm{ext}}=-\mathbf{H}.\mathbf{I}$.

(*b*) Self-energy density (for a non-conducting ellipsoid only): $E_{\mathrm{s}}=\frac{1}{2}\Sigma N^{\mathrm{s}}{}_j I_j^{\,2}$.

(*c*) Exchange energy density (Stoner and Wohlfarth 1948)*:

$$E_{\mathrm{exc}}=-\tfrac{1}{2}N_{\mathrm{w}}\mathbf{I}.\mathbf{I}+\tfrac{1}{2}C\Sigma[(\nabla I_i).(\nabla I_i)]$$
$$=-\tfrac{1}{2}N_{\mathrm{w}}\mathbf{I}.\mathbf{I}+\tfrac{1}{2}C\Sigma\left[\frac{\partial\mathbf{I}}{\partial X_i}.\frac{\partial\mathbf{I}}{\partial X_i}\right].$$

(*d*) Crystalline anisotropy energy for single crystals (Becker and Doring 1939):

Hexagonal crystals: $E_{\mathrm{c}}=K_1'(1-\alpha_1^{\,2})+K_2'(1-\alpha_2^{\,2})$.

Cubic crystals: $E_{\mathrm{c}}=K_1[\alpha_1^{\,2}\alpha_2^{\,2}+\alpha_2^{\,2}\alpha_3^{\,2}+\alpha_3^{\,2}\alpha_1^{\,2}]+K_2[\alpha_1^{\,2}\alpha_2^{\,2}\alpha_3^{\,2}]$
$=\frac{1}{2}K_1[1-(\alpha_1^{\,4}+\alpha_2^{\,4}+\alpha_3^{\,4})]+K_2[\alpha_1^{\,2}\alpha_2^{\,2}\alpha_3^{\,2}]$.

(*e*) Strain energy density for cubic single crystals (Becker and Doring 1939)†:

$$E_{\mathrm{st}}=-\tfrac{3}{2}\lambda_{100}\Sigma\alpha_i^{\,2}P_{ii}-3\lambda_{111}\{\alpha_1\alpha_2P_{12}+\alpha_2\alpha_3P_{23}+\alpha_3\alpha_1P_{31}\}.$$

In the above, α_1, α_2 and α_3 are the direction cosines of the magnetization vector with respect to the X_1, X_2, X_3 axes, taken along the cubic axes of the cubic crystal and taken with the X_1 axis in the direction of the principal crystalline axis of the hexagonal crystal, so that $\alpha_1=I_1/I=(\mathbf{I}.\mathbf{i}_1)/I$, where $\mathbf{i}_1$ is a unit vector along the X_1 axis, etc. The P_{ij}'s are the components of the stress tensor referred to the same coordinate system. K_1', K_2' and K_1, K_2 are crystalline anisotropy constants which may be determined experimentally. Recent values of these constants are quoted by Kittel (1949 b). The $N^{\mathrm{s}}{}_j$'s are the shape demagnetization constants applying when the coordinate system is taken along principal axes of the ellipsoidal specimen. N_{w} is the Weiss molecular field constant, and C is a constant approximately equal to $\frac{1}{3}a^2N_{\mathrm{w}}$, where a is the grating spacing of the material. The results of more accurate calculations of the quantity C are given by Lifshitz (1944) and by Stoner and Wohlfarth (1948). Finally, λ_{100} and λ_{111} are the saturation values of the magnetostriction constants of the ferromagnetic crystal in the [100] and [111] directions respectively. Numerical values of these constants for iron and nickel are given by Becker and Doring (1939, pp. 277–280).

* This formula has been derived only for substances having cubic structure.

† This expression is valid only for the region of elastic strain and for stress tensor elements independent of position (homogeneous stress).

Since the total energy density is to a very good approximation the sum of the individual energy density terms, the contribution to the internal field of each energy density term may be obtained by applying the operator $\mathfrak{P}$ to each term in turn. One then finds the following results:

$$\mathbf{H}^{\mathrm{i}}_{\mathrm{ext}} = \mathbf{H} \equiv \mathbf{H}_0 + \mathbf{h} \qquad \ldots\ldots(6)$$

$$(H^{\mathrm{i}}_{\mathrm{s}})_j = -\Sigma N^{\mathrm{s}}_j I_j \qquad \ldots\ldots(7)$$

$$\mathbf{H}^{\mathrm{i}}_{\mathrm{exc}} = N_{\mathrm{w}}\mathbf{I} + C\nabla^2\mathbf{I} \qquad \ldots\ldots(8)$$

$$\mathbf{H}^{\mathrm{i}}_{\mathrm{c}} = \left[\frac{2K_1'}{I} + \frac{4K_2'}{I}\left\{1 - \left(\frac{I_1}{I}\right)^2\right\}\right]\left(\frac{I_1}{I}\right)\mathbf{i}_1 \quad \text{Hexagonal} \qquad \ldots\ldots(9)$$

$$(H^{\mathrm{i}}_{\mathrm{c}})_j = \frac{2K_1}{I^4} I_j^3 - \frac{2K_2}{I^6} I_j I_k^2 I_l^2 \qquad (j,k,l = 1,2,3 \text{ and permutations})$$
Cubic $\qquad \ldots\ldots(10)$

$$(H^{\mathrm{i}}_{\mathrm{st}})_j = \frac{3}{I^2}\sum_k [(\lambda_{100} - \lambda_{111})\delta_{jk} + \lambda_{111}] P_{jk} I_k. \qquad \ldots\ldots(11)$$

Some of these equations are written directly in terms of vectors, others in terms of the jth component of the corresponding vector, in the interest of simplicity.

From the above expressions the direction and magnitude of each contribution to the total internal field may be obtained. Previously, Bozorth (1949) obtained the approximate maximum magnitude of the internal field contributions arising from several of the energy density terms considered here by equating the terms separately to $\mathbf{H}^{\mathrm{i}}.\mathbf{I}$. Further, Kittel (1948) computed the quantity $\mathbf{I} \times \mathbf{H}^{\mathrm{i}}_{\mathrm{c}}$ for the case of crystalline anisotropy for several special directions and planes in single crystals. Finally, Brown (1940) has used a different variational approach to obtain general equations equivalent to $(\mathbf{I}_0 \times \mathbf{H}_0^{\mathrm{i}})_j = 0$, expressing the balance of torques on the magnetization vector when no oscillating field is applied, and including the static effect of all the potential energy terms considered here but with these terms expressed somewhat differently. The present results, however, give both the magnitude and the general directional dependence of the various static and oscillating internal field contributions in convenient form. It should be noted, however, that the internal field contributions due to crystalline anisotropy and strain in cubic crystals are not unique, because the relation $\alpha_1^2 + \alpha_2^2 + \alpha_3^2 = 1$ may be used to transform the expressions for the energy densities to different forms from those used here. Nevertheless, such indeterminacy does not affect the term $\mathbf{I} \times \mathbf{H}^{\mathrm{i}}$ which determines the direction of $\mathbf{I}$; therefore both the direction of $\mathbf{I}$ and the effect of the above energy terms upon ferromagnetic resonance phenomena remain unique.

§ 4. FERROMAGNETIC RESONANCE EXPERIMENTS

The foregoing internal field contributions may be used to compute the dependence of the magnetization curves of ferromagnetic single crystals along different crystal directions upon ellipsoid shape, crystalline anisotropy and applied stress. Part of such a programme has been carried out by Stoner and Wohlfarth (1948), who, however, used the method of direct minimization of the total magnetic energy density to obtain the dependence of the magnetization components upon an applied static magnetic field. In solving such a problem, the actual internal field contributions derived here are unnecessary, although they shed additional light on the physical situation considered. In considering, however, the influence

of ellipsoid shape, exchange anisotropy, crystalline anisotropy and strain upon ferromagnetic resonance phenomena, explicit expressions for the internal field contributions are useful.

In a ferromagnetic resonance experiment two external magnetic fields are applied to an ellipsoidal ferromagnetic body. The specimen may be a single crystal or polycrystalline, non-conducting or conducting. The fields are usually taken along two mutually perpendicular principal axes of the ellipsoid. One of the fields is large and static but can be varied in magnitude over a wide range; the other is produced by incident microwave electromagnetic radiation and is very small in magnitude. In making ferromagnetic resonance experiments, the frequency of the incident radiation is commonly held constant and the magnitude of the static field varied. It is found that a maximum of the absorption of microwave power in the specimen occurs for a unique static field strength. This resonant field strength, H_0^r, is that field strength which makes the effective Larmor frequency of the spins of the ferromagnetic material, $(\gamma/2\pi)H^{\text{eff}}$, equal to the frequency of the applied radiation ν. Since the effective field H^{eff} involves all the internal field contributions, theoretical determination of the resonant field strength requires information concerning such contributions.

It is usually assumed in ferromagnetic resonance calculations that the externally applied static field is always of sufficient strength to cause the resulting static component of the total magnetization vector to be substantially equal to the saturation magnetization of the material and to lie in the direction of the static field. Crystalline anisotropy and applied stress may tend to pull the static magnetization vector away from the field direction, but if the field is sufficiently strong (as is usually the case experimentally) such effects may be neglected. Then any influence of shape, crystalline anisotropy, or strain on the resonance phenomena arises from the interaction between their internal field contributions and the very weak oscillating component of the magnetization vector produced by the oscillating magnetic field of the incident radiation.

There are two particularly important quantities which may be obtained from the results of a ferromagnetic resonance experiment. These are the Landé g-factor determined from the resonant magnetic field strength, and the damping factor which may be calculated from the shape of the microwave absorption resonance curve. The importance of these two factors in giving insight into the coupling between ferromagnetic electrons and between these electrons and the crystal field has been recently discussed by Kittel (1949a) and Van Vleck (1950). In the present treatment we are especially concerned with the calculation of the Landé g-factor for different ferromagnetic specimen shapes, orientation of applied fields, crystalline nature and applied stress, although other quantities, such as crystalline-anisotropy and magnetostriction constants, may also be obtained from the analysis of resonance experiments. It is not expected that the g-factor of a given ferromagnetic material should depend appreciably upon any of the above conditions; however, its calculation requires knowledge of the effects of these factors upon the resonant magnetic field. Such knowledge may be embodied in the explicit form of H^{eff}, and, given an experimental H_0^r for a specific microwave frequency, the corresponding g-value may be computed from the resonance condition $\nu=(ge/4\pi mc)H^{\text{eff}}$. The presence in an experimental material of any anisotropy which is not recognized by an appropriate modification of H^{eff} can obviously cause an incorrect value of g to be obtained from the experiment.

§ 5. THE GENERAL RESONANCE CONDITION

The ferromagnetic resonance condition may be obtained from the solution of the equation of motion (equation (5)) when the explicit form of the internal field components is known. The equation of motion may be solved in any convenient coordinate system; the most convenient is often the rectangular system (X_1, X_2, X_3), defined by coincident ellipsoid and single-crystal principal axes. For the present work it is useful to introduce another rectangular coordinate system (X_1', X_2', X_3') rotated with respect to the (X_1, X_2, X_3) axis with the static applied field $\mathbf{H}_0$ always taken along the X_3' axis and the oscillating field $\mathbf{h}$ along the X_1' axis. By solving the equation of motion in this primed system, general resonance conditions applicable to arbitrary orientations of the applied fields with respect to ellipsoid principal axes, single crystal axes, or an applied or intrinsic stress system may be obtained immediately.

In order to solve the equation of motion in the primed coordinate system, the internal field vector must be resolved in the primed system. The internal field contributions given in equations (7), (9), (10), and (11) involve magnetization vector components referred to the unprimed system; the transformation of the internal field expressions and the magnetization vector components to the primed system is straightforward and is accomplished by introducing the nine direction cosines γ_{ij} connecting an X_i' axis to an X_j axis. One finds that the internal field components in the primed system due to shape effects, crystalline anisotropy, or strain may each be written in the general form

$$(H_{\mathrm{a}}^{\mathrm{i}})_j' = \sum_k N^{\mathrm{a}}{}_{jk} I_k', \qquad \ldots\ldots(12)$$

where the index 'a' denotes anisotropy due to shape, single-crystal structure, or strain. The $N^{\mathrm{a}}{}_{jk}$ matrix elements are effective demagnetization constants due to anisotropy referred to the primed system; they will, in general, involve the γ_{ij}'s.

The equation of motion for arbitrary $N^{\mathrm{a}}{}_{jk}$ values may now be solved using equation (12). The components of the over-all internal field, including applied fields, are of the form

$$(H^{\mathrm{i}})_j' = H_j' - \sum_k N^{\mathrm{a}}{}_{jk} I_k', \qquad \ldots\ldots(13)$$

where $H_1' = h$, $H_2' = 0$, $H_3' = H_0$. Since the static field H_0 is taken as far greater than any static anisotropy field, the static magnetization vector will lie very nearly along the direction of the static applied field. In this case, the components of the magnetization vector are: $I_1' = i_1'$ $I_2' = i_2'$, $I_3' = I_0$. The solution of the equation of motion with the above form of H^{i} was first carried out by Kittel (1947, 1948). In Kittel's analysis the $[N^{\mathrm{a}}{}_{jk}]$ matrix was diagonal and the following expression for H^{eff} was obtained:

$$H^{\mathrm{eff}} = \{[H_0{}^{\mathrm{r}} + (N^{\mathrm{a}}{}_{22} - N^{\mathrm{a}}{}_{33})I_0][H_0{}^{\mathrm{r}} + (N^{\mathrm{a}}{}_{11} - N^{\mathrm{a}}{}_{33})I_0]\}^{1/2}, \qquad \ldots\ldots(14)$$

where $H_0{}^{\mathrm{r}}$ is the resonant value of the static field.

It turns out that the same result is an excellent approximation when the $[N^{\mathrm{a}}{}_{jk}]$ matrix is not diagonal, provided that H_0 is large enough to make I_0 lie along its direction. In the general case of arbitrary orientation between applied fields and crystal or ellipsoid axes, the off-diagonal elements of $[N^{\mathrm{a}}{}_{jk}]$ are not, in fact, zero. Nevertheless, the same resonance equation applies very closely. In order to compute the resonance shifts due to the various different sources of anisotropy, it is thus only necessary to calculate the diagonal elements of the corresponding $[N^{\mathrm{a}}{}_{jk}]$ matrices. When two or more sources of anisotropy are

present in a specimen to be used in a resonance experiment, the matrix elements occurring in the resonance condition are the sums of the matrix elements arising from the individual anisotropies, as can readily be seen from the linearity of equation (5) in $\mathbf{H}^1$ and of equation (12) in N^a_{ij}.

In the Appendix general expressions for the $(N^a_{11}-N^a_{33})$ and $(N^a_{22}-N^a_{33})$ factors occurring in the resonance condition are given for shape, crystalline anisotropy and strain anisotropy contributions. Special cases of these expressions for situations which have arisen or might be important in resonance experiments are considered in the following section.

§6. ANISOTROPY CONTRIBUTIONS TO THE RESONANCE CONDITION

(i) *Shape*

Ferromagnetic resonance experiments have thus far been carried out with spherical magnetic specimens of high resistivity (Hewitt 1948, Bickford 1950, Yager *et al.* 1950) and with either high resistivity ferritic or conducting metallic disc-shaped specimens (Griffiths 1951). In these cases the applied magnetic fields are always taken along principal ellipsoid axes (considering a thin disc as an oblate spheroid) and the general treatment in the Appendix is unnecessary; the results given in equations (23) are only required when field directions and principal axes do not coincide. The shape effects derived below apply both to polycrystalline and to single crystal materials.

The effective fields for the above specimen shapes are easily obtained by substituting the shape demagnetization constants N^s_{jj} directly for the N^a_{jj} elements occurring in equation (14). For a non-conducting isotropic sphere $N^s_1=N^s_2=N^s_3=4\pi/3$ and H_{eff} reduces to $H_0{}^r$. There is no shape anisotropy here and hence no resonance shift. For a non-conducting thin disc the demagnetization constants for fields lying in the plane of the disc are approximately π^2/m, while that for a field normal to the disc is $(4\pi-2\pi^2/m)$, where m is the ratio of disc diameter to thickness (Osborn 1945, Stoner 1945). There are two field orientations of experimental interest, both applied fields lying in the plane of the disc, and static field perpendicular to the disc. The demagnetization constants in these two cases are, respectively, $N_1=N_3=\pi^2/m$, $N_2=4\pi-2\pi^2/m$, and $N_1=N_2=\pi^2/m$, $N_3=4\pi-2\pi^2/m$. The corresponding effective fields are

$$H^{\text{eff}}{}_{\parallel}=\left[\left(B_0{}^r-\frac{3\pi^2}{m}I_0\right)H_0{}^r\right]^{1/2};\quad H^{\text{eff}}{}_{\perp}=\left[H_0{}^r-\left(4\pi-\frac{3\pi^2}{m}\right)I_0\right]$$

(non-conducting discs). .....(15)

When the resistivity of a specimen is not so high that it may be considered as virtually non-conducting, the skin effects begin to become important. Because of this effect, the magnetic fields in the specimen are inhomogeneous since there is a decay of the amplitudes of the oscillating components of the field as they penetrate into the disc. In this case the expression for the magnetic potential energy should contain terms arising from and depending upon the distribution of $\nabla.\mathbf{I}$, which would cause the simple expression for E_s given in §2 to be incorrect. A good approximation to the correct value of the effective field in this case may be obtained, however, by remembering that at the high frequencies employed the skin depth is always considerably less than the diameter or thickness of the disc. Then the demagnetization constants in the direction of oscillating field

components have approximately the values they would have if the disc were of infinite diameter. Therefore, for parallel fields, $N_1=0$, $N_2=4\pi$, $N_3=\pi^2/m$, while for perpendicular static fields, $N_1=0$, $N_2=0$, $N_3=4\pi-2\pi^2/m$. The effective field expressions are

$$H^{\text{eff}}{}_{\parallel}=\left[\left(B_0{}^{\text{r}}-\frac{\pi^2}{m}I_0\right)\left(H_0{}^{\text{r}}-\frac{\pi^2}{m}I_0\right)\right]^{1/2};\quad H^{\text{eff}}{}_{\perp}=\left[H_0{}^{\text{r}}-\left(4\pi-\frac{2\pi^2}{m}\right)I_0\right]$$

(conducting discs). .....(16)

Experiments designed to compare g_{sphere} with g_{disc} (parallel field orientation) for a polycrystalline ferrite of high resistivity were performed by Hewitt (1948), who obtained reasonably good agreement between the g-values, indicating that the resonance formulae for these cases are at least good approximations. Further, an experiment comparing $g_{\parallel}$ and $g_{\perp}$ for a supermalloy disc specimen was carried out by Kittel, Yager and Merritt (1949) who, found a difference between $g_{\parallel}$ and $g_{\perp}$ of 2·5%. Using the above expression for $H^{\text{eff}}{}_{\perp}$, which is slightly more accurate than that used by Kittel *et al.*, one obtains a difference of approximately 1·1%; this can probably be ascribed to inexact knowledge of I_0.

(ii) *Exchange*

In order to evaluate the effect of exchange anisotropy on the resonance condition it is necessary to add the exchange internal field contribution given in equation (8) to the equation of motion and solve it with this added term. If the magnetic material is non-conducting, however, the contribution will be zero since $\nabla^2\mathbf{I}$ will then be zero and $\mathbf{I}\times N_{\text{w}}\mathbf{I}$ is identically zero. Because of the skin effect present when the material is conducting, $\nabla^2\mathbf{I}$ is not zero and becomes $\nabla^2\mathbf{i}$. Exact solution of the equation of motion with such a term taken in conjunction with Maxwell's equations is a lengthy complicated process since the material becomes triply refracting to microwaves. The results of such a solution by the author (Macdonald 1950) concur with those of a perturbation treatment by Kittel and Herring (1950) in indicating no appreciable resonance shift from this cause for metals at room temperature.

(ii) *Magnetocrystalline Anisotropy*

Thus far no resonance experiments have been reported on hexagonal-close-packed single crystals. Experiments to determine the anisotropy constants K_1' and K_2' might be carried out with the static magnetic field always in a plane perpendicular to the principal crystal axis or, alternatively, with the static field lying in a plane containing the crystal axis. If θ is the angle between the static field and the crystal axis, the direction cosines in these two cases are, respectively, $\gamma_{21}=1$, $\gamma_{11}=\gamma_{31}=0$ and $\gamma_{11}=\sin\theta$, $\gamma_{31}=\cos\theta$, $\gamma_{21}=0$. The corresponding contributions from equations (24) (see Appendix) to the effective field are

$$(N^{\text{e}}{}_{11}-N^{\text{e}}{}_{33})I_0=0;\quad (N^{\text{e}}{}_{22}-N^{\text{e}}{}_{33})I_0=-\frac{2}{I_0}(K_1'+2K_2') \quad .....(17)$$

and $$(N^{\text{e}}{}_{11}-N^{\text{e}}{}_{33})I_0=\frac{2K_1'}{I_0}\cos 2\theta+\frac{4K_2'}{I_0}\sin^2\theta(1+2\cos 2\theta);$$

$$(N^{\text{e}}{}_{22}-N^{\text{e}}{}_{33})I_0=\frac{2K_1'}{I_0}\cos^2\theta+\frac{K_2'}{I_0}\sin^2 2\theta. \quad .....(18)$$

When $\theta = 0$ the last two equations reduce to a result first obtained by Kittel (1948), who considered terms in K_1' only. For cobalt the factors $2K_1'/I_0$ and K_2'/I_0 are approximately 6,000 and 700 gauss respectively, showing that crystalline anisotropy can affect the resonance condition greatly for this material.

Two interesting experiments have been carried out on cubic single crystals. Kip and Arnold (1949) investigated the dependence of the resonant field for a silicon–iron single crystal disc upon the angle θ between the static field and the [001] crystal direction when the static field was constrained to lie in the (010) plane. In this case the non-zero direction cosines are $\gamma_{11} = \gamma_{33} = \cos\theta$, $\gamma_{13} = -\gamma_{31} = \sin\theta$ and $\gamma_{22} = 1$. The contributions to the effective field from equations (25) are

$$(N^c_{11} - N^c_{32})I_0 = \frac{2K_1}{I_0}\cos 4\theta\,; \quad (N^c_{22} - N^c_{33})I_0 = \frac{K_1}{2I_0}(3 + \cos 4\theta) + \frac{K_2}{2I_0}\sin^2 2\theta. \qquad \ldots\ldots(19)$$

These results were first obtained by Kittel (1948, 1949a). Kip and Arnold found the expected dependence of H_0^r upon θ at constant applied frequency and obtained a good value of K_1 for silicon–iron as well as a g-value independent of θ.

Recently Yager, Galt, Merritt and Wood (1950) investigated the effect of rotating the static field applied to a single-crystal ferrite sphere in a (110) crystal plane. If θ is the angle between the applied field and the [001] direction, the non-zero direction cosines applying to this case are

$$\gamma_{11} = \gamma_{12} = \sqrt{(1/2)}\gamma_{33} = \sqrt{(1/2)}\cos\theta, \quad \gamma_{31} = \gamma_{32} = -\sqrt{(1/2)}\gamma_{13} = \sqrt{(1/2)}\sin\theta.$$

The general equation (25) then reduces to

$$\left.\begin{aligned}(N^c_{11} - N^c_{33})I_0 &= \frac{K_1}{I_0}(2 - \sin^2\theta - 3\sin^2 2\theta) + \frac{K_2}{16I_0}\sin^2\theta(1 - 60\cos^2\theta + 65\cos^4\theta);\\ (N^c_{22} - N^c_{33})I_0 &= \frac{2K_1}{I_0}\left(1 - 2\sin^2\theta - \frac{3}{8}\sin^2 2\theta\right) - \frac{K_2}{16I_0}\sin^2 2\theta(7 - 5\cos^2\theta).\end{aligned}\right\} \qquad \ldots\ldots(20)$$

The first-order terms in these equations have been reported earlier by Bickford (1950). Yager *et al.* found the θ-dependence indicated by the above equations and an excellent value of K_1 for the ferrite investigated: the K_2 terms were apparently negligible for this ferrite.

(iv) *Strain*

From the general equations (26) given in the Appendix it is relatively easy to compute the strain contribution to the resonance condition when the applied fields lie in a (010) or (110) crystal plane and none of the stress tensor elements is zero. Here, however, we shall consider some even simpler situations of more experimental interest.

In the case of uniform pressure P applied to a ferromagnetic ellipsoid, the stress tensor elements are given by $P_{ij} = -P\delta_{ij}$, and there is no contribution from the general equations (26) because there is no strain anisotropy. This is not the case, however, for plane stress even in the simplest and experimentally most interesting case of a purely radial stress T_0 (T_0 is positive for tension, negative for compression) applied at the circumference of a circular disc. Here the only

non-zero stress tensor elements are (for a disc with its normal in the [010] direction) $P_{11}=P_{33}=T_0$. On substituting these results into the relations (26), and simplifying, one obtains

$$(N^{st}{}_{11}-N^{st}{}_{33})I_0=\frac{3\lambda_{100}T_0}{I_0}(\gamma_{12}{}^2-\gamma_{32}{}^2);\quad (N^{st}{}_{22}-N^{st}{}_{33})I_0=\frac{3\lambda_{100}T_0}{I_0}(\gamma_{22}{}^2-\gamma_{32}{}^2). \qquad \ldots\ldots(21)$$

In an experiment to measure the effect of applied stress of this character, produced, for example, by means of a draw-strap around the disc, the applied magnetic fields would be taken either in the (010) crystal plane (the plane of the disc) or with the static field perpendicular to the disc. For these two conditions the above equations reduce to

$$\left.\begin{aligned}&\text{Parallel fields: } (N^{st}{}_{11}-N^{st}{}_{33})I_0=0;\quad (N^{st}{}_{22}-N^{st}{}_{33})I_0=3\lambda_{100}T_0/I_0,\\&\text{Perpendicular static field: } (N^{st}{}_{11}-N^{st}{}_{33})I_0=(N^{st}{}_{22}-N^{st}{}_{33})I_0=\frac{-3\lambda_{100}T_0}{I_0}.\end{aligned}\right\} \qquad \ldots\ldots(22)$$

In neither case is the contribution to the effective field zero, although rotation of the fields around the normal to the disc has no effect (crystalline anisotropy neglected) since there is no strain anisotropy in the plane of the disc. These non-zero results are somewhat unexpected and are discussed later in connection with actual experiments.

Another simple stress system of experimental interest consists of a unidirectional stress T applied in the $[\beta_1, \beta_2, \beta_3]$ crystallographic direction. Here the stress elements are $P_{ij}=\beta_i\beta_j T$. In the case where the applied fields lie in the plane of a single-crystal disc cut so that this plane coincides with the (010) crystallographic plane, and where the unidirectional stress is also applied in this plane, both the magnetostriction constants λ_{100} and λ_{111} may be obtained by measuring the change of H_0^r as the fields are rotated with respect to the crystal axes, keeping the stress direction fixed with respect to these axes or, alternatively, keeping the stress direction fixed and shifting the stress direction with respect to the crystal axes. No experiments of this type have been reported as yet.

The above strain contributions have all applied to cubic ferromagnetic single crystals. Ferromagnetic resonance experiments are often made, however, on polycrystalline materials in which the individual crystallites have approximately random orientation. The extension of the strain formulae to isotropic polycrystalline material may be made in two different ways. In the first method the complete resonance condition, including self-energy, crystalline anisotropy, and strain contributions, must be averaged over all possible directions of the crystallite axes, preferably taking into account absorption line broadening due to relaxation processes, etc. Since this would be extremely complicated to carry out, even if crystalline shape and size distributions were known, it is simpler to make the approximation of isotropic magnetostriction usual in dealing with polycrystalline aggregates of ferromagnetic crystallites. This approximation consists of taking $\lambda_{100}=\lambda_{111}=\lambda$. The effective strain demagnetization constants in equation (26) then simplify to give

$$(N^{st}{}_{11}-N^{st}{}_{33})I_0=\frac{3\lambda}{I_0}(P_{33}'-P_{11}');\quad (N^{st}{}_{22}-N^{st}{}_{33})I_0=\frac{3\lambda}{I_0}(P_{33}'-P_{22}'),$$

where the primed stress elements are referred now to the primed (field) coordinate system.

When isotropic stress T_0 is applied in the plane of a polycrystalline disc, the effective field contributions are given by equations (22) with λ_{100} replaced by λ. The sign of these factors depends both upon the sign of λ and upon whether the applied stress is tensile or compressive. The change in the resonance field caused by these factors may be quite appreciable; for example, Kittel (1949b) gives for $3\lambda T_0/I_0$ the values 600, 600, 4,000 gauss for iron, cobalt and nickel, respectively, when T_0 is taken as the breaking stress of the material.

No resonance experiments deliberately undertaken to observe stress effects on single crystals or polycrystalline materials have been published as yet. However, the resonant field dependence on applied plane stress has been verified by Macdonald (1950, 1951 a, b)*, who investigated resonance shifts for thin nickel films evaporated on mica. Here, applied isotropic plane stress (independently determined from magnetometer measurements) was found to be produced by differential contraction between mica and nickel on cooling after evaporation. Such stress was dependent on film thickness and produced an apparent dependence of the g-factor on film thickness. No dependence of the g-factor on applied stress was observed, however, when the stress-corrected resonance condition was used. In the course of making resonance measurements from room temperature to the Curie point on a nickel disc silver-soldered to a copper block, Standley (unpublished) observed a decrease in the apparent g-value with increasing temperature. Calculations by the author (Macdonald 1950) have shown that such decrease was only apparent, being caused by the temperature-dependent plane tension produced in the nickel disc by the greater expansion on heating of copper as compared with nickel. It may be postulated that a similar small decrease in g with increasing temperature for nickel found by Bloembergen (1950) and reported to be within experimental error was caused by the same phenomenon. Further, the 4% decrease in g with decreasing temperature over the range from room temperature to $-153°$ c. found by Bickford (1950) for a Fe_3O_4 single-crystal disc may be susceptible to the same general explanation, although the magnetostriction constant for magnetite may depend significantly upon temperature in this region. The dependence of the resonant field upon unidirectional stress applied to a polycrystalline specimen has not been verified in detail experimentally so far, although Macdonald (1950) observed some directional dependence of H_0^r upon the angle between the applied static field in the plane of an evaporated nickel disc and the coplanar direction of a magnetic field applied during annealing of the specimen.

§7. CONCLUSION

In all the resonance experiments discussed in §6 the g-values obtained were substantially greater than 2·00, the value to be expected for free electron spins. In fact the great majority of all g-values measured so far have significantly exceeded the free electron value, usually lying in the range between 2·1 and 2·3. One of the objects of the present work was to investigate fully the modifications in the resonance condition caused by internal fields arising from various types of anisotropy, with the hope that the results might possibly explain some or all of the anomalous g-values that have been reported.

* See also Griffiths (1951).

The bearing of the present results on the g-value problem may be summarized as follows:

(i) The use of the effective field expressions given in (16) for a conducting disc decreases the experimental discrepancy between $g_{\parallel}$ and $g_{\perp}$ found by Kittel, Yager and Merritt to about 1%. Since this is within the limits of experimental error, g is independent of field orientation. Nevertheless, the value of g found for supermalloy still remains about 2·19.

(ii) The work of Kittel and Herring (1950) and Macdonald (1950) shows that the high g-values found for metals cannot be ascribed to exchange force effects; such an explanation would not, in any event, apply to non-conducting materials.

(iii) The results of experiments on anisotropic single crystals are in excellent agreement with theory. There appears to be no g-dependence upon special crystalline directions, but the experimentally measured g-values are anomalously large.

(iv) The g-factor has been found independent of applied stress, and the use of the correction terms to the effective field found when isotropic plane stress is present in a disc-like ferromagnetic specimen has satisfactorily explained an apparent dependence of g upon evaporated film thickness and upon temperature for nickel discs. Stress effects may also be pertinent to the complete interpretation of the g-value temperature dependence found by Bickford (1950) for magnetite at low temperatures.

(v) The internal field results of the present paper, taken in conjunction with the experimental results of Macdonald on stressed and stress-free nickel films, would seem to render inapplicable Birks' (1948) suggestion that high g-values are due to internal anisotropy or strain fields.

There has been much speculation as to the reason for the anomalously large g-values. A critical survey of the reasons suggested for the effect has been given by Kittel (1949 a), see also Van Vleck (1950). None of the explanations seems able to account for the phenomenon in detail, although it is likely that the effect is connected with spin–orbit coupling as postulated by Polder (1949) and by Kittel (1949 a). There is as yet no detailed theory of the phenomenon, and it remains essentially unexplained.

APPENDIX

EFFECTIVE DEMAGNETIZATION CONSTANTS DUE TO ANISOTROPY

The problem considered here is the transformation of equations (7), (9), (10) and (11) for anisotropy internal-field contributions (referred to the fixed coordinate system (X_1, X_2, X_3)) to the rotated coordinate system (X_1', X_2', X_3') in order to obtain expressions of the form of equation (12) for the internal field contributions in the primed system. The N^a_{jk} demagnetization elements due to anisotropy defined by the transformation may then be used in equation (14) to give the general resonance condition for any orientation between primed and unprimed axes.

(i) *Shape* (cf. equation (7))

Since equation (7) is linear in I_j, the N^s_j shape demagnetization constants may be considered the diagonal elements of the demagnetization matrix referred to the unprimed principal-axis coordinate system. A coordinate tranformation of this matrix to the primed system then gives the desired result:

$$N^s_{jk} = \sum_l \gamma_{jl}\gamma_{kl} N^s_l.$$

Therefore the diagonal-element differences appearing in the resonance condition are

$$(N^s_{11}-N^s_{33})=\sum_l[\gamma_{1l}^2-\gamma_{3l}^2]N^s_l;\quad (N^s_{22}-N^s_{33})=\sum_l[\gamma_{2l}^2-\gamma_{3l}^2]N^s_l. \quad \ldots\ldots(23)$$

(ii) *Magnetocrystalline Anisotropy*: *Hexagonal Crystal* (cf. equation (9))

The above procedure for obtaining N^a_{jk} elements is not applicable to this case because $\mathbf{H}^i_c$ is here not a linear function of the I_j components. Instead, the $\mathbf{H}^i_c$ vector must be resolved directly in the primed system and the unprimed I_j components occurring in the resulting $(H^i_c)_j'$ field components expressed in terms of the I_j' components. A linear dependence of the $(H^i_c)_j'$ components upon I_k', as in equation (12), is then obtained by dropping terms containing powers of i_k' greater than unity. Such neglect is justified as long as $I_0 \gg i_k'$; this condition holds in practice. One obtains

$$\left.\begin{aligned}(N^c_{11}-N^c_{33})&=\frac{2}{I_0^2}[(K_1'+2K_2')(\gamma_{31}^2-\gamma_{11}^2)+2K_2'(3\gamma_{11}^2-\gamma_{31}^2)\gamma_{31}^2],\\(N^c_{22}-N^c_{33})&=\frac{2}{I_0^2}[(K_1'+2K_2')(\gamma_{31}^2-\gamma_{21}^2)+2K_2'(3\gamma_{21}^2-\gamma_{31}^2)\gamma_{31}^2],\end{aligned}\right\}\quad(24)$$

where I has been replaced by I_0.

(iii) *Magnetocrystalline Anisotropy*: *Cubic Crystal* (cf. equation (10))

To simplify the succeeding formulae, the following functions of the direction cosines are defined:

$$f_{jk}=\sum_l \gamma_{jl}^2\gamma_{kl}^2;\quad h_{l,m,n}=\gamma_{l1}\gamma_{m2}\gamma_{n3},$$

$$g_{l,m,n}=h_{l,m,n}[h_{l,m,n}+2\{h_{m,n,l}+h_{n,l,m}\}].$$

The desired demagnetization element differences obtained as in (ii) are then

$$\left.\begin{aligned}(N^c_{11}-N^c_{33})&=\frac{2}{I_0^2}[K_1(f_{33}-3f_{13})-K_2\{g_{3,3,3}-(g_{1,3,3}+g_{3,3,1}+g_{3,1,3})\}],\\(N^c_{22}-N^c_{33})&=\frac{2}{I_0^2}[K_1(f_{33}-3f_{23})-K_2\{g_{3,3,3}-(g_{2,3,3}+g_{3,3,2}+g_{3,2,3})\}].\end{aligned}\right\}\quad(25)$$

The terms in K_1 are in agreement with results obtained by Van Vleck (1950) from a quantum-mechanical treatment. General expressions for the second-order terms have not been given previously. As Van Vleck points out, it is noteworthy that the classical and quantum-mechanical treatments give exactly the same results, at least to first order.

(iv) *Strain* (cf. equation (11))

Define the following quantity in terms of the stress tensor elements referred to the unprimed crystal-axis coordinate system:

$$S_{jk}=\frac{3}{I^2}[(\lambda_{100}-\lambda_{111})\delta_{jk}+\lambda_{111}]P_{jk}.$$

Then the expression for the internal field contribution may be written

$$(H^i_{st})_j=\sum_k S_{jk}I_k.$$

Transforming the matrix $[S_{jk}]$ to the primed system, one obtains

$$N^{st}_{jk}=-\sum_l\sum_m \gamma_{jl}\gamma_{km}S_{lm}.$$

Therefore the general expressions for the strain demagnetization element differences are

$$(N^{st}_{11}-N^{st}_{33})=\sum_l\sum_m[\gamma_{3l}\gamma_{3m}-\gamma_{1l}\gamma_{1m}]S_{lm}\,;\quad (N^{st}_{22}-N^{st}_{33})=\sum_l\sum_m[\gamma_{3l}\gamma_{3m}-\gamma_{2l}\gamma_{2m}]S_{lm}. \qquad \ldots\ldots(26)$$

ACKNOWLEDGMENTS

It is a pleasure to acknowledge the helpful suggestions of Professor M. H. L. Pryce, Drs. J. H. E. Griffiths, C. Kittel and K. W. H. Stevens, and the referees. The author wishes further to thank the Rhodes Trustees for a Rhodes scholarship held during this investigation.

REFERENCES

Becker, R., and Doring, W., 1939, *Ferromagnetismus* (Berlin : Springer).
Bickford, L. R., Jr., 1950, *Phys. Rev.*, **78**, 449.
Birks, J. B., 1948, *Phys. Rev.*, **74**, 988.
Bloembergen, N., 1950, *Phys. Rev.*, **78**, 572.
Bozorth, R. M., 1949, *Physica*, **15**, 207.
Brown, W. F., 1940, *Phys. Rev.*, **58**, 736.
Griffiths, J. H. E., 1951, *Physica*, **17**, 253
Hewitt, W. H., Jr., 1948, *Phys. Rev.*, **73**, 1118.
Kip, A. F., and Arnold, R. D., 1949, *Phys. Rev.*, **75**, 1556.
Kittel, C., 1947, *Phys. Rev.*, **71**, 270 ; 1948, *Ibid.*, **73**, 155; 1949 a, *Ibid.*, **76**, 743; 1949 b, *Rev. Mod. Phys.*, **21**, 541.
Kittel, C., and Herring, C., 1950, *Phys. Rev.*, **77**, 725.
Kittel, C., Yager, W. A., and Merritt, F. R., 1949, *Physica*, **15**, 256.
Landau, L., and Lifshitz, E., 1935, *Phys. Z. Sowjet*, **8**, 153.
Lifshitz, E., 1944, *J. Phys. U.S.S.R.*, **8**, 337.
Lilley, B. A., 1950, *Phil. Mag.*, **41**, 792.
Macdonald, J. R., 1950, *D.Phil. Thesis* (Oxford); 1951 a, *Phys. Rev.*, **81**, 312; 1951 b, *Ibid.*, **81**, 329.
Osborn, J. A., 1945, *Phys. Rev.*, **67**, 351.
Polder, D., 1949, *Phil. Mag.*, **40**, 99.
Stoner, E. C., 1945, *Phil. Mag.*, **36**, 803.
Stoner, E. C., and Wohlfarth, E. P., 1948, *Phil. Trans. Roy. Soc.* A, **240**, 599.
Van Vleck, J. H., 1950, *Phys. Rev.*, **78**, 266.
Yager, W. A., Galt, J. K., Merritt, F. R., and Wood, E. A., 1950, *Phys. Rev.*, **80**, 744.

The Effect of the Mean Free Path of Electrons on the Electrical Properties of Non-Metals

By R. W. WRIGHT
Physics Department, University College, Ibadan, Nigeria

Communicated by J. P. Andrews; MS. received 8th January 1951, and in amended form 8th May 1951

ABSTRACT. The theories of the mean free path of electrons in various types of materials, under various conditions, are discussed. The conductivity, thermo-electric power, Hall coefficient, fractional change of conductivity in a magnetic field, and the Nernst, Ettinghausen and Righi–Leduc coefficients are all calculated upon the Lorentz–Sommerfeld theory for the various mean free path theories. The variations are discussed with particular respect to the changes of the reduced chemical potential η^*. The magnitude and sign of the coefficients are found to depend upon the mean free path theory assumed, that is, upon the type of material. In particular it is shown that the Ettinghausen and Nernst coefficients should be negligible in the majority of semiconductors with ionic lattices. Some of the assumptions usually made in semiconductor theory are shown to lead to erroneous conclusions. Experimental evidence is discussed and is found in general to support the theory given, both in impurity metals and semiconductors, except perhaps in the case of the thermo-electric power. No experimental results in non-metals are known for the thermo- and galvanomagnetic effects apart from the Hall coefficient, and it appears likely that such measurements will produce interesting information.

§1. INTRODUCTION

From the earliest days of the free-electron theory of conduction in solids the electrical properties and their temperature variations have been expressed in terms of two functions, namely the distribution function of the electrons in the solid, and the mean free path of the electrons. It is now accepted that the appropriate distribution function is the Fermi–Dirac, which under some conditions reduces to the simpler Maxwell–Boltzmann law. For the mean free path no universally applicable function has been obtained hitherto. On the contrary, the mean free path function differs according to the character of the solid (whether it possesses an atomic or an ionic lattice, for example), and according to the temperature and electron density. In the past the appropriate mean free path function has been by no means invariably used in discussions of experimental results, and assumptions of the mathematically simplest function have not infrequently resulted in an apparent failure to explain the experiments. Moreover this same avoidance of the correct procedure has led to theoretical results which, in the main, are approximations for the limiting cases of metals, or of materials containing so few conduction electrons that the Maxwell–Boltzmann statistics apply, leaving a wide gap into which many materials necessarily fall. The objects of this paper are to lay down a more general procedure employing the most appropriate mean free path function in all cases, and enabling intermediate substances to be considered. As a secondary objective, fuller consideration is given to the less familiar galvanomagnetic and thermomagnetic effects, from which valuable information is obtainable, but which have been much more neglected by the experimentalists. Therefore, in addition to conductivity,

thermo-electric and Hall effects as normally considered, we shall consider also the Nernst, Ettinghausen and Righi-Leduc effects, and finally the effect of change of resistance in a magnetic field. Since the theory of metals is already well understood, non-metals only will be considered here. Finally a comparison is made between the results predicted by the theory and those observed expe i-mentally. In order to do this, simple approximate formulae are obtained for the variation of the electrical properties with temperature, which are applicable over limited temperature ranges. The experimental results for many materials are found to be in good accord with the approximate formulae, and it seems likely that many more would be explained if the approximations were no longer used, and the full theoretical expressions compared with experiment.

§ 2. THE DISTRIBUTION FUNCTION AND DEGENERACY

It is necessary first to explain the manner in which the Fermi–Dirac distribution function will be employed. According to this function the concentration of free electrons n_f is given by

$$n_f = 4\pi h^{-3}(2m^* kT)^{3/2} F_{1/2}(\eta^*) \qquad \ldots\ldots(1)$$

where T is the absolute temperature, h and k are Planck's and Boltzmann's constants, m^* is the effective mass of the electron and $F_{1/2}(\eta^*)$ belongs to a group of functions defined by

$$F_m(\eta^*) = \int_0^\infty \frac{\eta^m \, d\eta}{1+\exp(\eta-\eta^*)}. \qquad \ldots\ldots(2)$$

In this definition $\eta = E/kT$ the 'reduced' energy of an electron, the value of E being the energy of the electron relative to the bottom of the conduction band. η^* is the reduced chemical potential, and its value is calculated by integrating the number of electrons in each energy state, and equating to the total number of electrons. The equation (1) may be regarded as expressing η^* in terms of the concentration n_f. In several important papers the reduced chemical potential η^* has already been used very effectively as a parameter indicative of the degree of degeneracy, and it will be so used here. It will be observed that η^* is independent of the mean free path but is dependent on the distribution of energy levels, and on the distribution of electrons in the energy bands. When the variation of η^* (and thus the degeneracy) with temperature is considered, non-metallic solids divide naturally into two groups: semiconductors in which the number of free electrons is zero at absolute temperature but increases as temperature rises, and impurity metals where the number of free electrons is a constant independent of temperature. In the first case it appears that η^* is large and negative at low temperatures, rising to a maximum as the temperature rises, and then decreasing again at still higher temperatures. In the second case η^* is large and positive at low temperatures, and decreases as the temperature rises. These two groups consist usually of substances in which the electrons are due to a non-stoichiometric excess of one component of the lattice, or to impurities.

In more detail, for impurity metals, since n_f is constant, and equal to the concentration of impurity centres, equation (1) expresses the variation of η^* with temperature. At low temperatures, or more precisely when $n_f h^3 \gg 4\pi(2m^* kT)^{3/2}$ and $\eta^* \gg 0$ we have

$$\eta^* = \left(\frac{3n_f}{8\pi}\right)^{2/3} \frac{h^2}{2mk} \frac{1}{T} \qquad \ldots\ldots(3)$$

showing that η^* is inversely proportional to the temperature. At high temperature, i.e. when $n_f h^3 \ll 4\pi (2m^* kT)^{3/2}$

$$\eta^* = \ln\left[\frac{n_f h^3}{2(2\pi m^* kT)^{3/2}}\right] \qquad \ldots\ldots(4)$$

showing that η^* varies but slowly with temperature, becoming large and negative as the temperature rises. At intermediate temperatures, however, the full expression (1) must generally be used.

In a semiconductor, however, the problem is more elaborate, as the number of free electrons varies with the temperature. Formula (1) still holds for the relation between n_f and η^*.

The equation for η^* is then :

$$n_b = 4\pi h^{-3}(2m^* kT)^{3/2}[1+\exp(\eta' + \eta^*)]\, F_{1/2}(\eta^*) \qquad \ldots\ldots(5)$$

where $\eta' = E'/kT$, and n_b is the concentration of impurity centres with energy levels a distance E' below the conduction band.

For low temperatures ($E' \gg kT$), then the following approximation will hold good :

$$\eta^* = -\tfrac{1}{2}\eta' + \tfrac{1}{2}\ln\left[\frac{n_b h^3}{2(2\pi m^* kT)^{3/2}}\right] \qquad \ldots\ldots(6)$$

which is such that η^* is inversely proportional to the temperature, and is large and negative. This is the case of the classical semiconductor.

As the temperature rises and kT becomes of the order of E' and greater, then the above approximation breaks down. The value of η^* increases from its large negative value inversely proportional to T whilst the approximation (equation (6)) holds good, then as it breaks down the value of η^* fails to increase so rapidly, reaches a maximum and begins to decrease again. Eventually, at sufficiently high temperatures, the situation will resemble that of the impurity metal at high temperatures since all the available free electrons will be free, and the value of η^* will decrease logarithmically with temperature as shown in equation (4).

§ 3. REVIEW OF MEAN FREE PATH THEORIES

In metals and substances with atomic lattices it has been shown (Wilson 1936), that if the energy E of an electron above the bottom of the conduction band is small, i.e. $E < kT$, then the mean free path is, to a first approximation, inversely proportional to the temperature, and independent of the energy E:

$$l = l_1/T \qquad \ldots\ldots(7)$$

where l_1 depends upon the constants of the lattice. Shifrin (1944) has shown that the presence of degeneracy which was assumed absent in Wilson's derivation, does not affect formula (7) to the first approximation. When the energy E of an electron is high, then its mean free path is given by (Wilson 1936)

$$l = l_2 T\eta^2 \qquad \ldots\ldots(8)$$

where $\eta = E/kT$, and is the reduced energy. This is the case which is applied to metals, and has of course been dealt with elsewhere in detail. The assumption is made that formula (8) may be applied to all the ' conduction ' electrons with reasonable approximation. The variation as predicted by formula (8) will not be discussed in this paper.

In an ionic lattice the mean free path is dependent upon whether the electron energy E above the bottom of the conduction band is greater or less than $h\nu$, the

energy of the characteristic vibrations of the lattice. For energies less than $h\nu$, Mott and Fröhlich (1939) and Davydov and Shmushkevitch (1940) have shown that

$$l = l_3\, e^{h\nu/kT} E^{1/2} = l_3 (kT)^{1/2}\, e^{h\nu/kT}\, \eta^{1/2} \qquad \ldots\ldots(9)$$

This formula will be applicable to the vast majority of electrons present in an ionic lattice if the temperature and concentration of free electrons are low, so that few electrons have high energies. Shifrin (1944) has suggested that this formula is only true when the concentration of free electrons is so small that classical statistics may be applied, and that the presence of degeneracy modifies the formula to the following:

$$l = l_3 (kT)^{1/2}\, e^{h\nu/kT}\, \eta^{1/2}(1-f) \qquad \ldots\ldots(10)$$

where $f = [1 + \exp(\eta - \eta^*)]^{-1}$ is the Fermi–Dirac function; and $\eta^* = E^*/kT$ is the reduced chemical potential. We shall see that this modification has very little effect upon the electrical properties of the material so long as $\eta^* < -4$. This is usually the case in 'classical' semiconductors with ionic lattices, and it is to this group of materials to which equation (9) may be considered applicable. Shifrin's modified, and more complicated, formula (10) whilst applicable to these materials need only be used when the degeneracy becomes appreciable, or $\eta^* > -4$. The modifications introduced by formula (10) are particularly important in connection with ionic latticed 'impurity metals'. These are materials which possess a constant concentration of free electrons in an 'impurity band' of permitted energy levels, due to the presence of foreign impurities or an excess of one constituent above stoichiometric proportion. At low temperatures the degeneracy in such materials is high, as in metals, and thus the factor $(1-f)$ has an appreciable effect. The application of formula (10) to ionic latticed impurity metals is restricted to cases where the concentration of free electrons is such that few have energies greater than $h\nu$.

For electron energies E greater than $h\nu$ the mean free path has been shown to be (Mott and Fröhlich 1939):

$$l = l_4 E/kT = l_4 \eta \qquad \ldots\ldots(11)$$

where l_4 is a constant for temperatures greater than the Debye temperature (Wright 1951). This equation may be applied to all ionic latticed semiconductors and impurity metals at high temperatures.

In certain cases equation (11) may be applied to all temperatures. If there is a high concentration of free electrons in the impurity band of an impurity metal, then at low temperatures the Fermi energy E^* will be large, viz. $E^* > h\nu$. Under these conditions all the effective 'conduction' electrons, i.e. those near the Fermi level, will have energies $E > h\nu$, and thus formula (11) may be used. Hence the use of equation (11) for all temperatures, for all the electrons, will result in a fair approximation.

Finally it may be pointed out that in the original theories of semiconductors the mean free path was assumed to be a constant, independent of temperature and energy:

$$l = l_5. \qquad \ldots\ldots(12)$$

Many conclusions derived from this assumption are extremely erroneous, as will be seen in the following discussion.

Summing up, we see that all the above expressions for the mean free path may be expressed in the form $l = l_0 f(\eta)$ where l_0 is independent of the energy E (i.e. η)

but is, in general, dependent upon the temperature, and $f(\eta)$ is a function of η only. The above results are collected in the Table.

In the following discussion the general form $l = l_0 f(\eta)$ will be used, both l_0 and $f(\eta)$ depending upon the actual material and conditions under consideration.

Material	Limits of application	Equation	l_0	$f(\eta)$
Classical case	—	(12)	l_5	1
Atomic latticed materials	Non-metals	(7)	l_1/T	1
Ionic latticed materials	Very high T	(11)	l_4	η
Ionic latticed semiconductors	Low T, low r_f	(9)	$l_3(kT)^{1/2}e^{h\nu/kT}$	$\eta^{1/2}$
Ionic latticed impurity metals	Low T, low r_f	(10)	$l_3(kT)^{1/2}e^{h\nu/kT}$	$\eta^{1/2}(1-f)$
Ionic latticed semiconductors	Low T, high r_f	(10)	$l_3(kT)^{1/2}e^{h\nu/kT}$	$\eta^{1/2}(1-f)$
Ionic latticed impurity metals	High r_f	(11)	l_4	η

§ 4. THE ELECTRICAL PROPERTIES

We are now in a position to write down expressions for the electrical properties calculated from the Lorentz–Sommerfeld theory in a generalized form suited to a discussion of the differences made by the different mean free path functions. These expressions are :

Electrical conductivity $\sigma = A\,16\pi m^* e^2 kT l_0/3h^3$ .....(13)

Thermo-electric power $\Theta = -B k/e$ .....(14)

Hall coefficient $R = -C/n_f e$ .....(15)

Fractional change of σ in a magnetic field H $d\sigma/\sigma = DH^2 e^2 l_0^2/2m^* kT$ .....(16)

Nernst coefficient $Q = E k l_0/(2m^* kT)^{1/2}$ .....(17)

Ettinghausen coefficient $P = 3F/2n_f k$ .....(18)

Righi–Leduc coefficient $S = -Gel_0/(2m^* kT)^{1/2}$ .....(19)

Where the letters $A, B \ldots\ldots G$ represent functions of the Fermi–Dirac functions $F_m(\eta^*)$. These functions differ according to which mean free path theory is used, and the various values are given in Appendix I. It must be remembered that l_0 is in general dependent upon the temperature.

The Nernst coefficient Q is defined by the equation $F_y = QH_z\, dT/dx$ where F_y is the electric field in the y direction, and the rest of the notation is as usual. The Ettinghausen coefficient P is defined similarly by $dT/dy = PH_z I_x$ where I_x is the current density in the x direction. The Righi–Leduc coefficient S is defined by $dT/dy = SH_z\, dT/dx$.

The majority of the expressions for the constants A, B and C have been derived before, but the expressions for D, E, F and G given in Appendix I are original, since these effects seem only to have been considered in the limiting cases of metals and the 'classical' case. The variations of the expressions A to G with η^* are shown in Figures 1 to 7. In each Figure there are four graphs: graph I shows the variation with η^* of the appropriate constant if the mean free path is assumed to vary as shown by equation (12) or equation (7); graph II if the mean free path is given by equation (9), graph III if by equation (10) and graph IV if by equation (11). The variations are shown with respect to the variations of η^*, because η^* is independent of the lattice structure and therefore of the mean free path. The manner of the

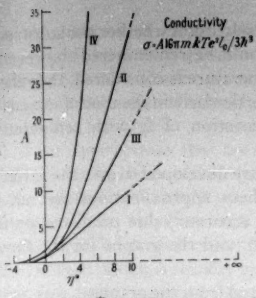

Figure 1.

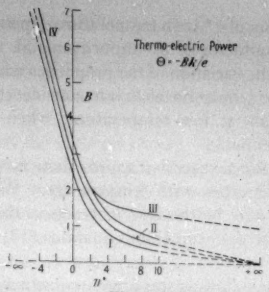

Figure 2.

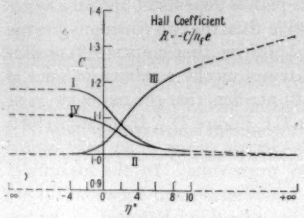

Figure 3.

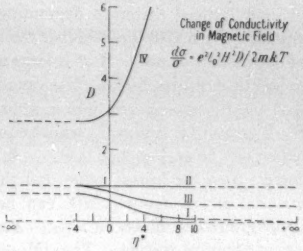

Figure 4.

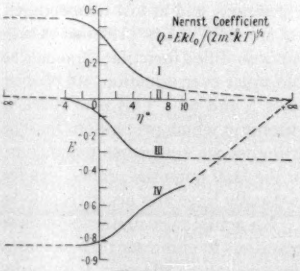

Figure 5.

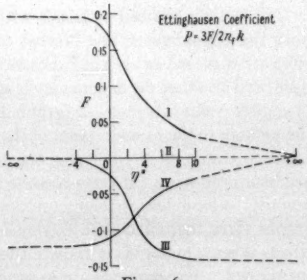

Figure 6.

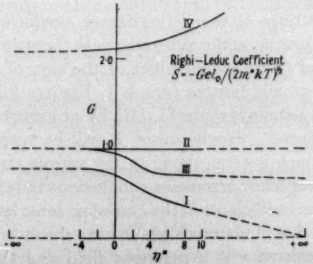

Figure 7.

Figures 1–7. Variations with η^* of the functions A–G of equations (13)–(19), as given by Appendix I.

variation of η^* with temperature depends entirely upon whether the substance is a semiconductor or an impurity metal. It should be remembered, however, that when the variation of the properties with temperature is considered, then the variation of l_0 must be taken into consideration, particularly in the case of ionic latticed materials at low temperature, when the variation of l_0 with temperature is exponential.

In the next section approximate formulae are developed to give the variation of the properties with temperature. Where these approximations are not valid, which may be the case in practice, then the accurate value predicted by theory must be deduced from equations (13) to (19), and the graphs for the functions *A–G*.

The following important points may be noted from the graphs:

(*a*) The variation of the thermo-electric power with η^* is completely different in ionic latticed materials depending upon whether the mean free path follows equation (9) or (10), i.e. whether the mean free path is dependent upon the degree of degeneracy or not. If η^* is large and negative then the two equations give rise to identical results, but as η^* becomes large and positive, then equation (9) predicts that the thermo-electric power approaches asymptotically a minimum value of $\Theta = 0$ (graph II, Figure 2) whilst equation (10) predicts that the minimum value which will be approached is $\Theta = -\boldsymbol{k}/\boldsymbol{e}$ (graph III, Figure 2). If equation (10) is correct then the lowest value that the thermo-electric power of an ionic latticed material at low temperature can have is 86 microvolts. In the majority of semiconductors, however, $\eta^* < -2$ and thus equation (9) and equation (10) give rise to identical results. The difference will be important, however, in the case of impurity metals at low temperature.

(*b*) In ionic latticed materials with low degeneracy, and at low temperatures, both the Ettinghausen and Nernst coefficients are zero. Any presence of such effects in these materials will indicate that Shifrin's modified formula (10) should be used, and also that the degeneracy is appreciable, since even equation (10) predicts negligible values if $\eta^* < -2$ (graph III, Figures 5 and 6). This is of practical importance in the measurement of the Hall constant in which precautions must be taken to eliminate any E. M. F.s due to the Ettinghausen transverse temperature gradient producing a thermo-electric E. M. F. in the Hall potential probes. In the majority of ionic latticed semiconductors η^* is usually large and negative, and the graphs show that effects are extremely small. No actual measurements of these effects in such materials is known, though precautions to eliminate them are often mentioned. Experiments are in progress to measure these effects in an impurity metal, CdO, where they should be appreciable.

(*c*) The actual directions of the Ettinghausen coefficient P and the Nernst coefficient Q are dependent upon the mean free path theory adopted. It should be noticed that both P and Q are independent of the sign of charge carried by the current carrier, yet in atomic lattices (graph I, Figures 5 and 6) the effects are positive, whilst in ionic lattices (graphs II, III, IV of Figures 5 and 6) coefficients, if appreciable, are negative. Furthermore, it will be seen that the assumption that l_0 is a constant, which is often made in the simple classical theory of semiconductors, leads to completely erroneous conclusions in respect of both the sign and the magnitude of the coefficients in the case of an ionic latticed material.

(*d*) It will be noted that in materials which are subject to equation (11), such as CdO, the change of resistance in a magnetic field and the Righi–Leduc effect should both be comparatively large.

(*e*) The thermodynamical relationship that $Q = KP/T$ (where K is the thermal conductivity of the electrons) is obeyed for all values of η^* and all the theories of the mean free path. The empirical relationship $RQ/PS = K/\sigma T$ is correct when η^* is large and the material is highly degenerate, as in a metal, where the relationship is found to be obeyed.

(*f*) If the assumptions that are made in the classical theory, viz. $\eta^* \ll 0$ and $l = l_3$, are taken, the above equations lead to the values for the electrical properties shown in Appendix II, which are the same as those which have been obtained previously. There are, however, no substances to which such simplifying assumptions can be considered applicable. It will be noted from Appendix II that $R = 3\pi/8n_f\mathbf{e}$, which is usually assumed for semiconductors, is deduced only if the mean free path is assumed constant. In the majority of semiconductors with ionic lattices it will be seen that $R = 1/n_f\mathbf{e}$ is more nearly correct.

§ 5. COMPARISON WITH EXPERIMENTAL RESULTS

(i) *Conductivity*

In atomic latticed materials such as silicon and germanium several investigations have been made of the variation of conductivity with temperature. Consider such a semiconductor with a small activation energy E' and number of impurity centres n_b. At all temperatures the mean free path is given by equation (7), and thus the expression for σ may be found as in Appendix I:

$$\sigma = \frac{16\pi m^* \boldsymbol{k} \mathbf{e}^2 l_1}{3\boldsymbol{h}^3} \ln(1 + \exp \eta^*) \qquad \ldots\ldots(20)$$

where it should be remembered that l_1 is independent of the temperature. At low temperatures η^* is large and negative, so that equation (6) may be used as an approximation for η^*, giving

$$\sigma = \frac{8n_b^{1/2}\mathbf{e}^2 l_1}{3(\boldsymbol{h}^2 T)^{3/4}} \left(\frac{\pi m^* \boldsymbol{k}}{2}\right)^{1/4} e^{-E'/2\boldsymbol{k}T} \qquad \ldots\ldots(21)$$

Thus $\ln \sigma$ is proportional to $1/T$ as is usually found in poorly conducting semiconductors. As the temperature increases, however, η^* increases beyond the limits where equation (6) is a good approximation, and eventually reaches a maximum, after which it decreases. Shifrin (1944) has shown by calculation that η^* decreases in such a way that $\ln(1 + \exp \eta^*)$ decreases linearly with temperature. The conductivity should therefore follow equation (21) at low temperatures, reach a maximum, and then decrease proportionally as T increases. Precisely this variation has been observed by Putley (1949) for Si and Ge†. At higher temperatures still, intrinsic conduction occurs and masks the impurity conduction. Pearson and Bardeen (1949) obtained results for silicon very similar to those of Putley's. They also showed that as the concentration of impurity increased, the material became an impurity metal, as was shown by the Hall coefficient (and thus the concentration of free electrons n_f) becoming independent of the temperature.

The conductivity in atomic latticed impurity metals is given by equation (20), but η^* varies with the temperature in the manner described in § 2. At low temperatures, when $\eta^* > 2$, we may use equation (3) so that

$$\sigma \simeq \frac{8\pi \mathbf{e}^2 l_1}{3\boldsymbol{h}} \left(\frac{3n_b}{8\pi}\right)^{2/3} \frac{1}{T} \qquad \ldots\ldots(22)$$

† Hutner, Rittner and du Pré (1950) have shown that the agreement is good except below 150° K. when the additional scattering due to the impurity centres (not considered here) must be considered to give good agreement.

At high temperatures, when $\eta^* < -2$, we may use equation (4) for η^* so that

$$\sigma \simeq \frac{4e^2 l_i n_b}{3(2\pi m^* k)^{1/2}} \frac{1}{T^{3/2}} \qquad \ldots\ldots(23)$$

Although some of Pearson and Bardeen's specimens became impurity metals when the concentration of impurities was sufficiently high, neither of the above variations with temperature was compared with those found experimentally, though such a type of variation seems to be indicated by the graphs given in their paper.

In ionic latticed semiconductors, the theory indicates that at low temperatures $\ln \sigma$ should be proportional to $1/T$, as in the usual semiconductor theory :

$$\sigma = (2\pi kT)^{3/4} m^{*1/4} n^{1/2} e^2 l_3 h^{-3/2} \exp(2h\nu - E')/2kT \qquad \ldots\ldots(24)$$

Such a variation has been observed in the majority of poorly conducting semiconductors, and was, at one time, considered to be a test of whether a material was a semiconductor. It should be noted that in equation (24) the variation of the mean free path with temperature has been allowed for, and the slope of the graph of $\ln \sigma$ against $1/T$ should be $(2h\nu - E')/2k$, and not, as is often assumed $-E'/2k$. Usually, however, $2h\nu \ll E'$. When η^* increases and approaches zero, then the approximation given by equation (6) breaks down, and equation (24) is no longer applicable. Such a change has been noticed by Busch and Labhardt (1946) in SiC. The graph of $\ln \sigma$ against $1/T$ is no longer a straight line. They found that use of the accurate expression for the conductivity (see Appendix I) was in good agreement with the theory. When η^* increases and reaches its maximum, then at higher temperatures η^*, and thus $F_{1/2}(\eta^*)$ and n_f, will no longer vary rapidly with temperature. Shifrin (1944) has shown that for many specimens n_f should vary roughly proportionally to T. In this case the variation of the conductivity will be mainly controlled by the exponential term in the mean free path, and so the conductivity should decrease exponentially as the temperature rises. No simple analytical expression can be obtained. Such a variation of conductivity with temperature has been observed in several materials, but is capable of a different explanation, and such results will be discussed later.

In an ionic latticed impurity metal, we may consider first the case in which there are sufficient free electrons, such that equation (11) is valid at all temperatures. In this case Appendix I tells us that

$$\sigma = \frac{16\pi m^* e^2 l_4 k}{3h^3} TF_1(\eta^*). \qquad \ldots\ldots(25)$$

At low temperatures, when $\eta^* > 2$, this approximates to

$$\sigma = \frac{3^{1/3} e^2 h n_b^{4/3}}{4m^* k \pi^{1/3}} \frac{l_4}{T}. \qquad \ldots\ldots(26)$$

The variation of conductivity with T predicted by this equation, has been found to hold very well in the case of specimens of CdO (Wright 1951). It should be noted, however, that at temperatures less than the Debye temperatures, l_4 is no longer independent of the temperature, and the conductivity should approach a uniform maximum value as T decreases to zero. At high temperatures when $\eta^* < -2$, then equation (25) approximates to

$$\sigma = \frac{8e^2 l_4 n_b}{3(2\pi m^* k)^{1/2}} \frac{1}{T^{1/2}}. \qquad \ldots\ldots(27)$$

The second type of ionic latticed impurity metal is that in which the concentration of free electrons is sufficiently small that the vast majority of free electrons has energies less than $h\nu$, and thus equation (10), for the mean free path, is valid. It is not quite certain whether this type exists since the concentration of impurity centres, and thus free electrons, must be large for the material to become an impurity metal. The conductivity of such materials, if they exist, is given at low temperatures when $\eta^* > 2$ by

$$\sigma = \frac{n_b e^2 l_3}{2^{3/2} m^{1/2}} e^{h\nu/kT}. \qquad \ldots\ldots(28)$$

The conductivity should therefore increase logarithmically as $1/T$. At high temperatures the conductivity should vary as equation (27), as should all ionic latticed materials at very high temperatures.

Interesting experimental results have been obtained using specimens of PbS by Devajatkova, Maslakovec and Sominskij (1941), with specimens of PbSe by Bauer (1940), with specimens of PbTe by Putley (private communication), and with specimens of V_2O_3 by Foëx (1949), which have not been fully explained theoretically. For the curves given for the resistivity of PbS against temperature, there appears a definite indication of a variation in agreement with equation (26) as a highly conductive impurity metal. Shifrin has suggested that the conductivity is proportional to $\exp(h\nu/kT)$, and thus indicates either a highly conductive semiconductor or an impurity metal as in equation (28). It is difficult from the graphs given in the paper to decide between the two variations. Unfortunately, no measurements of the Hall constant were made, which would have instantly distinguished between a semiconductor and an impurity metal. In PbSe, also, the conductivity appears to increase in proportion to $\exp(h\nu/kT)$ and is therefore following equation (28) as an impurity metal, or is acting as a highly conductive semiconductor. Similarly in V_2O_3 the conductivity increases exponentially at low temperatures as expected of semiconductors, reaches a maximum, and then decreases such that a graph of $\ln\sigma$ against $1/T$ is a straight line. In PbTe the conductivity is also found to be proportional to $\exp(h\nu/kT)$, in this case for both excess and defect conduction, in the region of temperature where the Hall constant is practically independent of temperature. The conductivity is therefore represented by equation (28). In both V_2O_3 and PbTe it seems likely that the material is a semiconductor, and the conductivity follows equation (28) when the majority of the impurity centres are ionized.

(ii) *Thermo-electric Power*

In general the results for the thermo-electric power have agreed less with theory than the other electrical properties investigated. This may be due to the fact that the theory of the thermo-electric power contains many over-simplifying assumptions.

In atomic latticed semiconductors the theory predicts that

$$\Theta = -\frac{k}{e}\left[\frac{2F_1(\eta^*)}{F_0(\eta^*)} - \eta^*\right]. \qquad \ldots\ldots(29)$$

When the temperature is low, then equation (6) is applicable, and $F_1 = F_0$,

so

$$\Theta = -\frac{k}{e}\left[2 + \frac{E'}{2kT} - \tfrac{1}{2}\ln\left\{\frac{n_b h^3}{2(2\pi m^* kT)^{3/2}}\right\}\right]. \qquad \ldots\ldots(30)$$

This is the type of variation which was considered typical of a semiconductor, but there are but few atomic latticed semiconductors, and none seem to obey this type of equation. As the temperature rises so η^* increases and eventually reaches its maximum, and then starts to decrease again; so the thermo-electric power should decrease in proportion to $1/T$ at low temperatures, and at higher temperatures reach a minimum, and finally increase in proportion to $\ln T$. Putley's measurements (1948) on silicon and germanium found that the thermo-electric power increased rapidly with temperature, over part of its range roughly proportional to temperature, thus contradicting the above theory.

Atomic latticed impurity metals should obey equation (29) and at low temperatures we may approximate for η^* by equation (3) when $\eta^* > 2$

$$\Theta = -\frac{k}{e}\frac{\pi^2}{3}\left(\frac{8\pi}{3n_b}\right)^{2/3}\frac{2mk}{h^2}T. \qquad \ldots\ldots(31)$$

The thermo-electric power should therefore be proportional to the temperature. This is more in accord with results found for specimens of silicon and germanium by Putley, but these specimens, as far as conductivity is concerned, acted as semiconductors. At high temperatures when $\eta^* < -2$ the variation with temperature should be the same as that predicted for semiconductors, i.e. proportional to $\ln T$.

In ionic latticed semiconductors at low temperatures, the thermo-electric power is the same as equation (30), except that the constant 2 in the parentheses should be changed to 5/2. The thermo-electric power should therefore be inversely proportional to temperature. This type of relation is found in many good insulating semiconductors. In NiO (Wright and Andrews 1949) the numerical values which may be deduced from the graph of Θ against $1/T$ were found to be in good relation with those deduced from both conductivity and Hall coefficient measurements. As the temperature rises, so η^* increases to its maximum, and then decreases; but for values of η^* in the region of zero then the only accurate formula is the full one

$$\Theta = -\frac{k}{e}\left(\frac{5}{3}\frac{F_{3/2}(\eta^*)}{F_{1/2}(\eta^*)} - \eta^*\right). \qquad \ldots\ldots(32)$$

The thermo-electric power should therefore decrease to a minimum and then increase, and eventually, at sufficiently high temperatures, become proportional to $\ln T$.

Impurity metals, with an ionic lattice and a high concentration of free electrons so that equation (11) applies to all temperatures, have at low temperatures when $\eta^* > 2$

$$\Theta = -\frac{k}{e}\frac{2\pi^2}{3}\left(\frac{8\pi}{3n_b}\right)^{2/3}\frac{2mk}{h^2}T. \qquad \ldots\ldots(33)$$

Such a variation has been found definitely to exist in specimens of CdO which acted as impurity metals.

A similar type of variation has been observed by Busch, Lundt and Spodlin (1941) in SiC, but whether the material acted as an impurity metal in other respects is not known. At high temperatures, $\eta^* < -2$, then

$$\Theta = -\frac{k}{e}\left[3 - \ln\left(\frac{n_b h^3}{2(2\pi m^* kT)^{3/2}}\right)\right], \qquad \ldots\ldots(34)$$

so that as the temperature increases, the rate of increase of Θ with temperature decreases until it is proportional to $\ln T$. If the concentration of the free electrons in the impurity metal is low, we have at low temperatures

$$\Theta = -\frac{k}{e}\left[1+\left(\frac{8\pi}{3n_h}\right)^{2/3}\frac{mk}{h^2}\left(\pi^2+\frac{9}{2}\right)T\right]. \qquad \ldots\ldots(35)$$

This formula indicates only a slow variation with temperature. At high temperatures such a material would follow equation (34). Considering the case of the experimental values obtained by Devajatokowa, Maslakovitz and Sominiskii (1941) on PbS, they obtained values which seem at low temperatures to be proportional to the temperature, but whether according to equation (35) or equation (33), depends upon the specimen. Both types of variations do seem to be present. At high temperatures there are indications that Θ is proportional to $\ln T$. These observations would indicate that the specimens of PbS used were impurity metals, and this agrees with some of the deductions based upon the variation of the conductivity with temperature.

(iii) *The Hall Coefficient*

The function C in equation (15) is seen in Figure 3 to vary between unity and 1·33 for all types of materials and all temperatures. Variations of C with temperature is therefore very slow, and C may usually be taken as a constant, so that the variation of the Hall coefficient with temperature is purely dependent upon the variation of the concentration of free electrons. In semiconductors at low temperatures, then, $\ln R$ should be proportional to $1/T$, and this has been observed in many semiconductors. As the temperature increases this simple variation should disappear and only the accurate formula suffices (Busch and Labhardt (1946) found this to be the case in SiC). At higher temperatures, R should decrease linearly with temperature, and finally approach a minimum constant value. In impurity metals the concentration of free electrons is independent of temperature; thus so is the Hall coefficient. Several substances have recently been found to illustrate this type of material, such as some specimens of Si, PbSe, PbTe and CdO. The invariance of the Hall coefficient with temperature is a sure indication of an impurity metal.

(iv) *Change of Resistance in a Magnetic Field*

Very little experimental work has been done on this phenomenon. It will be seen from Figure 4 that except for material for which $\eta^* > 0$ the variation of D with η^* is of little consequence. Thus in the case of semiconductors D may be considered a constant, and the variation with temperature will depend entirely upon the remainder of equation (16). It will be seen that investigations of this effect will therefore give direct information upon the variation of the mean free path with temperature. Putley (private communication) has shown by observations at one temperature on PbTe that $d\sigma/\sigma$ is proportional to H^2, and that the fractional change of Hall coefficient with magnetic field dR/R is also proportional to H^2. Recently Estermann and Föner (1950) have measured $d\sigma/\sigma$ for specimens of germanium, and their results are in reasonable accord with theory. The only other results are those of Kapitza (1929) on much more impure specimens of germanium, which gave much smaller values for $d\sigma/\sigma$. This is to be expected,

since the degeneracy is much higher, and thus, as will be seen from graph I, Figure 4, the value of D should be much less.

For impurity metals η^* may be greater than zero and the variations of D must be taken into account. For atomic latticed materials at low temperatures

$$\frac{d\sigma}{\sigma} = \left(\frac{8\pi}{3n_b}\right)^{2/3} \frac{e^2 l_1^2 H^2}{h^2} \frac{1}{T^2}, \qquad \ldots\ldots(36)$$

whilst at high temperatures

$$\frac{d\sigma}{\sigma} = \frac{\pi}{4} \frac{e^2 l_1^2 H^2}{2mk} \frac{1}{T^3}. \qquad \ldots\ldots(37)$$

In ionic latticed impurity metals with a high concentration of free electrons, at low temperatures $\eta^* > 2$

$$\frac{d\sigma}{\sigma} = \left(\frac{3n_b}{8\pi}\right)^{2/3} \left(\frac{el_4 hH}{2mk}\right)^2 \frac{1}{T^2}, \qquad \ldots\ldots(38)$$

whilst at high temperatures $\eta^* < -2$

$$\frac{d\sigma}{\sigma} = \frac{225}{256} \frac{\pi e^2 l_4^2 H^2}{2mk} \frac{1}{T}. \qquad \ldots\ldots(39)$$

If the material has but comparatively few free electrons, and is still an impurity metal, then at low temperatures

$$\frac{d\sigma}{\sigma} = \frac{2e^2 l_3^2 H^2}{9m} e^{2h\nu/kT}, \qquad \ldots\ldots(40)$$

whilst at high temperatures all ionic materials will obey equation (39). No experimental results have been obtained to compare with the predictions made above.

(v) *The Nernst, Ettinghausen and Righi–Leduc Coefficients*

No measurements of these coefficients have been made upon materials other than metals. The assumptions made in the theory appear to be as far-reaching as those made in the theory of the thermo-electric power, where experiment does not agree very well with theory. It would therefore appear that experimental investigation may lead to a further understanding of the deficiences of the theory, and thus give rise to a more adequate theory. In this section we shall discuss the manner in which the present theory predicts that the effects should vary with temperature.

In semiconductors with an ionic lattice, it has already been pointed out that both the Ettinghausen and Nernst coefficients should be negligible unless the specimens are very degenerate. In semiconductors with an atomic lattice,

$$Q = \frac{\pi^{1/2}}{4} \frac{kl_1}{(2mk)^{1/2}} \frac{1}{T^{3/2}} \qquad \ldots\ldots(41) \qquad \text{and} \qquad P = \frac{3\pi}{32 n_i k}, \qquad \ldots\ldots(42)$$

so long as η^* is negative, which is the usual case.

In an impurity metal with an atomic lattice, at low temperatures with $\eta^* > 2$, the Nernst coefficient Q is independent of temperature, and inversely proportional to the concentration of impurity electrons, whilst the Ettinghausen coefficient is given by

$$P = \left(\frac{8\pi}{3}\right)^{2/3} \frac{m}{h^2 n_b^{5/3}} T. \qquad \ldots\ldots(43)$$

At high temperatures the variations are those predicted by equations (41) and (42). If the impurity metal has an ionic lattice with a large number of free electrons, then at low temperatures the Nernst coefficient is again independent of temperature, and as the temperature rises and η^* becomes less than -2

$$Q = \frac{15\boldsymbol{k}l_4\pi^{1/2}}{32(2m^*\boldsymbol{k}T)^{1/2}}. \qquad \ldots\ldots(44)$$

At low temperatures, the Ettinghausen coefficient P is given by equation (43) but with a negative sign. As the temperature rises P approaches a constant negative value. If, however, there are but few impurity electrons in the impurity metal, then at low temperatures

$$Q = -\frac{kl_3}{3(2m^*)^{1/2}} e^{h\nu/kT}, \qquad \ldots\ldots(45)$$

and as the temperature rises the value of Q will gradually approach to zero. The Ettinghausen effect is constant at low temperatures when $\eta^* > 2$, but reduces to zero when the temperature has risen such that $\eta^* < -2$.

The Righi–Leduc coefficient S in atomic semiconductors is

$$S = \frac{-7\pi^{1/2}l_1\boldsymbol{e}}{16(2m^*\boldsymbol{k})^{1/2}} \frac{1}{T^{3/2}} \qquad \ldots\ldots(46)$$

whilst in ionic latticed semiconductors

$$S = -\frac{l_3\boldsymbol{e}}{(2m^*)^{1/2}} e^{h\nu/kT}. \qquad \ldots\ldots(47)$$

In an atomic latticed impurity metal at high temperatures equation (46) would hold, but at low temperatures, with $\eta^* > 2$,

$$S = -\frac{l_1\boldsymbol{e}}{\boldsymbol{h}}\left(\frac{8\pi}{3n_b}\right)^{1/3} \frac{1}{T}. \qquad \ldots\ldots(48)$$

In an ionic latticed material with a high concentration of free electrons, at low temperatures $\eta^* > 2$

$$S = -\left(\frac{3n_b}{8\pi}\right)^{1/3} \frac{l_4\boldsymbol{e}\boldsymbol{h}}{2m^*\boldsymbol{k}T} \qquad \ldots\ldots(49)$$

whilst at high temperatures $\eta^* < -2$ and

$$S = -\frac{75}{64} \frac{\pi^{1/2}l_4\boldsymbol{e}}{(2m^*\boldsymbol{k}T)^{1/2}}. \qquad \ldots\ldots(50)$$

If the material has a low concentration of free electrons, then at high temperatures $\eta^* < -2$ and equation (47) will hold, whilst at low temperatures S will have one-third the value given by equation (47).

(vi) *Conclusions*

In this section we have attempted to compare the theoretically predicted variations with temperature of the phenomena with those found experimentally. It has only been possible to do this by deriving approximate formulae for the electrical properties which only apply over specific temperature ranges. The accurate formulae, given in Appendix I, must be directly compared with experimental results, as Putley (1949) did with Si and Ge, before it can be decided that the formulae do not explain the observed variations in any particular case.

APPENDIX I

Expressions for the Electrical Phenomena when $l = l_0\eta^r$

In monatomic lattices with low concentration of free electrons equation (1) is applicable, and $l_0 = l_1/T$ and $r = 0$.

In 'classical' semiconductors with ionic lattices ('classical' semiconductors being taken as those in which $\eta^* \ll 0$), $l_0 = l_3(\boldsymbol{k}T)^{1/2}e^{h\nu/\boldsymbol{k}T}$ and $r = \frac{1}{2}$.

In ionic latticed materials at very high temperatures, and in impurity metals with a high concentration of free electrons at all temperatures, $l_0 = l_4$ and $r = 1$.

In the following F_m is written to indicate $F_m(\eta^*)$.

$$\sigma = \frac{16\pi m^*\boldsymbol{e}^2\boldsymbol{k}Tl_0}{3\boldsymbol{h}^3}(r+1)F_r, \qquad \Theta = -\frac{\boldsymbol{k}}{\boldsymbol{e}}\left[\frac{(2+r)}{(1+r)}\frac{F_{r+1}}{F_r} - \eta^*\right],$$

$$R = -\frac{1}{n_i\boldsymbol{e}}\frac{3}{2}\frac{(2r+\frac{1}{2})}{(r+1)^2}\frac{F_{1/2}F_{2r-1/2}}{F_r^2}, \qquad \frac{d\sigma}{\sigma} = \frac{\boldsymbol{e}^2l_0^2}{2m^*\boldsymbol{k}T}H^2\left[\frac{(2r+\frac{1}{2})F_{2r-1/2}}{(r+1)F_r}\right]^2,$$

$$Q = \frac{\boldsymbol{k}l_0}{(2m^*\boldsymbol{k}T)^{1/2}}\left[\frac{(r+2)(2r+\frac{1}{2})F_{r+1}F_{2r-1/2} - (2r+\frac{3}{2})(r+1)F_rF_{2r+1/2}}{(r+1)^2F_r^2}\right],$$

$$P = \frac{3}{2n_i\boldsymbol{k}}\frac{F_{1/2}}{(r+1)F_r}\left[\frac{(r+1)(2r+\frac{3}{2})F_rF_{2r+1/2} - (r+2)(2r+\frac{1}{2})F_{r+1}F_{2r-1/2}}{(r+2)^2F_{r+1}^2 - (r+3)(r+1)F_{r+2}F_r}\right],$$

$$S = -\frac{l_0\boldsymbol{e}}{(2m^*\boldsymbol{k}T)^{1/2}} \times$$

$$\left[\frac{2(r+1)(r+2)(2r+\frac{3}{2})F_rF_{r+1}F_{2r+1/2} - (r+1)^2(2r+\frac{5}{2})F_r^2F_{2r+3/2} - (r+2)^2(2r+\frac{1}{2})F_{r+1}^2F_{2r-1/2}}{(r+1)F_r\{(r+2)^2F_{r+1}^2 - (r+1)(r+3)F_rF_{r+2}\}}\right].$$

These relations are all deduced upon the assumption of relatively small magnetic fields.

In the case of ionic latticed materials at low temperatures and low concentrations of free electrons equation (4) may be applied. The electrical properties may be obtained from the above equations by setting $l_0 = l_3(\boldsymbol{k}T)^{1/2}e^{h\nu/\boldsymbol{k}T}$ and making the following substitutions

$$(r+1)F_r = \tfrac{3}{4}(F_{1/2} + \tfrac{1}{2}F_{1/2}) \qquad (2r+\tfrac{1}{2})F_{2r-1/2} = \tfrac{1}{2}F_{1/2} + \tfrac{3}{8}F_{-1/2} - \tfrac{1}{12}F_{-3/2}$$

$$(r+2)F_r = \tfrac{5}{4}(F_{3/2} + \tfrac{3}{2}F_{1/2}) \qquad (2r+\tfrac{3}{2})F_{2r+1/2} = \tfrac{5}{6}F_{3/2} + \tfrac{15}{8}F_{1/2} + \tfrac{5}{10}F_{-1/2}$$

$$(r+3)F_r = \tfrac{7}{4}(F_{5\,2} + \tfrac{5}{2}F_{3/2}) \qquad (2r+\tfrac{5}{2})F_{2r+3/2} = \tfrac{7}{8}F_{5/2} + \tfrac{35}{8}F_{3/2} + \tfrac{35}{16}F_{1/2}$$

APPENDIX II

The various values taken by the functions $A - G$ when η^* is large and negative are shown in the Table.

l	A	B	C	D	E	F	G
l_0	e^{η^*}	$2-\eta^*$	$3\pi/8$	$\pi/4$	$\pi^{1/2}/4$	$\pi/16$	$+\frac{7}{16}\pi^{1/2}$
$l_0\eta^{1/2}$ $l_0\eta^{1/2}(1-f)$	$\frac{3}{4}\pi^{1/2}e^{\eta^*}$	$\frac{5}{2}-\eta^*$	1·00	1·00	0	0	+1·00
$l_0\eta$	$2e^{\eta^*}$	$3-\eta^*$	$\frac{45\pi}{128}$	$\frac{225\pi}{256}$	$-\frac{15}{32}\pi^{1/2}$	$-\frac{5\pi}{128}$	$+\frac{75}{64}\pi^{1/2}$

All the formulae when $l = l_0$ agree with those predicted by the classical theory of semiconductors.

ACKNOWLEDGMENT

The author wishes to thank Professor J. P. Andrews for his help during discussions and in preparation of this paper.

REFERENCES

BAUER, K., 1940, *Ann. Phys., Lpz.*, **38**, 84.
BUSCH, G., and LABHARDT, H., 1946, *Helv. phys. Acta*, **19**, 463.
BUSCH, G., SCHMIDT, P., and SPÖDLIN, R., 1947, *Helv. phys. Acta*, **20**, 461.
DAVYDOV, B., and SHMUSHKEVITCH, I., 1940, *J. Phys. U.S.S.R.*, **3**, 359.
DEVAJATKOVA, E. D., MASLAKOVEC, J. P., and SOMINSKIJ, M. S., 1941, *Bull. Acad. Sci., U.S.S.R.*, **5**, 409.
ESTERMANN, I., and FÖNER, A., 1950, *Phys. Rev.*, **79**, 365.
FOËX, M., 1949, *C.R. Acad. Sci., Paris*, **229**, 880.
HUTNER, K. A., RITTNER, E. S., and DU PRÉ, E. K., 1950, *Phillips Res. Rep.*, **5**, 188.
KAPITZA, P., 1929, *Proc. Roy. Soc.* A, **123**, 292.
MOTT, N. F., and FRÖHLICH, H., 1939, *Proc. Roy. Soc.* A, **171**, 496.
PEARSON, G. L., and BARDEEN, J., 1949, *Phys. Rev.*, **75**, 865.
PUTLEY, E. H., 1948, *Thesis*, London, 1949, *Proc. Phys. Soc.* A, **62**, 284.
SHIFRIN, K., 1944, *J. Phys. U.S.S.R.*, **8**, 242.
WILSON, A. H., 1936, *Theory of Metals* (Cambridge : University Press).
WRIGHT, R. W., 1951, *Proc. Phys. Soc.* A, **64**, 350.
WRIGHT, R. W., and ANDREWS, J. P., 1949, *Proc. Phys. Soc.* A, **62**, 446.

The Magnetic g-Factors of a Nucleon

BY C. CANDLER
Canynge Hall, University of Bristol

MS. received 30*th August* 1950, *and in final form* 13*th July* 1951

ABSTRACT. The nuclear magnetic moment is a two-valued function of the spin, and Schmidt's argument is used in reverse to induce the orbital and spin g-factors. g_l is shown to be unity in odd-proton and zero in odd-neutron nuclei, as theory has assumed, but g_s varies from nucleus to nucleus with a mean value about half that found in the free proton or neutron. The magnetic spin ratio G, defined as $g_s/g(\mathrm{p})$ in odd-proton and as $g_s/g(\mathrm{n})$ in odd-neutron nuclei, measures the approach of an empirical moment to a Schmidt line; it is shown to obey much the same rules in odd-proton and odd-neutron nuclei.

§1. ORBITAL AND SPIN g-FACTORS

A PLOT of the magnetic moment against the spin in either odd-proton or odd-neutron nuclei shows that all moments lie near to one of two lines, which are roughly parallel (Latham 1947). In odd-proton nuclei the magnetic moment increases with the spin (Figure 1), while in odd-neutron nuclei it is nearly constant (Figure 2) (nuclei lighter than $A=20$ are excluded). The two lines are explained if both spin and magnetic moment are due to a single odd nucleon, which can only exist in a π-state with **l** and **s** parallel, or in an α-state with **l** and **s** anti-parallel. In developing this thesis Schmidt (1937) assumed that the g-factors of orbit and spin are those found in the free proton and neutron, but his lines are too far apart, and with many accurate magnetic moments available, the argument is better reversed.

When two vectors **l** and **s** combine to a resultant **I**, the magnetic splitting factor g_I is obtained from g_l and g_s by the equation

$$g_I = \frac{I(I+1)+l(l+1)-s(s+1)}{2I(I+1)} g_l + \frac{I(I+1)+s(s+1)-l(l+1)}{2I(I+1)} g_s. \quad \ldots\ldots(1)$$

When **l** and **s** are parallel, write $l=(I-\frac{1}{2})$ and the magnetic moment $\mu(\pi)$, so that

$$2\mu(\pi) = (2I-1)g_l + g_s, \quad \ldots\ldots(2)$$

while when **l** and **s** are anti-parallel, write $l=(I+\frac{1}{2})$ and the magnetic moment $\mu(\alpha)$, and obtain

$$-2\mu(\alpha)(I+1)/I = -(2I+3)g_l + g_s. \quad \ldots\ldots(3)$$

Each equation is linear in the unknowns g_l and g_s, so that the latter can be obtained from each separately by inserting the mean empirical magnetic moments for a series of spin values. In the form here given the lines have the same slope g_l and the same intercept g_s, provided that $2\mu(\pi)$ is plotted against $(2I-1)$ when **l** and **s** are parallel, and $-2\mu(\alpha)\,(I+1)/I$ against $-(2I+3)$, when they are anti-parallel (Figure 3).

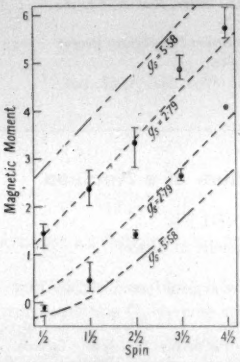

Figure 1. The magnetic moments of odd-proton nuclei measured in nuclear magnetons. The broken curves show the values predicted for two values of g_s, the outer pair being the Schmidt lines.

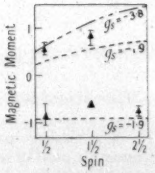

Figure 2. The magnetic moments of odd-neutron nuclei measured in nuclear magnetons.

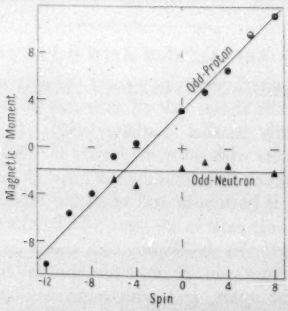

Figure 3. The magnetic moment as a function of the spin in odd-proton and odd-neutron nuclei. The ordinate is $2\mu(\pi)$ when **l** and **s** are parallel, and $-2\,\mu(\alpha)\,(I+1)/I$ when they are anti-parallel. The corresponding abscissa are $2I-1)$ and $-(2I+3)$.

The line obtained for odd-proton nuclei shows conclusively that the slope g_l is unity, as theory (Bohr 1951) requires, while the intercept g_s is not 5·58, but about half this value. In odd-neutron nuclei the points are less consistent, but theory argues strongly that g_l shall be zero and this gives as good a fit as any other value. The mean value of g_s is about $-1{\cdot}95$ or half that found in the free neutron.

This conclusion might have been reached by a simpler if less conclusive argument, for the direction of the Schmidt lines is determined by g_l and their distance apart by g_s. As the empirical lines are parallel to those predicted, but nearer together, the value of g_l postulated by Schmidt is correct, but his value of g_s is too large.

§2. THE MAGNETIC SPIN RATIO

When the magnetic orbital factor is taken as unity in odd-proton and zero in odd-neutron nuclei, an empirical magnetic moment determines the magnetic spin factor g_s, provided one knows whether **l** and **s** are parallel or anti-parallel. In odd-neutron nuclei the distinction is between negative in π-nuclei and positive in α-nuclei. In odd-proton nuclei magnetic moments between $(I-\frac{1}{2})$ and $I(I+1\frac{1}{2})/(I+1)$ are ambiguous, but only three stable nuclei have been found in this range, and of these ^{127}I and ^{209}Bi are so near one limit that the correct assignment is hardly open to doubt. The third ^{75}As is not well established.

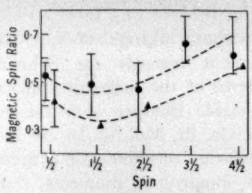

Figure 4.

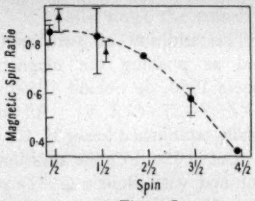

Figure 5.

Figure 4. The magnetic spin ratio of π-nuclei. The circles and triangles show the mean values of the ratio for all known odd-proton and odd-neutron nuclei respectively. The curves are intended only to show the general trend of the values.

Figure 5. The magnetic spin ratio of α-nuclei.

The more nearly the empirical g_s approaches the values $g(\mathrm{p})=5{\cdot}58$ and $g(\mathrm{n})=-3{\cdot}83$ found in the free proton and neutron, the nearer the magnetic moment lies to one of the Schmidt lines, so introduce the magnetic spin ratio G, and define it as $g_s/g(\mathrm{p})$ in odd-proton and $g_s/g(\mathrm{n})$ in odd-neutron nuclei. G may be derived from the empirical moment using equations (2) and (3), or explicitly

$$\left.\begin{array}{lll} Z \text{ odd.} & \pi\text{-state} & G\mu(\mathrm{p})=\mu(\mathrm{P},\pi)-(I-\frac{1}{2}) \\ & \alpha\text{-state} & G\mu(\mathrm{p})=I+1\frac{1}{2}-(1+1/I)\mu(\mathrm{P},\alpha) \\ N \text{ odd.} & \pi\text{-state} & G\mu(\mathrm{n})=\mu(\mathrm{N},\pi) \\ & \alpha\text{-state} & G\mu(\mathrm{n})=-(1+1/I)\mu(\mathrm{N},\alpha). \end{array}\right\} \quad \ldots\ldots(4)$$

The magnetic spin ratio G is convenient, because it often obeys the same rules in odd-proton and odd-neutron nuclei and lends itself to a concise statement of certain empirical rules.

(i) Among stable nuclei with A greater than 20 the range of G is 0·29 in ^{127}I to 0·94 in ^{197}Au in odd-proton nuclei, and the range is almost the same in odd-neutron nuclei, 0·31 in ^{113}Cd to 0·95 in ^{195}Pt.

(ii) The mean values of G for all nuclei of the same spin and type are plotted in Figures 4 and 5. In π-nuclei G is nearly independent of the spin, ranging round values of 0·52 in odd-proton and 0·42 in odd-neutron nuclei. In α-nuclei on the other hand G falls continuously from 0·9 when the spin is $\frac{1}{2}$ to less than 0·5 when the spin is $4\frac{1}{2}$.

(iii) When an odd-proton nucleus with r protons is compared with an odd-neutron nucleus with r neutrons, the magnetic spin ratios are closely the same (Table). This rule is valid only when $r \leqslant 49$ and when both nuclei have the same spin, but six pairs conform and no exception is known (Schawlow and Townes 1951).

The Magnetic Spin Ratio of Nuclei having the same spin and either r protons or r neutrons

r	Nuclei	I	G
5	^{9}Be ^{11}B	$1\frac{1}{2}$	0·61, 0·61
7	^{13}C ^{15}N	$\frac{1}{2}$	1·10, 1·02
13	^{25}Mg ^{27}Al	$2\frac{1}{2}$	0·45, 0·58
17	^{33}S ^{35}Cl	$1\frac{1}{2}$	0·55, 0·58
37	^{67}Zn ^{85}Rb	$2\frac{1}{2}$	0·66, 0·40
49	^{87}Sr ^{113}In	$4\frac{1}{2}$	0·57, 0·53

(iv) The addition of two neutrons without change of spin has been described as pushing the magnetic moment towards the Schmidt lines (Wangsness 1950, de Schalit 1950). In terms of the magnetic spin ratio this reads $G(Z, N+2) > G(Z, N)$. All known stable isotopes obey this rule, the fifteen pairs established being H, Cl, K, Cu, Ga, Br, Mo, Ag, In, Sn(2), Te, Ba, Re, Tl. But in I and Cs the addition products are unstable, and G decreases.

Combined with Bohr's (1951) rule for quadrupole moments, this means that when the addition of two neutrons produces a stable nucleus of the same spin, the numerical value of the quadrupole moment is reduced, so that the nucleus is more nearly spherical. Five isotopic pairs (Cl, Cu, Ga, Br, Re) conform; Eu seems to be an exception, but is easily distinguished because the addition of the two neutrons drives the odd proton from a π- to an α-state, while in the five conforming pairs the state of the odd proton is unaltered.

ACKNOWLEDGMENTS

I have much pleasure in acknowledging the help and encouragement which I have received from Professors C. F. Powell and M. H. L. Pryce and from Dr. J. A. Spiers.

REFERENCES

Bohr, A., 1951, *Phys. Rev.*, **81**, 134.
Latham, R., 1947, *Phys. Soc. Proc.*, **59**, 979.
de Schalit, A., 1950, *Phys. Rev.*, **80**, 103L.
Schawlow, A. L., and Townes, C. H., 1951, *Phys. Rev.*, **82**, 268L.
Schmidt, T., 1937, *Z. Phys.*, **106**, 358.
Wangsness, R. K., 1950, *Phys. Rev.*, **78**, 620L.

X-Ray Diffraction by a Crystal Possessing Periodicities within the Unit Cell

By J. W. JEFFERY
Birkbeck College Research Laboratory, London University

MS. received 16*th January* 1951, *and in amended form* 5*th June* 1951

ABSTRACT. The Fourier transform of a crystal is used to explain the appearance of the x-ray reflections from the true crystal lattice of tricalcium silicate as satellites of the strong reflections corresponding to a pseudo-lattice. Similar but more general diffraction effects are also discussed.

§1. INTRODUCTION

In the course of an x-ray crystallographic investigation of tricalcium silicate (Jeffery 1950, 1951) a rather peculiar diffraction effect was encountered. The crystal symmetry is strongly pseudo-rhombohedral, with a marked pseudo-halving of the hexagonal *a*-axis, but the real symmetry is monoclinic, one of the pseudo-hexagonal *a*-axes being the monoclinic *b*-axis. The monoclinic face-centred cell ($a=33{\cdot}1$ A, $b=7{\cdot}1$ A., $c=18{\cdot}6$ A., $\beta=94°$) is twelve times the volume of the primitive rhombohedral cell (Hex. $a=7{\cdot}0$ A., $c=25{\cdot}0$ A.). The ' extra ' reflections

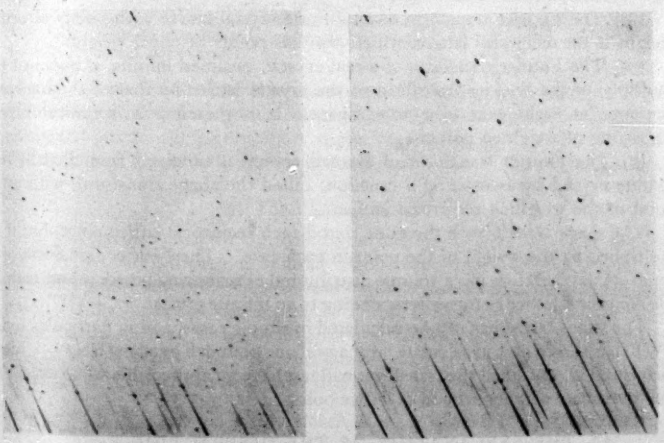

(*a*) (*b*)

Figure 1. Equivalent portions of two zero layer Weissenberg photographs.
(*a*) About that hexagonal *a*-axis which is equivalent to the monoclinic *b*-axis ; (*b*) about one of the other *a*-axes.

corresponding to the monoclinic lattice are all fairly weak and occur as satellites of the strong rhombohedral reflections. In between these rhombohedral reflections and their satellites are large areas in which the monoclinic reflections

are undetectable, so that even the establishment of the dimensions of the monoclinic cell was not an easy task. This is shown in Figure 1, which consists of the corresponding parts of two zero-layer Weissenberg photographs. One, about the monoclinic *b*-axis, shows satellites grouped round each strong rhombohedral reflection, the second, about one of the other pseudo-hexagonal *a*-axes, shows only the rhombohedral reflections; both photographs are heavily exposed and the satellite spots show up much more strongly than would be the case if the photographic densities were proportional to the x-ray intensities.

A similar effect has been described by Vand (1951) in the more general case of long chain compounds. Here, within a large unit cell, regions of order occur corresponding to a smaller unit cell, but there is no simple relation between the two lattices. In this case strong reflections corresponding to the effectively infinite lattice with the large unit cell only appear around the points where reflections would be produced by an infinite lattice based on the smaller cell.

The purpose of this note is to show that these effects can be simply explained on the basis of the Fourier transform conception. The results derived by Ewald (1940) will be used, and are summarized below.

§2. PROPERTIES OF THE FOURIER TRANSFORM

(i) The Fourier transform of a given electron density distribution describes the scattering of x-rays by that distribution.

(ii) In the case of the contents of the unit cell of a crystal the Fourier transform is, in general, a continuous function.

(iii) The Fourier transform of an infinite crystal lattice with points of equal weight is the reciprocal lattice, which also has points of equal weight.

(iv) The Fourier transform of a real crystal, assumed infinite, is obtained by multiplying the Fourier transform of the crystal lattice by that of the unit cell contents, at each point in Fourier space. It is therefore a reciprocal lattice consisting of weighted points.

(v) The Fourier transform of a small crystal is obtained from that of the infinite crystal by associating a function, called the shape transform, with each point of the weighted reciprocal lattice.

The shape transform is the same round each reciprocal lattice point, but it is multiplied by the weight of the point in each case. The Fourier transform of a small crystal therefore has a volume distribution of scattering power round each of the reciprocal lattice points corresponding to an infinite crystal.

The shape transform can be calculated in simple cases, and in particular Laue (1936) has shown how to calculate it for any shape bounded by plane faces. Unless the crystal is very small the transform will not have an appreciable value except in the immediate neighbourhood of lattice points.

§3. THE EXPLANATION OF THE DIFFRACTION EFFECTS

(i) *Tricalcium Silicate*

We now apply the above considerations to the case of tricalcium silicate. As a first approximation consider the monoclinic cell as a number of rhombohedral cells, i.e. consider it as a very small crystal with a true rhombohedral lattice. The Fourier transform of this will be a weighted rhombohedral reciprocal lattice with the shape transform of the monoclinic cell associated with each lattice point. This will be an approximation to the Fourier transform of the monoclinic cell contents.

To obtain the transform for the whole crystal, considered as infinite, we multiply the transform of the cell contents by the monoclinic reciprocal lattice, with all points having equal weight. The transform of the cell contents has appreciable

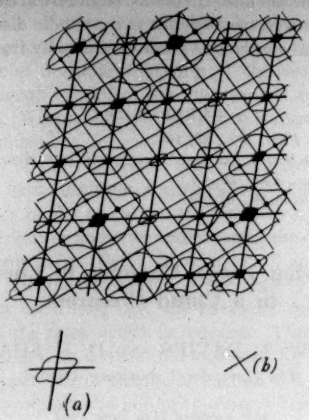

Figure 2. Schematic diagram showing the production of satellite reciprocal lattice points in the case of tricalcium silicate.
(*a*) Regions in which the Fourier transform of the monoclinic cell contents has an appreciable value. The shapes of the regions are the same but their relative extents are determined by the weight of the rhombohedral reciprocal lattice points.
(*b*) Monoclinic reciprocal lattice points.

values only near the rhombohedral lattice points. Therefore after multiplication only those monoclinic lattice points coincident with or near to heavily weighted rhombohedral points will have weights appreciably different from zero, and the monoclinic lattice points will appear as satellites of the rhombohedral points (Figure 2).

(ii) *The General Case*

In the more general case the contents of the large unit cell are made up of two parts. The first part is the region of order which can be considered as a very small crystal with a small unit cell. The second part is the rest of the contents of the large cell. If the former predominates, its Fourier transform is a good approximation to the transform of the large cell contents. The argument then proceeds as before, except that none of the reciprocal lattice points corresponding to the large cell are necessarily coincident with those derived from the smaller one.

(iii) *Conclusions*

These considerations give a descriptive explanation of the observed diffraction effects which can form a foundation for a more detailed and quantitative analysis.

§4. FURTHER CONSIDERATIONS

Vand (1951) has shown that even in the more general case the simple structure of the small cell can usually be solved fairly easily and the phases of the reflections corresponding to this are then known. From a consideration of the Laue function giving the shape transform of the very small crystal contained in the true

cell, it is then possible to deduce the phases of the 'satellite' reflections and thus solve the complete structure.

In the case of tricalcium silicate it can be shown (Jeffery 1951) that the increase in relative intensity of the satellite reflections, from zero at the origin to comparative equality for the high orders, corresponds to a periodic distortion of the rhombohedral lattice rather than a periodic variation of density from cell to cell within an undistorted lattice.

REFERENCES

EWALD, P. P., 1940, *Proc. Phys. Soc.*, **52**, 167.
JEFFERY, J. W., 1950, *Ph.D. Thesis*, London University; 1951, *Acta Crystallogr.*, in the press.
LAUE, M., 1936, *Ann. Phys., Lpz.*, **26**, 55.
VAND, V., 1951, *Acta Crystallogr.*, **4**, 104.

A Search for Sudden Large Changes of Energy of Beta-Rays in a Cloud Chamber

BY W. T. DAVIES AND D. F. SHAW
The Clarendon Laboratory, Oxford

MS. received 11*th June* 1951

ABSTRACT. Measurements are presented of the changes of curvature of β-ray tracks in a cloud chamber containing air at approximately N.T.P. situated in a magnetic field of 400 gauss. These are examined for evidence of processes involving the reversible production of electrons of rest mass a small multiple of the normal value. Indications from a study of earlier investigations, that such processes might exist, are not substantiated, and the results confirm and extend those of Bleuler. It is shown that this type of cloud chamber investigation is unsuitable for obtaining useful information on inelastic scattering of fast β-particles, and that multiple scattering and observational bias are adequate to explain the anomalies previously reported.

§1. INTRODUCTION

CLOUD chamber experiments have yielded conflicting results on the inelastic scattering of fast β-particles. Several investigators* have concluded that scattering with an energy loss of more than about 20% occurs with a frequency 10 to 100 times that predicted by the theory of Bethe and Heitler (1934) in which the loss of energy is due to emission of radiation. This has led to suggestions that the excessive frequency of sudden energy losses is due to the occurrence of an additional process having the appearance of a radiative collision, but involving a third particle which must be non-ionizing. Measurements of the energy distribution of the X-radiation produced when electrons of 1 to 3 MEV. are absorbed in different materials have confirmed the accuracy of the Bethe–Heitler theory in this energy region. Calorimetric experiments have shown that, in the absorption of fast electrons, any process involving the emission of non-ionizing radiation, if it exists at all, must have a probability small compared with that for bremsstrahlung production.

The most recently reported search for inelastic scattering in the gas of a magnetic cloud chamber is that of Bleuler (1942) who found no evidence for an excessive number of cases of sudden energy loss in fluorine. While 19 cases

* A bibliography of earlier work is given under general headings at the end of the list of references.

of single scattering were observed exhibiting apparent losses of over 10% of the incident kinetic energy, 25 cases were observed in which scattering was accompanied by an apparent gain of energy of more than 10%. The expected number of losses of this amount of energy or more, by radiation, was about three for these experimental conditions. Bleuler accounted for his observations on the assumption that the changes of curvature were not in fact due to changes of energy, but were simply the result of multiple scattering of the electron in the gas of the cloud chamber. Although this effect was encountered at an early stage in cloud chamber development (Wilson 1923), it was left to Williams (1939) to present the first quantitative treatment.

If the momentum of the electron is determined from the curvature of the track in a magnetic field, multiple scattering will introduce an error in the measured value of this radius of curvature (Bethe 1946). This error increases with increase of gas pressure and with reduction of the length of the track used in the curvature measurement (Bethe 1946, eqns. 12 and 13). Apart from the fact that the effect of multiple scattering on curvature is less likely to cancel out for a short track than for a long one, the curvature measurements themselves will be less precise as the track length is reduced. Thus, if a single event such as a nuclear deflection divides a track into two parts for the purpose of analysis, it may frequently happen that a change of curvature is recorded.

Although one may explain the failure to observe cases of curvature decrease in other work than that of Bleuler as due to an observational bias which causes them to be rejected as of no significance, there is another feature of previous work which has not been satisfactorily explained, viz. the occurrence of cases of almost complete energy loss (see for instance Williams and Terroux 1930, Barber and Champion 1938, Davies 1939). In such cases, when the track observed after the process has been very short and heavily ionizing, the question of a multiple scattering error in the curvature hardly arises.

§ 2. THE PRESENT INVESTIGATION

It is conceivable that multiple scattering may not be the only process which could give rise to a decrease or an increase of curvature following a nuclear collision. A process which might be imagined to take place is one in which the rest mass of the electron is increased at the expense of its kinetic energy relative to the nucleus. Such a process has in fact been previously suggested by Zwicky (1938)* and it is of interest to consider the implications in more detail.

Let E and p represent the total energy and momentum respectively of the primary electron of rest mass m_0 (measured relative to a colliding nucleus). Then

$$p^2 = E^2/\mathbf{c}^2 - m_0{}^2\mathbf{c}^2. \qquad \ldots\ldots(1)$$

If the electron undergoes an elastic collision with the nucleus in which its rest mass changes to nm_0 $(n>1)$ and its momentum decreases by an amount Δp with the recoiling nucleus contributing to the momentum conservation:

$$(p-\Delta p)^2 = E^2/\mathbf{c}^2 - (nm_0)^2\mathbf{c}^2. \qquad \ldots\ldots(2)$$

Solution of equations (1) and (2) gives:

$$\Delta p = p - \{p^2 - (n^2-1)m_0{}^2\mathbf{c}^2\}^{1/2} \qquad \ldots\ldots(3)$$

taking the negative square root since $p>\Delta p>0$ for $n>1$.

* The possible existence of a spectrum of rest masses for the fundamental particles has also been suggested by Møller (1947) and Bhabha (1947). Also Jánossy and McCusker (1949) have discussed the existence of cosmic-ray particles of rest mass $3m_0$ and $10m_0$.

To comply with the results of the calorimetric experiments it would be necessary to assume that the inverse process can occur, i.e. the increase of translational kinetic energy with decrease in rest mass. For this case, taking as the initial rest mass nm_0 and the final value m_0 the corresponding increase in momentum $\Delta p'$ is :

$$\Delta p' = \{p^2 + (n^2-1)m_0^2c^2\}^{1/2} - p \qquad \ldots\ldots(4)$$

with the requirement $\Delta p' > 0$ for $n > 1$.

In Figure 1 are plotted curves showing the relationship between $H\rho$ and $\Delta(H\rho)$ on the assumption that the rest mass can increase from m_0 to 2, 3 or $4m_0$, or can change in the reverse sense. Included in this figure are the published results of Barber and Champion (1938) and Leprince-Ringuet (1935), chosen because they were in a form suitable for this analysis. It will be seen that, while this evidence cannot be said to corroborate the hypothesis, it certainly would not exclude the occurrence of such a process.

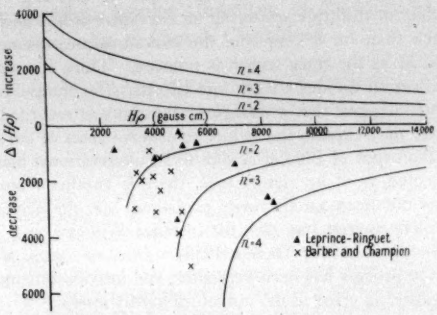

Figure 1.

Besides the obvious discrete values of possible changes in momentum, the distribution shown in Figure 1 differs from that expected to arise from multiple scattering in two other respects which should be capable of experimental test: (*a*) for initial $H\rho$ values below 2,800 gauss cm. one would expect to observe only increases in momentum, whereas multiple scattering errors could contribute apparent increases and decreases; (*b*) for $H\rho$ values above 2,800 gauss cm. both increases and decreases could occur with the magnitude of the decreases significantly greater than that of the increases, whereas multiple scattering would give approximately equal positive and negative changes.

§3. EXPERIMENTAL WORK

In an effort to obtain further experimental evidence, particularly since Bleuler's data were not given in sufficient detail for us to analyse in the manner indicated, we have made new measurements on the curvature of electron tracks in a cloud chamber situated in a uniform magnetic field of about 400 gauss. Air at approximately atmospheric pressure was used as the cloud chamber filling. The measured tracks of electrons from a ^{32}P source covered the range of $H\rho$ from 2,300 to 6,600 gauss cm. This is a region in which the effect of an integral change in rest mass as postulated would be most pronounced.

The photographs were projected to original size on a screen on which were drawn reference circles of radii from 6 cm. to 15 cm. at 1 cm. intervals. The

radius of curvature of each track was determined by fitting to one of these reference circles. Our criterion for circle fitting was that there should be no radial deviations exceeding the width of the image of the track ($\frac{1}{2}$ to 1 mm.) from a circular arc at least 5 cm. long. This length was adopted, after trials by different observers on a selection of tracks, and by the same observer at different times, as the minimum which allowed a decision to be made between adjacent circles.* The length and radius of curvature of each track, and single deflections greater than 3° were recorded. Examples of cases when a track did not fit the selected circle along its whole length are illustrated in Figures 2, 3 and 4 (Plate†) and the method of treatment detailed below.

(*a*) In Figure 2, track *abc*, a nuclear deflection of 4° occurs at *b*. It is necessary, therefore, to measure the radii of curvature of portions *ab* and *bc* separately.

(*b*) In Figure 3, track *defg*, the portion *ef* is almost straight due to plural scattering. This results in a division of the track into two sections and again circles have to be fitted separately to the portions *de* and *fg*. Since the portion *ef* is less than 5 cm. long, no attempt would be made to measure the radius of curvature of this section.

(*c*) In Figure 4, track *hjk* is typical of several found in which the curvature appeared to change continuously along its length. In such cases it was usually possible to represent the track very closely by two arcs of circles of different radii intersecting on the track. It often happened that the two selected circles best fitted the track when intersecting at a small angle (2° or 3°) so that in representing the track in this way a small deflection was introduced where none was at first apparent. It is not considered that this affects the significance of the results.

The measurements covered 350 metres of track in the selected range of momenta; 252 cases were found in which a change of 1 cm. or more in the radius

Table 1. Distribution of Track Length and Changes of Curvature

	ρ (cm.)	6	7	8	9	10	11	12	13	14	15	Total 6–15
	$H\rho$ range (gauss cm.)	2300–2700	2700–3100	3100–3600	3600–4000	4000–4400	4400–4900	4900–5300	5300–5700	5700–6200	6200–6600	2300–6600
	Actual track length (m.)	32·1	53·1	65·3	64·9	52·0	38·0	21·8	11·2	6·0	1·4	346
	Effective track length (m.)	5·2	10·3	15·7	17·8	14·9	12·6	7·3	3·8	1·9	0·5	90
Distribution of observed changes in curvature	Number of decreases in curvature: Total	27	30	26	19	16	6	3	4	0	0	131
	$\Delta\rho > 4$ cm.	1	0	4	0	1	0	0	0	0	0	6
	$\Delta\rho = 4$ cm.	1	2	0	0	0	0	0	0	0	0	3
	$\Delta\rho = 3$ cm.	4	5	5	2	0	1	0	0	0	0	17
	$\Delta\rho = 2$ cm.	11	15	12	6	8	2	2	0	0	0	56
	$\Delta\rho = 1$ cm.	10	8	5	11	7	3	1	4	0	0	49
	Number of increases in curvature: $\Delta\rho = 1$ cm.	7	9	8	7	10	6	4	0	0	0	51
	$\Delta\rho = 2$ cm.	3	6	3	11	8	5	4	0	2	0	42
	$\Delta\rho = 3$ cm.	0	1	2	4	5	2	2	1	0	1	18
	$\Delta\rho = 4$ cm.	0	0	0	1	0	0	1	1	0	1	4
	$\Delta\rho > 4$ cm.	0	1	0	0	0	2	1	1	0	1	6
	Number of increases in curvature: Total	10	17	13	23	23	15	12	3	2	3	121
	Number of tracks showing no change	142	235	326	325	235	175	106	53	33	5	1635

* Bothe (1948) has discussed various other criteria for circle fitting. We do not consider the difference between them to be significant when the radial interval between the circles to be fitted is as large as in our case.

† For Plates see end of issue.

of curvature of a track was observed. The distribution of track length and changes in curvature is shown in Table 1. Any sudden change in curvature occurring within 5 cm. of either end of the visible portion of a track could not meet our requirements for acceptance. Therefore, in computing the effective track length (row 4) the first and last 5 cm. of each track have been excluded. In addition, the track length has been reduced from the experimental conditions (65 cm. Hg pressure at 16° C.) to the equivalent at N.T.P. The effective track length for curvature changes was 90 metres.

§4. DISCUSSION AND CONCLUSIONS

It is evident from the results that cases of increase and decrease in curvature occur with equal frequency. There was no apparent periodicity in the curvature changes such as would have accompanied changes in rest mass. In the lower momentum intervals the number of cases of curvature decrease significantly exceeds the number in which it increases. This may be attributed to the fact that the electrons producing these tracks entered the cloud chamber at an angle such that their path was convex to the chamber radius. If then, a change occurred to increase the curvature their path before striking the chamber wall would be less than if the curvature decreased. The requisite minimum track length required for circle fitting would therefore be more readily achieved in the latter case. This effect was less pronounced at the higher momenta where the electrons entered the chamber in a different direction.

We verified that the observed changes were not produced by lack of homogeneity in the magnetic field or by distortions in the chamber, the cameras or the reprojecting system. The spread of curvature changes is much greater than would be expected from our errors in circle fitting. We conclude therefore that most of the changes result from the effect of multiple scattering since this is the only other factor which might produce an almost symmetrical distribution in curvature about the mean value. The results of this experiment do not exclude the occurrence of a process, such as an increase in rest mass, with a frequency small compared with the random changes of curvature.* A more direct way of investigating this effect would be to observe the collisions between primary β-particles and atomic electrons. Ruark and Jones (1938) analysed the results of Champion (1932) and found no evidence for a change in rest mass, but the number of collisions observed was comparatively small.

We analysed a selection of our tracks using the method of Groetzinger, Berger and Ribe (1950), by measuring the angles between successive chords 1·5 cm. long on 34 sections of track varying in length from 6 cm. to 15 cm. The root mean square deviation from the mean angle varied between 0·5° and 2·5°; the corresponding value obtained for measurements on true circles was rather less than 1°. In the case of an electron of initial $H\rho = 5{,}000$ which experiences a change of rest mass, the predicted values for the root mean square angle of multiple scattering α in air at 65 cm. Hg pressure are given in Table 2. These results show that this method cannot be used to detect a change of rest mass under our conditions.

In the track length we examined, the Bethe–Heitler theory predicts about one case of radiation loss greater than 20% whereas over 70 changes of curvature

* The number of cases found of a change in radius of curvature corresponds roughly to the expected number of single scattering events in which the projected deflection is greater than 5°.

both positive and negative were observed corresponding to an energy change greater than this amount. In order that a difference of 2% between the number of apparent gains and losses may be statistically significant one would need sufficient track length to yield about 5,000 such changes. Under our conditions this would mean measuring nearly 15 kilometres of track, a tedious investigation unless assisted by such improvements in cloud chamber technique as those introduced by Champion and Roy (1948) and Hodson, Loria and Ryder (1950).

The last point for discussion is the occurrence of cases of almost complete energy loss of which we observed three. If plotted on Figure 1, all three would lie close to the curve for $n=2$. We prefer, however, to regard them as due to the chance production of a δ-ray as the β-particle passes out of the illuminated region of the cloud chamber. A vertical section of the light beam gives a region, fairly accurately 1 cm. deep, of intense illumination bounded top and bottom by strips approximately 2 mm. deep in which the illumination falls to a value insufficient

Table 2. Predicted Root Mean Square Angles of Multiple Scattering for electrons of different rest masses in air at 65 cm. Hg pressure and 16° C.

Initial conditions			Final conditions		
$H\rho$	Rest mass	α	$H\rho$	Rest mass	α
5,000	m_0	2°	4,000	$2m_0$	3°
5,000	$2m_0$	2·5°	6,000	m_0	1·5°
5,000	$3m_0$	3°	6,500	m_0	2°

to photograph δ-rays. It is reasonable to assume that a δ-ray produced within the last centimetre of a track which is passing out of the light beam because of obliquity may be mistaken for a case of very large energy loss. We have counted in 27 metres of track 18 δ-rays of projected length greater than 5 mm.* The total number of tracks which passed out of the light in crossing the chamber was about 1,300. Hence one would expect roughly nine cases of this kind. Clearly it seems unjustified to consider any other process.

We conclude that there is no reliable cloud chamber evidence that the frequency of occurrence of significant energy losses due to radiation is greater than predicted by theory. The results of most of the earlier cloud chamber experiments are invalidated by the limitations on the method imposed by multiple scattering.

ACKNOWLEDGMENTS

We are grateful to Professor Lord Cherwell for his encouragement and advice. One of us (D.F.S.) is indebted to the Department of Scientific and Industrial Research for a maintenance grant.

REFERENCES

Barber, A., and Champion, F. C., 1938, *Proc. Roy. Soc.* A, **168,** 159.
Bethe, H. A., 1946, *Phys. Rev.*, **70,** 821.
Bethe, H., and Heitler, W., 1934, *Proc. Roy. Soc.* A, **146,** 83.
Bhabha, H. J., 1947, *Report of International Conference on Fundamental Particles and Low Temperatures*, Vol. I (London : Physical Society), p. 22.
Bleuler, E., 1942, *Helv. Phys. Acta*, **15,** 613.
Bothe, W., 1948, *S.B. Heidelberger Akad. Wiss.*, No. **5,** 107.

* Our choice of 5 mm. as the minimum projected length is not entirely arbitrary since in the cases reported, including our own, the low-energy track has been in the neighbourhood of 1 cm. in length.

CHAMPION, F. C., 1932, *Proc. Roy. Soc.* A, **136,** 630.
CHAMPION, F. C., and ROY, R. R., 1948, *Proc. Phys. Soc.*, **61,** 532.
DAVIES, W. T., 1939, *Ph.D. Thesis*, Cambridge.
GROETZINGER, G., BERGER, M. J., and RIBE, F. L., 1950, *Phys. Rev.*, **77,** 584.
HODSON, A. L., LORIA, A., and RYDER, N. V., 1950, *Phil. Mag.*, **41,** 826.
JÁNOSSY, L., and MCCUSKER, C. B. A., 1949, *Nature, Lond.*, **163,** 181.
LEPRINCE-RINGUET, L., 1935, *C.R. Acad. Sci., Paris*, **201,** 712.
MØLLER, C., 1947, *Report of International Conference on Fundamental Particles and Low Temperatures*, Vol. I (London : Physical Society), p. 184.
RUARK, A., and JONES, C. C., 1938, *Phys. Rev.*, **53,** 454.
WILLIAMS, E. J., 1939, *Proc. Roy. Soc.* A, **169,** 531 (see also *Phys. Rev.*, 1940, **48,** 292).
WILLIAMS, E. J., and TERROUX, F. R., 1930, *Proc. Roy. Soc.* A, **126,** 289.
WILSON, C. T. R., 1923, *Proc. Roy. Soc.* A, **104,** 1, 192.
ZWICKY, F., 1938, *Phys. Rev.*, **53,** 611.

In addition to those specifically mentioned in the text the following authors' work is referred to in the Introduction :

(*a*) *Cloud Chamber Experiments*

KLARMANN, H., and BOTHE, W., 1936, *Z. Phys.*, **101,** 489.
LECOIN, M., 1936, *C.R. Acad. Sci., Paris*, **202,** 839.
RANDELS, R. B., CHAO, K. T., and CRANE, H. R., 1945, *Phys. Rev.*, **68,** 64.
STEPANOWA, E. G., 1939, *J. Phys., U.S.S.R.*, **1,** 204.

(*b*) *Ionization Chamber Experiments*

ARCIMOVIČ, L. A., and CHRAMOV, V. A., 1938, *C. R. Acad. Sci., U.R.S.S.*, **18,** 415.
BUECHNER, W. W., VAN DE GRAAFF, R. J., BURRILL, E. A., and SPERDUTO, A., 1948, *Phys. Rev.*, **74,** 1348.
PETRAUSKAS, A. A., VAN ATTA, L. C., and MYERS, F. E., 1943, *Phys. Rev.*, **63,** 389.
WU, C. S., 1941, *Phys. Rev.*, **59,** 481.

(*c*) *Calorimetric Experiments*

BUECHNER, W. W., and VAN DE GRAAFF, R. J., 1946, *Phys. Rev.*, **70,** 174.
IVANOV, A. V., WALTER, A. K., SINELNIKOV, K. D., TARANOV, A. J., and ABRAMOVICH, A. M., 1941, *J. Phys., U.S.S.R.*, **4,** 319.

The First Order Raman Effect in Crystals, particularly in Diamond

BY O. THEIMER*
Department of Mathematical Physics, University of Edinburgh

Communicated by M. Born; MS. received 9th April 1951

ABSTRACT. The theory of the first order Raman effect in crystals is presented in a form which takes into account the finiteness of the wavelength of the incident radiation. The theory is applied to calculate the relative intensities of the first order Raman line and of the Brillouin components of diamond, which are interpreted as the Stokes and anti-Stokes Raman lines produced by those elastic vibrations, whose wave vector **Q** fulfils the condition $\mathbf{Q}=\mathbf{Q}''-\mathbf{Q}'$. ($\mathbf{Q}'$ and $\mathbf{Q}''$ are the wave vectors of the incident and scattered radiation.) The calculated intensities are in good agreement with experiments of Krishnan. A formula derived by Leontowitsch and Mandelstamm is discussed and is shown to be inadequate to calculate the intensities of the Brillouin components.

* On leave of absence from Physics Department, Technische Hochschule, Graz, Austria.

§1. INTRODUCTION

SCATTERING phenomena in crystals can be divided into two groups: scattering with frequency changes and scattering without frequency shifts. A process of the latter kind occurs only with radiation whose wavelength is of the same order of magnitude as the lattice constants*. For longer waves, the scattered radiation which is of the same frequency cancels out by interference, if the crystal is perfect. In this case only those scattering processes yield a finite intensity, which are connected with vibrational transitions producing frequency shifts between the scattered and the incident light. These latter processes are all of the nature of the Raman effect. They are called first order effects if only transitions $v \rightarrow v \pm 1$ are involved. (Here v denotes the vibrational states of the crystal.)

Max Born (Born and Bradburn 1947) has developed a general theory for the Raman effect in crystals, which yields explicit formulae for the intensity of the Raman spectrum of the first and second order. This theory has been found to be in good agreement with experiments of different kinds. The theory implies a simplifying assumption which can be completely justified for the Raman effect with optical waves; it is however not admissible when dealing with some of the phenomena which have been investigated experimentally during the last few years. Born's approximation consists in assuming that the wavelength of the incident light is long compared with the dimensions of the scattering crystal, i.e. practically infinite.

In this paper the theory of the Raman effect is presented in a form that takes into account the finite wavelength of the radiation. This allows us to investigate theoretically the Brillouin scattering of diamond, which appears to be the most important of the problems for which the finite wavelength has to be taken into account and which justify the increased complexity of the formulae. The Brillouin components have been discussed previously by other authors; their treatment is however not quite satisfactory.

The Brillouin components of diamond have been investigated by Krishnan (1947). Using the elastic constants of diamond, he calculated the frequency shifts and found good agreement with experiment. In order to derive the intensity values from the theory, however, he applied a simple formula of Leontowitsch and Mandelstamm, which is not adequate to give all the required details. Further, this formula does not allow calculation of the intensity ratio between the Brillouin components and the first order Raman line with frequency 1332 cm^{-1}. These deficiences are removed in the present paper.

§2. LATTICE DYNAMICS

In this section we summarize some of the results obtained previously by Born (1942) and Born and Begbie (1947).

The position vector of a lattice particle may be written

$$\mathbf{r}\begin{pmatrix} l \\ k \end{pmatrix} = \mathbf{r}(l) + \mathbf{r}(k), \qquad \ldots\ldots(2.1)$$

where

$$\mathbf{r}(l) = l_1\mathbf{a}_1 + l_2\mathbf{a}_2 + l_3\mathbf{a}_3\,; \qquad \ldots\ldots(2.2)$$

* This is exactly true if the internal forces and the polarizability changes are linear functions of the displacements of the single atoms. The unavoidable non-linear effects are, however, negligibly small in most cases of light scattering in crystals.

here l_1, l_2, l_3 are integers, $\mathbf{a}_1$, $\mathbf{a}_2$, $\mathbf{a}_3$ are the three elementary vectors of the lattice cell and $\mathbf{r}(k)$ $(k=1,2,\ldots p)$ are the position vectors of the p particles in the cell.

The rectangular components of $\mathbf{r}\begin{pmatrix} l \\ k \end{pmatrix}$ are $x_\alpha \begin{pmatrix} l \\ k \end{pmatrix}$ $(\alpha = 1, 2, 3)$.

The second derivatives of the potential Φ of the disturbed lattice will be denoted by

$$\Phi_{\alpha\beta}\begin{pmatrix} l-l' \\ kk' \end{pmatrix} = \left[\frac{\partial^2 \Phi}{\partial x_\alpha \begin{pmatrix} l \\ k \end{pmatrix} \partial x_\beta \begin{pmatrix} l' \\ k' \end{pmatrix}}\right]. \qquad \ldots\ldots(2.3)$$

The equations of motion for small vibrations, of amplitude

$$u_\alpha \begin{pmatrix} l \\ k \end{pmatrix} = v_\alpha \begin{pmatrix} l \\ k \end{pmatrix} \Big/ \sqrt{m_k} = X_\alpha \begin{pmatrix} l \\ k \end{pmatrix} - X_\alpha{}^0 \begin{pmatrix} l \\ k \end{pmatrix} \qquad \ldots\ldots(2.4)$$

are

$$\ddot{v}_\alpha \begin{pmatrix} l \\ k \end{pmatrix} = - \sum_{\beta l' k'} D_{\alpha\beta}\begin{pmatrix} l-l' \\ kk' \end{pmatrix} v_\beta \begin{pmatrix} l' \\ k' \end{pmatrix}, \qquad \ldots\ldots(2.5)$$

where

$$D_{\alpha\beta}\begin{pmatrix} l \\ kk' \end{pmatrix} = (m_k m_{k'})^{-1/2} \Phi_{\alpha\beta}\begin{pmatrix} l \\ kk' \end{pmatrix}. \qquad \ldots\ldots(2.6)$$

The equations of motion (2.5) are satisfied by plane waves which may be written in the form

$$v_\alpha \begin{pmatrix} l \\ k \end{pmatrix} = V_\alpha(k) \exp(-i\omega t) \exp\{i\mathbf{q} \cdot \mathbf{r}(l)\}, \qquad \ldots\ldots(2.7)$$

or in the form

$$v_\alpha \begin{pmatrix} l \\ k \end{pmatrix} = W_\alpha(k) \exp(-i\omega t) \exp\left\{i\mathbf{q} \cdot \mathbf{r}\begin{pmatrix} l \\ k \end{pmatrix}\right\}, \qquad \ldots\ldots(2.8)$$

where

$$W_\alpha(k) = V_\alpha(k) \exp\{-i\mathbf{q} \cdot \mathbf{r}(k)\}. \qquad \ldots\ldots(2.9)$$

The equations of motion can be expressed in the compact form

$$\Omega W = C(\mathbf{q}) W \qquad \ldots\ldots(2.10) \qquad \text{and} \qquad \Omega V = D(\mathbf{q}) V \qquad \ldots\ldots(2.11)$$

where $\Omega = \omega^2$ and W and V are one-column matrices:

$$W = \{W_1(1), W_2(1), W_3(1), W_1(2) \ldots, W_3(p)\}. \qquad \ldots\ldots(2.12)$$

The elements of the matrices $C(\mathbf{q})$ and $D(\mathbf{q})$ are

$$C_{\alpha\beta}(\mathbf{q}|kk') = D_{\alpha\beta}(\mathbf{q}|kk') \exp\{-i\mathbf{q} \cdot \mathbf{r}(kk')\} = \sum_l D_{\alpha\beta}\begin{pmatrix} l \\ kk' \end{pmatrix} \exp\left\{i\mathbf{q} \cdot \mathbf{r}\begin{pmatrix} l \\ kk' \end{pmatrix}\right\},$$

with

$$\mathbf{r}(kk') = \mathbf{r}(k) - \mathbf{r}(k'). \qquad \ldots\ldots(2.13)$$

It is convenient to introduce normal coordinates, with the help of which the expressions for the kinetic and potential energy are transformed into sums of squares:

$$\mathbf{v}\begin{pmatrix} l \\ k \end{pmatrix} = \sqrt{m_k}\,\mathbf{u}\begin{pmatrix} l \\ k \end{pmatrix} = \sum_{qj} \mathbf{e}\left(k \middle| \begin{matrix} q \\ j \end{matrix}\right) \exp\{i\mathbf{q} \cdot \mathbf{r}(l)\} \xi\begin{pmatrix} q \\ j \end{pmatrix}. \qquad \ldots\ldots(2.14)$$

The $\mathbf{e}\left(k \middle| \begin{matrix} q \\ j \end{matrix}\right)$ are the components of the eigenvectors of the lattice, i.e. $\mathbf{e}\left(k \middle| \begin{matrix} q \\ j \end{matrix}\right)$ is the displacement $\mathbf{v}(k)$ of the atom $\begin{pmatrix} 0 \\ k \end{pmatrix}$ when the lattice performs the normal vibration $\begin{pmatrix} q \\ j \end{pmatrix}$. They satisfy the orthogonality relations

$$\sum_{\alpha k} e_\alpha\left(k \middle| \begin{matrix} q \\ j \end{matrix}\right) e_\alpha{}^*\left(k \middle| \begin{matrix} q \\ j' \end{matrix}\right) = \delta(jj'), \qquad \sum_j e_\alpha\left(k \middle| \begin{matrix} q \\ j \end{matrix}\right) e_\beta{}^*\left(k' \middle| \begin{matrix} q \\ j \end{matrix}\right) = \delta(\alpha\beta)\delta(kk')$$

and the equations of motion

$$\ldots\ldots(2.15)$$

$$\Omega(j) e(j) = D\begin{pmatrix} q \\ j \end{pmatrix} e(j). \qquad \ldots\ldots(2.16)$$

For long elastic waves the amplitudes $W(k)/\sqrt{m_k}$ as defined by (2.8), (2.9) do not depend to the zero order in $\mathbf{q}$ on k and satisfy the ordinary equations for waves in an elastic substance. These can be written (ρ is the density of the crystal)

$$\rho\omega^2 W = D'(\mathbf{q})W, \qquad \ldots\ldots(2.17)$$

where the elements of $D'(\mathbf{q})$ are referred to the elastic constants c_{ik} by the matrix equation

$$\begin{vmatrix} D'_{11}(q) \\ D'_{22}(q) \\ D'_{33}(q) \\ D'_{23}(q) \\ D'_{31}(q) \\ D'_{12}(q) \end{vmatrix} = \begin{vmatrix} c_{11} & c_{66} & c_{55} & c_{65} & c_{51} & c_{16} \\ c_{66} & c_{22} & c_{44} & c_{24} & c_{46} & c_{62} \\ c_{55} & c_{44} & c_{33} & c_{43} & c_{35} & c_{54} \\ c_{65} & c_{24} & c_{43} & \tfrac{1}{2}(c_{23}+c_{44}) & \tfrac{1}{2}(c_{45}+c_{36}) & \tfrac{1}{2}(c_{64}+c_{25}) \\ c_{51} & c_{46} & c_{35} & \tfrac{1}{2}(c_{45}+c_{36}) & \tfrac{1}{2}(c_{31}+c_{55}) & \tfrac{1}{2}(c_{56}+c_{14}) \\ c_{16} & c_{62} & c_{54} & \tfrac{1}{2}(c_{64}+c_{25}) & \tfrac{1}{2}(c_{56}+c_{14}) & \tfrac{1}{2}(c_{12}+c_{66}) \end{vmatrix} \begin{vmatrix} q_1^2 \\ q_2^2 \\ q_3^3 \\ 2q_2q_3 \\ 2q_3q_1 \\ 2q_1q_2 \end{vmatrix}$$

$\ldots\ldots(2.18)$

To the first order in $\mathbf{q}$ the displacements $\mathbf{W}(k)$ of the different atoms in the elementary cell differ a little from each other. This difference must be taken into account in calculating the intensity of the Brillouin components. The first order terms $\mathbf{W}^{(1)}$ are given by the matrix equation

$$C^{(0)}W^{(1)} = C^{(1)}(\mathbf{q})W, \qquad \ldots\ldots(2.19)$$

where

$$C^{(0)}_{\alpha\beta}(kk') = \sum_l D_{\alpha\beta}\begin{pmatrix} l \\ kk' \end{pmatrix} \qquad \ldots\ldots(2.20)$$

$$C^{(1)}_{\alpha\beta}(\mathbf{q}|kk') = -i\sum_l\sum_\gamma D_{\alpha\beta}\begin{pmatrix} l \\ kk' \end{pmatrix} x_\gamma\begin{pmatrix} l \\ kk' \end{pmatrix} q_\gamma. \qquad \ldots\ldots(2.21)$$

In a finite lattice the wave vector $\mathbf{q}$ is restricted by the cyclic lattice condition in the following way:

We define the basic vectors $\mathbf{b}_\alpha$ of the reciprocal lattice by

$$\mathbf{a}_\alpha \cdot \mathbf{b}_\beta = \begin{cases} 1 \text{ if } \alpha = \beta, \\ 0 \text{ if } \alpha \neq \beta, \end{cases} \qquad \ldots\ldots(2.19)$$

and write

$$\mathbf{q} = 2\pi q_1\mathbf{b}_1 + 2\pi q_2\mathbf{b}_2 + 2\pi q_3\mathbf{b}_3. \qquad \ldots\ldots(2.20)$$

Then

$$\mathbf{q}\cdot\mathbf{r}(l) = 2\pi(q_1l_1 + q_2l_2 + q_3l_3) \qquad \ldots\ldots(2.21)$$

and

$$q_1 = \frac{h_1}{n}, \quad q_2 = \frac{h_2}{n}, \quad q_3 = \frac{h_3}{n} \qquad (h_1, h_2, h_3 = 0, 1, 2, \ldots(n-1)), \qquad \ldots\ldots(2.22)$$

where $n^3 = N$ is the total number of atoms in a simple lattice.

Equation (2.22) ensures that for any function of the lattice points

$$f[\mathbf{r}(L)] = f[\mathbf{r}(l)], \text{ if } L_\alpha = l_\alpha + n \qquad (\alpha = 1, 2, 3). \qquad \ldots\ldots(2.23)$$

§3. GENERAL THEORY OF THE RAMAN EFFECT IN CRYSTALS

According to Placzek (1934) the scattered intensity corresponding to the transition between two vibrational states v, v', is proportional to the matrix element $[\mathbf{M}]^2_{vv'}$, where $\mathbf{M} = \alpha\mathbf{E}$ is the electric moment induced by the electric field $\mathbf{E}$ of the incident wave and α is the polarizability tensor of the scattering crystal.

$\mathbf{M}$ can, in first approximation, be considered as the sum of the contributions of the single atoms. In each atom the external field $\mathbf{E}$ acts with a different phase,

depending on its position. Further another relative retardation must be taken into account, because of the different distances of the scattering atoms from the observer.

Let $$\mathbf{Q}'=2\pi\mathbf{s}'/\lambda, \quad \mathbf{Q}''=2\pi\mathbf{s}''/\lambda, \quad |\mathbf{s}'|=|\mathbf{s}''|=1 \qquad \ldots\ldots(3.1)$$

be the wave vectors of the incident and scattered wave (neglecting the change of wavelength λ) and let

$$\mathbf{Q}=\mathbf{Q}''-\mathbf{Q}'=2\pi(\mathbf{s}''-\mathbf{s}')/\lambda, \quad Q=|\mathbf{Q}|=(4\pi/\lambda)\sin\tfrac{1}{2}\chi, \quad \ldots\ldots(3.2)$$

where χ is the angle of deflection. Then an elliptically polarized harmonic wave

$$\mathbf{E}=R[\mathbf{A}\exp\{-i(\omega t-\mathbf{Q}'\cdot\mathbf{r})\}]=\tfrac{1}{2}[\mathbf{A}\exp\{-i(\omega t-\mathbf{Q}'\cdot\mathbf{r})\}+\mathbf{A}^*\exp\{i(\omega t-\mathbf{Q}'\cdot\mathbf{r})\}] \qquad \ldots\ldots(3.3)$$

produces the retarded moment

$$M_\varrho=\sum_{k\sigma}\alpha_{\varrho\sigma}\left(\begin{matrix}l\\k\end{matrix}\middle|\,\mathbf{u}\right)\exp\left\{i\mathbf{Q}\cdot\left[\mathbf{r}\left(\begin{matrix}l\\k\end{matrix}\right)+\mathbf{u}\left(\begin{matrix}l\\k\end{matrix}\right)\right]\right\}A_\sigma=\sum_\sigma\alpha_{\varrho\sigma}A_\sigma \quad (\rho,\sigma=1,2,3). \qquad \ldots\ldots(3.4)$$

The polarizability of the atom $\left(\begin{matrix}l\\k\end{matrix}\right)$ depends on the displacements $\mathbf{u}$, which is indicated by the symbol used.

If $\mathbf{s}$ is a unit vector normal to $\mathbf{s}''$ the intensity becomes

$$I_{vv'}=(\omega+\omega_{vv'})^4[\mathbf{M}\cdot\mathbf{s}]^2_{vv'}=(\omega+\omega_{vv'})^4\sum_{\varrho\sigma}\sum_{\mu\nu}[i_{\varrho\sigma,\mu\nu}]_{vv'}A_\sigma A_\nu^* s_\varrho s_\mu, \qquad \ldots\ldots,(3.5)$$

where $$[i_{\varrho\sigma,\mu\nu}]_{vv'}=[\alpha_{\varrho\sigma}]_{vv'}[\alpha_{\mu\nu}{}^*]_{vv'}. \qquad \ldots\ldots(3.6)$$

Since $\omega_{vv'}\ll\omega$ for visible or ultra-violet incident light, we may omit $(\omega+\omega_{vv'})^4$, which has practically the same value for all Raman lines. The whole scattered intensity is now obtained by forming the thermal average over all the initial states v:

$$\langle i_{\varrho\sigma,\mu\nu}\rangle_{\mathrm{av}}=\frac{\sum_v[i_{\varrho\sigma,\mu\nu}]_{vv'}\exp-(\epsilon_v/kT)}{\sum_v\exp(-\epsilon_v/kT)} \qquad \epsilon_v=\text{the energy of the state } v. \qquad \ldots\ldots(3.7)$$

For natural incident light and scattered light observed without an analyser, we must average over the polarization of the incident and scattered radiation:

$$\left.\begin{aligned}\overline{A_\varrho A_\sigma{}^*}&=-I_0 s_\varrho{}' s_\sigma{}', \quad (\rho\neq\sigma), & \overline{A_\varrho A_\varrho{}^*}&=I_0(1-s_\varrho{}'^2)\\ \overline{s_\varrho s_\sigma}&=-\tfrac{1}{2}s_\varrho{}'' s_\sigma{}'', \quad (\rho\neq\sigma), & \overline{s_\varrho s_\varrho}&=\tfrac{1}{2}(1-s_\varrho{}''^2)\end{aligned}\right\}\ \rho,\sigma=1,2,3. \qquad \ldots\ldots(3.8)$$

$I_0=\frac{1}{2}E^2$ is intensity of the incident light.

§4. EXPANSION OF THE POLARIZABILITY IN TERMS OF NORMAL COORDINATES

We expand the polarizability tensor in powers of the small displacements $\mathbf{u}\left(\begin{matrix}l\\k\end{matrix}\right)$:

$$\alpha_{\varrho\sigma}\left(\begin{matrix}l\\k\end{matrix}\middle|\,\mathbf{u}\right)=\alpha^{(0)}_{\varrho\sigma}\left(\begin{matrix}l\\k\end{matrix}\right)+\alpha^{(1)}_{\varrho\sigma}\left(\begin{matrix}l\\k\end{matrix}\right)+\ldots, \qquad \ldots\ldots(4.1)$$

where $$\alpha^{(0)}_{\varrho\sigma}\left(\begin{matrix}l\\k\end{matrix}\right)=\alpha^{(0)}_{\varrho\sigma}(k), \qquad \alpha^{(1)}_{\varrho\sigma}\left(\begin{matrix}l\\k\end{matrix}\right)=\sum_{l'k'}\sum_\mu\alpha_{\varrho\sigma,\mu}\left(\begin{matrix}l-l'\\kk'\end{matrix}\right)u_\mu\left(\begin{matrix}l'\\k'\end{matrix}\right). \qquad \ldots\ldots(4.2)$$

The zero-order terms do not depend on the cell index l. The first order terms are regarded as produced by the contributions of the displacements $\mathbf{u}\begin{pmatrix} l' \\ k' \end{pmatrix}$ of any point $\begin{pmatrix} l' \\ k' \end{pmatrix}$ to the change of the polarizability of a given atom $\begin{pmatrix} l \\ k \end{pmatrix}$; the coefficients in the corresponding sum depend of course only on the difference $(l-l')$.

The total polarizability of the perturbed crystal is

$$\alpha_{\varrho\sigma}=\sum_{lk}\left[\alpha^{(0)}_{\varrho\sigma}(k)+\alpha^{(1)}_{\varrho\sigma}\begin{pmatrix} l \\ k \end{pmatrix}\right]\exp\left\{i\mathbf{Q}.\left[\mathbf{r}\begin{pmatrix} l \\ k \end{pmatrix}+\mathbf{u}\begin{pmatrix} l \\ k \end{pmatrix}\right]\right\}$$
$$=\sum_{lk}\left\{\left[\alpha^{(0)}_{\varrho\sigma}(k)+\sum_{l'k'}\sum_{\mu}\alpha_{\varrho\sigma,\mu}\begin{pmatrix} l-l' \\ kk' \end{pmatrix}u_\mu\begin{pmatrix} l' \\ k' \end{pmatrix}\right]\exp\left\{i\mathbf{Q}.\left[\mathbf{r}\begin{pmatrix} l \\ k \end{pmatrix}+\mathbf{u}\begin{pmatrix} l \\ k \end{pmatrix}\right]\right\}\right\}. \quad \ldots\ldots(4.3)$$

As $\mathbf{Q}.\mathbf{u}\begin{pmatrix} l \\ k \end{pmatrix}\ll 1$, put $\exp\left\{i\mathbf{Q}.\mathbf{u}\begin{pmatrix} l \\ k \end{pmatrix}\right\}=1+i\mathbf{Q}.\mathbf{u}\begin{pmatrix} l \\ k \end{pmatrix}$ and express $\mathbf{u}$ in terms of normal coordinates, according to (2.14). Omitting the constant term $\alpha^{(0)}_{\varrho\sigma}$ and the product $\alpha^{(1)}_{\varrho\sigma}\begin{pmatrix} l \\ k \end{pmatrix}\mathbf{u}\begin{pmatrix} l \\ k \end{pmatrix}$ one obtains

$$\alpha^{(1)}_{\varrho\sigma}=\sum_{lk}\sum_{\mu}\sum_{qj}\left[i\frac{\alpha^{(0)}_{\varrho\sigma}(k)}{\sqrt{m_k}}Q_\mu e_\mu\left(k\middle|\begin{matrix} q \\ j \end{matrix}\right)\exp\{i\mathbf{q}.\mathbf{r}(l)\}\right.$$
$$\left.+\sum_{l'k'}\frac{\alpha_{\varrho\sigma,\mu}\begin{pmatrix} l-l' \\ kk' \end{pmatrix}}{\sqrt{m_{k'}}}e_\mu\left(k'\middle|\begin{matrix} q \\ j \end{matrix}\right)\exp\{i\mathbf{q}.\mathbf{r}(l')\}\right]\exp\left\{i\mathbf{Q}.\mathbf{r}\begin{pmatrix} l \\ k \end{pmatrix}\right\}\xi\begin{pmatrix} q \\ j \end{pmatrix}. \quad \ldots\ldots(4.4)$$

Introducing $\mathbf{r}(l')=\mathbf{r}\begin{pmatrix} l \\ k \end{pmatrix}-\mathbf{r}\begin{pmatrix} l-l' \\ k \end{pmatrix}$ one can immediately see that $\alpha^{(1)}_{\varrho\sigma}$ is a δ-function of $(\mathbf{Q}+\mathbf{q})$. With $l-l'=l$ one gets

$$\alpha^{(1)}_{\varrho\sigma}=\sum_j\alpha_{\varrho\sigma}\begin{pmatrix} Q \\ j \end{pmatrix}\xi\begin{pmatrix} Q \\ j \end{pmatrix}, \quad \ldots\ldots(4.5)$$

where
$$\alpha_{\varrho\sigma}\begin{pmatrix} Q \\ j \end{pmatrix}=N\sum_{\mu}\sum_{k}\left[i\frac{\alpha^{(0)}_{\varrho\sigma}(k)}{\sqrt{m_k}}Q_\mu e_\mu\left(k\middle|\begin{matrix} Q \\ j \end{matrix}\right)\exp\{i\mathbf{Q}.\mathbf{r}(k)\}\right.$$
$$\left.+\sum_{lk'}\frac{\alpha_{\varrho\sigma,\mu}\begin{pmatrix} l \\ kk' \end{pmatrix}}{\sqrt{m_{k'}}}e_\mu\left(k'\middle|\begin{matrix} Q \\ j \end{matrix}\right)\exp\left\{i\mathbf{Q}.\mathbf{r}\begin{pmatrix} l \\ k \end{pmatrix}\right\}\right]. \quad \ldots\ldots(4.6)$$

Equation (4.6) shows that only those lattice vibrations are active in the Raman effect whose wave vector $\mathbf{q}$ equals $-\mathbf{Q}$ given by (3.2).

For visible and ultra-violet incident light the scalar product $\mathbf{Q}.\mathbf{r}\begin{pmatrix} l \\ k \end{pmatrix}\ll 1$, if l is restricted to the small values $\pm1, \pm2, \pm3, \ldots$ belonging to the atoms which are not too distant from the atom k. This restriction is admissible as the $\alpha_{\varrho\sigma,\mu}\begin{pmatrix} l \\ kk' \end{pmatrix}$ fall rapidly with l. Hence one can expand the exponential and neglect terms of second or higher order in $\mathbf{Q}$:

$$\alpha_{\varrho\sigma}\begin{pmatrix} Q \\ j \end{pmatrix}=N\sum_{\mu}\sum_{k}\left\{i\frac{\alpha^{(0)}_{\varrho\sigma}(k)}{\sqrt{m_k}}Q_\mu e_\mu\left(k\middle|\begin{matrix} Q \\ j \end{matrix}\right)\right.$$
$$\left.+\sum_{lk'}\frac{\alpha_{\varrho\sigma,\mu}\begin{pmatrix} l \\ kk' \end{pmatrix}}{\sqrt{m_{k'}}}\left[1+i\mathbf{Q}.\mathbf{r}\begin{pmatrix} l \\ k \end{pmatrix}\right]e_\mu\left(k'\middle|\begin{matrix} Q \\ j \end{matrix}\right)\right\}. \quad \ldots\ldots(4.7)$$

The physical meaning of (4.7) becomes more evident if the relative difference

$$\Delta_\mu\left(kk'\left|\frac{Q}{j}\right.\right)=\frac{e_\mu\left(k'\left|\frac{Q}{j}\right.\right)\Big/\sqrt{m_{k'}}-e_\mu\left(k\left|\frac{Q}{j}\right.\right)\Big/\sqrt{m_k}}{e_\mu\left(k\left|\frac{Q}{j}\right.\right)\Big/\sqrt{m_k}}=\frac{u_\mu\left(k'\left|\frac{Q}{j}\right.\right)-u_\mu\left(k\left|\frac{Q}{j}\right.\right)}{u_\mu\left(k\left|\frac{Q}{j}\right.\right)} \qquad \ldots\ldots(4.8)$$

of the displacements of the different atoms in the elementary cell is introduced. Equation (4.7) is transformed into

$$\alpha_{\varrho\sigma}\left(\frac{Q}{j}\right)=N\sum_{\mu}\sum_{k}\Big\{i\alpha^{(0)}_{\varrho\sigma}(k)\,Q_\mu + \sum_{lk'}\alpha_{\varrho\sigma,\mu}\left(\frac{l}{kk'}\right)\left[1+i\mathbf{Q}\cdot\mathbf{r}\left(\frac{l}{k}\right)\right]\left[1+\Delta_\mu\left(kk'\left|\frac{Q}{j}\right.\right)\right]\Big\}u_\mu\left(k\left|\frac{Q}{j}\right.\right). \qquad \ldots\ldots(4.9)$$

In the second term of this equation all terms not depending on l and k' can be eliminated with the help of the general invariance relation

$$\sum_{lk'}\alpha_{\varrho\sigma,\mu}\left(\frac{l}{kk'}\right)=0, \qquad \ldots\ldots(4.10)$$

which follows from the invariance of $\alpha_{\varrho\sigma}$ against rigid translations of the whole lattice. Hence, (4.9) becomes

$$\alpha_{\varrho\sigma}\left(\frac{Q}{j}\right)=N\sum_{\mu}\sum_{k}\Big\{i\alpha^{(0)}_{\varrho\sigma}(k)Q_\mu+\sum_{lk'}\alpha_{\varrho\sigma,\mu}\left(\frac{l}{kk'}\right)\left[i\mathbf{Q}\cdot\mathbf{r}(l)+\Delta_\mu\left(kk'\left|\frac{Q}{j}\right.\right)+i\mathbf{Q}\cdot\mathbf{r}\left(\frac{l}{k}\right)\Delta_\mu\left(kk'\left|\frac{Q}{j}\right.\right)\right]\Big\}u_\mu\left(k\left|\frac{Q}{j}\right.\right). \qquad \ldots\ldots(4.11)$$

This expression behaves very differently for elastic vibrations (index e) and optical vibrations (index o). For elastic vibrations it is convenient to express $\Delta_\mu\left(kk'\left|\frac{Q}{j_e}\right.\right)$ as the sum of two terms:

$$\Delta_\mu\left(kk'\left|\frac{Q}{j_e}\right.\right)=\Delta^{(0)}_\mu\left(kk'\left|\frac{Q}{j_e}\right.\right)+\Delta^{(1)}_\mu\left(kk'\left|\frac{Q}{j_e}\right.\right). \qquad \ldots\ldots(4.12)$$

Here $\Delta^{(0)}_\mu\left(kk'\left|\frac{Q}{j_e}\right.\right)$ represents the contribution of the zero order displacement $\mathbf{W}$ of equation (2.17) and $\Delta^{(1)}_\mu\left(kk'\left|\frac{Q}{j_e}\right.\right)$ the contribution of $\mathbf{W}^{(1)}$ of (2.19). Both terms are simple functions of the wave vector $\mathbf{Q}$.

As mentioned in § 2 after equation (2.16) the zero order amplitudes $\mathbf{W}(k)/\sqrt{m_k}$ are independent of k; hence $\mathbf{u}\left(k\left|\frac{Q}{j_e}\right.\right)=\mathbf{V}(k)/\sqrt{m_k}=(\mathbf{W}/\sqrt{m_k})\exp\{-i\mathbf{Q}\cdot\mathbf{r}(k)\}$ depend on k only through the exponential factor and one has

$$\Delta^{(0)}_\mu\left(kk'\left|\frac{Q}{j_e}\right.\right)=i\mathbf{Q}\cdot\mathbf{r}(kk')=i\sum_\nu Q_\nu r_\nu(kk'). \qquad \ldots\ldots(4.13)$$

The second term of (4.12) has according to (2.19), (2.20), (2.21) the form

$$\Delta^{(1)}_\mu\left(kk'\left|\frac{Q}{j_e}\right.\right)=i\sum_{\nu\eta}\Gamma_{\mu\nu\eta}Q_\eta u_\nu\left(k\left|\frac{Q}{j_e}\right.\right)\Big/u_\mu\left(k\left|\frac{Q}{j_e}\right.\right). \qquad \ldots\ldots(4.14)$$

Substitute (4.13) and (4.14) in (4.11) and neglect all terms of second or higher order in $\mathbf{Q}$, then

$$\alpha_{\varrho\sigma}\left(\frac{Q}{j_e}\right)=iN\sum_{\mu}\sum_{k}\left\{\alpha^{(0)}_{\varrho\sigma}(k)Q_\mu+\sum_{lk'}\sum_{\nu}\left[\alpha_{\varrho\sigma,\mu}\left(\frac{l}{kk'}\right)Q_\nu\mathfrak{T}_\nu\left(\frac{l}{kk'}\right)\right.\right.$$
$$\left.\left.+\sum_{\eta}\Gamma_{\mu\nu\eta}Q_\eta u_\nu\left(k\left|\frac{Q}{j_e}\right.\right)\Big/u_\mu\left(k\left|\frac{Q}{j_e}\right.\right)\right]\right\}u_\mu\left(k\left|\frac{Q}{j_e}\right.\right). \quad \ldots\ldots(4.15)$$

Arrange with respect to the $u_\mu\left(k\left|\frac{Q}{j_e}\right.\right)$, then

$$\alpha_{\varrho\sigma}\left(\frac{Q}{j_e}\right)=\sum_{\mu}\alpha_{\varrho\sigma,\mu}\left(\frac{Q}{j_e}\right)u_\mu\left(\frac{Q}{j_e}\right), \quad \ldots\ldots(4.16)$$

where
$$\alpha_{\varrho\sigma,\mu}\left(\frac{Q}{j_e}\right)=iN\sum_{k}\left\{\alpha^{(0)}_{\varrho\sigma}(k)Q_\mu+\sum_{lk'}\sum_{\nu}\left[\alpha_{\varrho\sigma,\mu}\left(\frac{l}{kk'}\right)Q_\nu\mathfrak{T}_\nu\left(\frac{l}{kk'}\right)\right.\right.$$
$$\left.\left.+\sum_{\eta}\alpha_{\varrho\sigma,\eta}\left(\frac{l}{kk'}\right)\Gamma_{\eta\mu\nu}Q_\nu\right]\right\}. \quad \ldots\ldots(4.17)$$

This is the general formula for the polarizability changes connected with elastic waves. It consists of two parts: the second term (summation over ν, l, k') describes the effective changes of the polarizability of the single atoms, the first the variations of the phase relations during a vibration. It will be seen in (6.47) that both terms have the same order of magnitude and that the phase term is indispensable to obtain agreement between theory and experiment.

In the case of optical vibrations there does not exist a simple relation between the $\Delta_\mu\left(kk'\left|\frac{Q}{j_o}\right.\right)$ and the wave vector $\mathbf{Q}$. One can only say that $\Delta_\mu\left(kk'\left|\frac{Q}{j_o}\right.\right)$ is of the order 1, i.e. 10^3 times bigger than for those long elastic vibrations which produce the Raman effect with ultra-violet and visible light. One can, therefore, neglect in (4.11) all terms containing $\mathbf{Q}$ and obtain

$$\alpha_{\varrho\sigma,\mu}\left(\frac{Q}{j_o}\right)=N\sum_{k}\sum_{lk'}\alpha_{\varrho\sigma,\mu}\left(\frac{l}{kk'}\right)\Delta_\mu\left(kk'\left|\frac{Q}{j_o}\right.\right). \quad \ldots\ldots(4.18)$$

Summarizing, the stituation is this: With regard to the scattering power the essential difference between the optical and the elastic vibrations is represented by the different values of $\Delta_\mu\left(kk'\left|\frac{Q}{j_o}\right.\right)$ and $\Delta_\mu\left(kk'\left|\frac{Q}{j_e}\right.\right)$. For optical vibrations the local distortion of the lattice, measured by $\Delta_\mu\left(kk'\left|\frac{Q}{j}\right.\right)$ is large and the scattering power is strong. For elastic vibrations the local distortion is nearly zero and the scattering power at 0° K. is extremely weak. This difference, however, is less pronounced with increasing temperature, which can be shown as follows:

The thermal average $\langle i_{\varrho\sigma,\mu\nu}\rangle_{\mathrm{av}}$ for a single transition $v\rightarrow v\pm1$ of the vibration $\left(\frac{Q}{j}\right)$ is, with the notation of Smith (1948),

$$\langle i_{\varrho\sigma,\mu\nu}\rangle_{\mathrm{av}}=2C\left(\frac{Q}{j}\right)\left\{\alpha_{\varrho\sigma}\left(\frac{Q}{j}\right)\alpha_{\mu\nu}{}^{*}\left(\frac{Q}{j}\right)\right\}\begin{cases}1 \text{ for Stokes lines}\\ \exp(-h\nu_j/kT) \text{ for anti-Stokes lines,}\end{cases} \quad \ldots\ldots(4.19)$$

where
$$C\left(\frac{Q}{j}\right)=\frac{h}{2\pi N\nu\left(\frac{Q}{j}\right)}\frac{1}{1-\exp\left\{-h\nu\left(\frac{Q}{j}\right)\Big/kT\right\}}. \quad \ldots\ldots(4.20)$$

Hence, for the elastic branches, where $h\nu \ll kT$

$$C\left(\frac{Q}{j_e}\right) = kT \Big/ 2\pi N \nu^2 \left(\frac{Q}{j_e}\right). \qquad \ldots\ldots (4.21)$$

According to (4.21) the intensity of the Raman effect with elastic waves is proportional to T and increases considerably if the temperature is raised. On the contrary, for the high-frequency optical waves, which are only weakly thermally excited at room temperature, $C\left(\frac{Q}{j}\right)$ of (4.20) does not depend very much on T and there is no strong increase of scattering intensity with temperature. This different temperature dependence favours the intensity of the Raman effect with elastic waves as compared with the optical Raman effect and compensates the fact that the local distortion is much bigger for the optical than for the elastic vibrations.

Further, according to (4.21) the Raman effect for elastic waves should vanish if $T = 0°$ K. But as the condition $h\nu \ll kT$ loses its validity even for the low frequency elastic vibrations if $T \to 0$, (4.21) is no more applicable andonly (4.20) gives a correct expression for the intensity. Here $C\left(\frac{Q}{j_e}\right) \neq 0$ if $T = 0°$ K.

§ 5. THE BRILLOUIN COMPONENTS OF THE SCATTERED LIGHT

As mentioned in the introduction, there is no light scattering with unchanged frequency in perfect crystals if the wavelength of the light is greater than the lattice constants. Instead a set of six lines will appear in the scattering spectrum, which forms two groups symmetrical with respect to the frequency of the incident radiation. The frequency shifts $\Delta\nu$ are usually extremely small and can be detected only by very subtle interferometric methods. Only under particularly favourable conditions does $\Delta\nu$ assume larger values which, however, do not exceed 10 cm^{-1} for ultra-violet incident light. Such favourable conditions actually occur if the index of refraction and the eigen-frequencies of the scattering crystal are high. This happens in the case of diamond. These lines had been predicted by Brillouin in 1922, six years before the discovery of the Raman effect, from an ingenious consideration, and they are called the Brillouin components of the scattered light.

Brillouin interpreted the effect as reflection of the light waves on the elastic waves with Doppler shift. He showed that, in analogy to the Bragg condition, the wave vectors $\mathbf{Q}$, $\mathbf{Q}'$ and $\mathbf{Q}''$ of the elastic, the incident and the scattered wave must fulfil equation (3.2); further that the frequency shifts can be explained as Doppler effect, the reflecting waves moving with the velocity of sound. This explanation implies that the thermal excitation of the eigen-vibrations is a necessary condition for the Brillouin scattering.

The explanation suggested here regards the Brillouin components as Raman lines produced by the elastic waves. They are the Stokes and anti-Stokes Raman lines of those vibrations of the three elastic branches of the crystal, whose wave vector $\mathbf{Q}$ fulfils the condition (3.2); the small number of Raman lines is due to the fact expressed by equation (4.6) that most of the vibrations of the crystal are ineffective, due to mutual interference of the scattered light.

The treatment of the Brillouin components as Raman lines allows a rigorous calculation of their intensities. The attempts to obtain the intensities from

Brillouin's own interpretation have so far not been quite successful. An intensity formula has been derived by Leontowitsch and Mandelstamm (1931), namely

$$I=\frac{\pi^2}{2\lambda^4}kTn^8\left\{\frac{2(p_{12}^2+p_{44}^2)}{c_{11}+c_{12}+2c_{44}}+\frac{p_{44}^2}{c_{44}}\right\}, \qquad \ldots\ldots(5.1)$$

where λ is the wavelength of the incident light, n the index of refraction, T the temperature, c_{ik} = elastic constants and p_{ik} Pockel's elasto-optical constants.

This formula has been developed by an immediate extension of Einstein's scattering formula for liquids to crystals. It is based on classical continuum theory and on classical electrodynamics and statistics. The applicability of the theory is therefore confined to temperatures for which the classical approximation is still valid. According to (5.1) the intensity should vanish at 0° K., whereas the correct quantum mechanical formula predicts a finite intensity, which is in the case of diamond about 50 times smaller than it is at room temperature.

A further simplification of Leontowitsch and Mandelstamm consists in neglecting the time dependency of the thermal fluctuations in the crystal. Hence there is no frequency shift between the incident and the scattered light and the frequencies of the active lattice vibrations do not appear explicitly in the formula. A rather important detail is omitted by this approximation, as the intensities are in fact inversely proportional to the square of the lattice frequencies (see equation (4.21)).

In Müller's (1938) derivation of (5.1), which is based on Brillouin's theory for liquids, the wave character, i.e. the time dependence of the thermal fluctuations, is taken into account. Here the individual frequencies of the lattice vibrations vanish by averaging over all the wave vectors. Hence (5.1) represents the total scattering of a thermally excited crystal and not the light scattered by a single elastic wave for a single angle of deflection betwen the incident and observed light. (This was the case investigated experimentally by Krishnan.) Finally, (5.1) does not contain the phase term $\alpha_{\varrho\sigma}^{(0)}Q_\mu$ so that it neglects a decisive contribution to the intensity of the Brillouin components.

§ 6. THE BRILLOUIN COMPONENTS OF DIAMOND

(i) *Lattice Dynamics of Diamond*

Frequency and eigen-vectors of the elastic vibrations of diamond can be calculated from equation (2.17), which for cubic crystals has the form (**s** unit vector with direction of **Q**)

$$\begin{vmatrix} As_x^2-E & s_xs_y & s_zs_x \\ s_xs_y & As_y^2-E & s_ys_z \\ s_zs_x & s_ys_z & As_z^2-E \end{vmatrix} W=0, \qquad \ldots\ldots(6.1)$$

where

$$\frac{\rho v^2-c_{44}}{c_{12}+c_{44}}=E, \frac{c_{11}-c_{44}}{c_{12}+c_{44}}=A, v=\frac{\omega}{|\mathbf{Q}|}=\text{velocity of sound}, \rho=\frac{m}{a^3}=3{\cdot}5 \text{ for diamond.} \qquad \ldots\ldots(6.2)$$

This equation can easily be solved for some special cases. For the case $Q_x=Q_y=Q_z$,

$$\left.\begin{aligned} &E_{1,2}=s_x^2(A-1), E_3=s_x^2(A+2), \\ &\mathbf{W}_1=\left(\frac{1}{\sqrt{2}},-\frac{1}{\sqrt{2}},0\right), \mathbf{W}_2=\left(\frac{1}{\sqrt{6}},\frac{1}{\sqrt{6}},-\frac{2}{\sqrt{6}}\right), \mathbf{W}_3=\left(\frac{1}{\sqrt{3}},\frac{1}{\sqrt{3}},\frac{1}{\sqrt{3}}\right). \end{aligned}\right\} \qquad (6.3)$$

For the case $Q_x, Q_y = Q_z = 0$,

$$E_{1,2} = 0, E_3 = s_x^2 A, \quad \mathbf{W}_1 = (0,1,0), \mathbf{W}_2 = (0,0,1), \mathbf{W}_3 = (1,0,0). \qquad \ldots\ldots (6.4)$$

For the case $Q_x = 0$, Q_y, Q_z,

$$E_{1,3} = \tfrac{1}{2}A[s_y^2 + s_z^2 \pm \{A^2(s_y^2 - s_z^2) + 4 s_y^2 s_z^2\}^{1/2}], \; E_2 = 0. \qquad \ldots\ldots (6.5)$$

The eigen-vectors are found by substituting (6.5) in (6.1).

A general solution for all wave vectors can be obtained with the help of a perturbation method used in quantum mechanics, starting from the fact that the isotropic case can be solved rigorously. In this case one has $c_{11} - c_{44} = c_{12} + c_{44}$, $A = 1$.

We put $A = 1 + \gamma$ and introduce the matrices

$$H^{(0)} = \begin{vmatrix} s_x^2 & s_x s_y & s_x s_z \\ s_x s_y & s_y^2 & s_y s_z \\ s_x s_z & s_y s_z & s_z^2 \end{vmatrix}, \quad H^{(1)} = \begin{vmatrix} s_x^2 & 0 & 0 \\ 0 & s_y^2 & 0 \\ 0 & 0 & s_z^2 \end{vmatrix}. \qquad \ldots\ldots (6.6)$$

Then (6.1) reads $$(H^{(0)} + \gamma H^{(1)})\, W = EW. \qquad \ldots\ldots (6.7)$$

For $\gamma = 0$ we have $$H^{(0)} W^{(0)} = E^{(0)} W^{(0)}, \qquad \ldots\ldots (6.8)$$

with the solutions (θ, ϕ polar coordinates of $\mathbf{s}$)

$$E_1^{(0)} = 0, \; \mathbf{W}_1^{(0)} = (\sin\phi, -\cos\phi, 0), \qquad \ldots\ldots (6.9)$$

$$E_2^{(0)} = \theta, \; \mathbf{W}_2^{(0)} = (\cos\theta\cos\phi, \cos\theta\sin\phi, -\sin\theta), \qquad \ldots\ldots (6.10)$$

$$E_3^{(0)} = 1, \; \mathbf{W}_3^{(0)} = (\sin\theta\cos\phi, \sin\theta\sin\phi, \cos\theta) = \mathbf{s}, \qquad \ldots\ldots (6.11)$$

which express that in the isotropic medium there are one strictly longitudinal and two transverse waves, i.e.

$$\mathbf{W}_1^{(0)} \cdot \mathbf{s} = \mathbf{W}_2^{(0)} \cdot \mathbf{s} = \mathbf{W}_1^{(0)} \cdot \mathbf{W}_2^{(0)} = 0, \quad \mathbf{W}_3^{(0)} \cdot \mathbf{s} = 1. \qquad \ldots\ldots (6.12)$$

Equations (6.9) and (6.10) are not the only possible solutions. Each linear superposition $x_1 \mathbf{W}_1^{(0)} + x_2 \mathbf{W}_2^{(0)}$ can be chosen as well. If $\gamma \neq 0$ we expand

$$E_\alpha = E_\alpha^{(0)} + \gamma E_\alpha^{(1)}, \quad \mathbf{W}_\alpha = \mathbf{W}_\alpha^{(0)} + \gamma \mathbf{W}_\alpha^{(1)} \qquad \ldots\ldots (6.13)$$

and obtain the first order equation

$$(H^{(0)} - E_\alpha^{(0)})\, W_\alpha^{(1)} = (E_\alpha^{(1)} - H^{(1)})\, W_\alpha^{(0)}. \qquad \ldots\ldots (6.14)$$

The condition for the solubility of (6.14) is

$$\text{for } \alpha = 1, 2: \quad (a - E_{1,2}^{(1)})\, x_1 + c x_2 = 0, \quad c x_1 + (b - E_{1,2}^{(1)}) x_2 = 0 \qquad \ldots\ldots (6.15)$$

$$\text{for } \alpha = 3: \quad (d - E_3^{(1)}) x_3 = 0,$$

$$\text{where} \quad \begin{aligned} (H^{(1)} \mathbf{W}_1^{(0)} \cdot \mathbf{W}_1^{(0)}) &= \tfrac{1}{2}\sin^2\theta \sin^2 2\phi = a, \\ (H^{(1)} \mathbf{W}_2^{(0)} \cdot \mathbf{W}_2^{(0)}) &= \tfrac{1}{32}\sin^2 2\theta\,(\cos 4\phi + 14) = b, \\ (H^{(1)} \mathbf{W}_1^{(0)} \cdot \mathbf{W}_2^{(0)}) &= \tfrac{1}{4}\sin^2\theta \cos\theta \sin 4\phi = c, \\ (H^{(1)} \mathbf{s} \cdot \mathbf{s}) \quad &= \tfrac{1}{8}\sin^4\theta\,(\cos 4\phi + 6) + \cos^4\theta = d. \end{aligned} \qquad \ldots\ldots (6.16)$$

The solutions are

$$E_{1,2}^{(1)} = \tfrac{1}{2}\{a + b \pm \sqrt{g}\}, \; E_3^{(1)} = d,$$

$$(x_1)_{1,2} = -\frac{2c}{(4g)^{1/4}(a - b \pm \sqrt{g})^{1/2}}, \quad (x_2)_{1,2} = \frac{(a - b \pm \sqrt{g})^{1/2}}{(4g)^{1/4}}. \qquad \ldots\ldots (6.17)$$

Equations (6.17) together with (6.9) and (6.10) gives the eigen-vectors of the zero th order in γ. These are still normal to **s** and describe a pair of transverse waves. In the higher approximation of (6.14) the pure transversality of the waves generally vanishes.

Up to now all formulae in § 6(i) referred to the displacements **W** of zero order in **Q**, which are independent of the index k. For the calculation of the intensity of the Brillouin components, however, the relative differences $\Delta_\mu^{(1)}\left(kk'\left|\begin{matrix}Q\\ j_e\end{matrix}\right.\right)$ introduced in (4.14) must be known. They have been given by Smith (1948) by the following matrix equation:

$$\Delta^{(1)}\left(1,2\left|\begin{matrix}Q\\ j_e\end{matrix}\right.\right)=\frac{i\alpha\beta}{2\alpha}\begin{vmatrix}0 & Q_z/W_x & Q_y/W_x\\ Q_z/W_y & 0 & Q_x/W_y\\ Q_y/W_z & Q_x/W_z & 0\end{vmatrix}W \qquad \ldots\ldots(6.18)$$

where $\beta/\alpha=0{\cdot}66$ is the ratio of the force constants of diamond.

Comparison between (6·18) and (4.14) yields

$$\Gamma_{\mu\nu\eta}=a\beta/2\alpha \quad \text{for} \quad \mu\neq\nu\neq\eta. \qquad \ldots\ldots(6.19)$$

All the other $\Gamma_{\mu\nu\eta}$ are zero.

The determination of the eigen-frequencies and eigen-vectors for the optical branches is more complicated than for the elastic ones. Using the notation of Smith (1948) equation (2.16) for diamond becomes

$$\begin{vmatrix}F-\Lambda & J & K & A & B & C\\ J & G-\Lambda & L & B & A & E\\ K & L & H-\Lambda & C & E & A\\ A^* & B^* & C^* & F-\Lambda & J & K\\ B^* & A^* & E^* & J & G-\Lambda & L\\ C^* & E^* & A^* & K & L & H-\Lambda\end{vmatrix}e=0. \qquad \ldots\ldots(6.20)$$

The $A, B, \ldots L$ are known functions of the wave vector **Q**. Equation (6.20) can be written in matrix form

$$M_{11}e_1+M_{12}e_2=0, \qquad M_{12}^*e_1+M_{11}e_2=0. \qquad \ldots\ldots(6.20\,a)$$

e_1, e_2 are the column matrices which represent the displacements $\mathbf{e}_1, \mathbf{e}_2$ of the two atoms in the elementary cell of diamond and

$$M_{11}=\begin{vmatrix}F-\Lambda & J & K\\ J & G-\Lambda & L\\ K & L & H-\Lambda\end{vmatrix}, \quad M_{12}=\begin{vmatrix}A & B & C\\ B & A & E\\ C & E & A\end{vmatrix}. \qquad \ldots\ldots(6.21)$$

M_{11} and M_{12} are both symmetrical, hence

$$M_{11}=\tilde{M}_{11},\ M_{12}=\tilde{M}_{12},\ M_{11}.M_{12}=M_{21}.M_{11}. \qquad \ldots\ldots(6.22)$$

Multiply (6.20 *a*) by M_{11}, then

$$M_{11}^2e_1+M_{12}.M_{11}e_2=0, \quad M_{12}^*M_{11}e_1+M_{11}^2e_2=0. \qquad \ldots\ldots(6.23)$$

Substituting for $M_{11}e_2 = -M_{12}^* e_1$ and $M_{11}e_1 = -M_{12}e_2$ from (6.20 *a*)

$$(M_{11}^2 - M_{12}M_{12}^*)e_1 = 0\,,\ (M_{11}^2 - M_{12}^* M_{12})e_2 = 0\,. \qquad \ldots\ldots (6.24)$$

We have thus reduced equation (6.19) of the sixth order to two equations (6.24) of the third order†. Each of them gives the eigen-values. The eigen-vectors $\mathbf{e}_1$ and $\mathbf{e}_2$ cannot be completely determined from the homogeneous equations (6.24): two complex factors λ_1 and λ_2 remain undetermined, which can be found by inserting $\lambda_1\mathbf{e}_1$ and $\lambda_2\mathbf{e}_2$ in (6.19) and by making use of the orthogonality relations (2.15).

The special case used in the following is that for which $Q_x = Q_y = Q_z$ and $\mathbf{Q}\cdot\mathbf{r}(k') \ll 1$. The eigen-vectors are found to be

$$e_1(1) = -e_2(1) = \left(\frac{1}{\sqrt{2}}, -\frac{1}{\sqrt{2}}, 0\right),\ e_1(2) = -e_2(2) = \left(\frac{1}{\sqrt{6}}, \frac{1}{\sqrt{6}}, -\frac{2}{\sqrt{6}}\right),$$

$$e_1(3) = -e_2(3) = \left(\frac{1}{\sqrt{3}}, \frac{1}{\sqrt{3}}, \frac{1}{\sqrt{3}}\right). \qquad \ldots\ldots (6.25)$$

(ii) *The Symmetry of Diamond*

Notations used in text and figures are those of Smith (1948). Figure 1 shows the elementary cell of diamond.

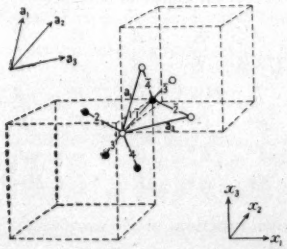

Figure 1. First neighbours of the two carbon atoms in the unit cell of diamond.

The values of the rectangular components of $\mathbf{r}\begin{pmatrix} l \\ kk' \end{pmatrix}$ for the first neighbours of O and O′ are given in Table 1.

Table 1

r \ l	1	2	3	4	r \ $\bar{l}$	$\bar{1}$	$\bar{2}$	$\bar{3}$	$\bar{4}$
x_1	$\frac{1}{2}a$	$-\frac{1}{2}a$	$-\frac{1}{2}a$	$\frac{1}{2}a$	x_1	$-\frac{1}{2}a$	$\frac{1}{2}a$	$\frac{1}{2}a$	$-\frac{1}{2}a$
x_2	$\frac{1}{2}a$	$-\frac{1}{2}a$	$\frac{1}{2}a$	$-\frac{1}{2}a$	x_2	$-\frac{1}{2}a$	$\frac{1}{2}a$	$-\frac{1}{2}a$	$\frac{1}{2}a$
x_3	$\frac{1}{2}a$	$\frac{1}{2}a$	$-\frac{1}{2}a$	$-\frac{1}{2}a$	x_3	$-\frac{1}{2}a$	$-\frac{1}{2}a$	$\frac{1}{2}a$	$\frac{1}{2}a$

a = lattice constant $= 1{\cdot}78 \times 10^{-8}$ cm. It follows from Table 1 that

$$\Sigma_l \mathbf{Q}\cdot\mathbf{r}(l) = 0,\ \Sigma_l \mathbf{Q}\cdot\mathbf{r}(\bar{l}) = 0,\ \ l = -\bar{l}. \qquad \ldots\ldots (6.26)$$

† A similar reduction has been given already by Born (1914).

The symmetry operations of the diamond lattice can be described by six transformations together with a re-labelling of the lattice points (see Born and Begbie 1947).

$$T_1 = \left|\begin{matrix} 0 & 1 & 0 \\ 0 & 0 & 1 \\ 1 & 0 & 0 \end{matrix}\right| \quad \begin{matrix} (1) & (2,3) & (3,4) & (4,2) \\ (\bar{1}) & (\bar{2},\bar{3}) & (\bar{3},\bar{4}) & (\bar{4},\bar{2}) \end{matrix} \qquad \ldots\ldots(6.27)$$

$$T_2 = \left|\begin{matrix} -1 & 0 & 0 \\ 0 & -1 & 0 \\ 0 & 0 & -1 \end{matrix}\right| \quad (1,\bar{1}) \quad (2,\bar{2}) \quad (3,\bar{3}) \quad (4,\bar{4}) \qquad \ldots\ldots(6.28)$$

$$T_3 = \left|\begin{matrix} 0 & 1 & 0 \\ 1 & 0 & 0 \\ 0 & 0 & 1 \end{matrix}\right| \quad (1) \quad (2) \quad (3,4) \quad (\bar{1}) \quad (\bar{2}) \quad (\bar{3},\bar{4}) \qquad \ldots\ldots(6.29)$$

$$T_4 = \left|\begin{matrix} 0 & -1 & 0 \\ 0 & 0 & -1 \\ 1 & 0 & 0 \end{matrix}\right| \quad \begin{matrix} (3) & (1,2) & (2,4) & (4,1) \\ (\bar{3}) & (\bar{1},\bar{2}) & (\bar{2},\bar{4}) & (\bar{4},\bar{1}) \end{matrix} \qquad \ldots\ldots(6.30)$$

$$T_5 = \left|\begin{matrix} 0 & 1 & 0 \\ 0 & 0 & -1 \\ -1 & 0 & 0 \end{matrix}\right| \quad \begin{matrix} (2) & (1,4) & (3,1) & (4,3) \\ (\bar{2}) & (\bar{1},\bar{4}) & (\bar{3},\bar{1}) & (\bar{4},\bar{3}) \end{matrix} \qquad \ldots\ldots(6.31)$$

$$T_6 = \left|\begin{matrix} 0 & -1 & 0 \\ 0 & 0 & 1 \\ -1 & 0 & 0 \end{matrix}\right| \quad \begin{matrix} (4) & (1,3) & (2,1) & (3,2) \\ (\bar{4}) & (\bar{1},\bar{3}) & (\bar{2},\bar{1}) & (\bar{3},\bar{2}) \end{matrix} \qquad \ldots\ldots(6.32)$$

By applying the transformation matrices T, lattice tensors of different rank are transformed in the following way :

$$X_\alpha' = \sum_{\alpha'} T_{\alpha\alpha'} X_{\alpha'} \text{ or } X' = TX \qquad \text{(first rank)} \qquad \ldots\ldots(6.33)$$

$$X'_{\alpha\beta} = \sum\sum_{\alpha'\,\beta'} T_{\alpha\alpha'} T_{\beta\beta'} X_{\alpha'\beta'} \text{ or } X' = TX\tilde{T} \qquad \text{(second rank)} \qquad \ldots\ldots(6.34)$$

$$X'_{\alpha\beta\gamma} = \sum\sum\sum_{\alpha'\,\beta'\,\gamma'} T_{\alpha\alpha'} T_{\beta\beta'} T_{\gamma\gamma'} X_{\alpha'\beta'\gamma'} \qquad \text{(third rank)} \qquad \ldots\ldots(6.35)$$

Application of (6.27) to (6.32), (6.35) and (4.9) gives the results of Table 2.

Table 2.

$\alpha_{\varrho\sigma,\mu}\begin{pmatrix} l \\ OO' \end{pmatrix}$ \ l	0	1	2	3	4
$\alpha_{11,1}$	0	A	$-A$	$-A$	A
$\alpha_{22,2}$	0	A	$-A$	A	$-A$
$\alpha_{33,3}$	0	A	A	$-A$	$-A$
$\alpha_{11,2}=\alpha_{33,2}$	0	B	$-B$	B	$-B$
$\alpha_{22,3}=\alpha_{11,3}$	0	B	B	$-B$	$-B$
$\alpha_{33,1}=\alpha_{22,1}$	0	B	$-B$	$-B$	B

$\alpha_{\varrho\sigma,\mu}\begin{pmatrix} l \\ OO' \end{pmatrix}$ \ l	0	1	2	3	4
$\alpha_{12,1}=\alpha_{23,3}=\alpha_{21,1}=\alpha_{32,3}$	0	E	$-E$	E	$-E$
$\alpha_{23,2}=\alpha_{31,1}=\alpha_{32,2}=\alpha_{13,1}$	0	E	E	$-E$	$-E$
$\alpha_{31,3}=\alpha_{12,2}=\alpha_{13,3}=\alpha_{21,2}$	0	E	$-E$	$-E$	E
$\alpha_{12,3}=\alpha_{21,3}$	$-4D$	D	D	D	D
$\alpha_{23,1}=\alpha_{32,1}$	$-4D$	D	D	D	D
$\alpha_{31,2}=\alpha_{13,2}$	$-4D$	D	D	D	D

The $\alpha_{\varrho\sigma,\mu}\begin{pmatrix} \bar{l} \\ O'O \end{pmatrix}$ are found with the help of the relation

$$\alpha_{\varrho\sigma,\mu}\begin{pmatrix} l \\ OO' \end{pmatrix} = -\alpha_{\varrho\sigma,\mu}\begin{pmatrix} \bar{l} \\ O'O \end{pmatrix}. \qquad \ldots\ldots(6.36)$$

(iii) *The Frequency Shifts of the Brillouin Components of Diamond*

Corresponding to the experimental work of Krishnan we shall now treat the case that $\mathbf{Q}''$ is normal to $\mathbf{Q}'$ and that $\mathbf{Q}$ has the direction of the cubic diagonal: $Q_x = Q_y = Q_z$. From (3.2) we find

$$|\mathbf{Q}| = \frac{2\pi\sqrt{2}}{\lambda} = \frac{2\sqrt{2}\pi\nu_0 n}{c_0} = 9{\cdot}14 \times 10^5\,\mathrm{cm}^{-1}; \qquad \ldots\ldots(6.37)$$

ν_0 is the frequency of the incident light $= 1{\cdot}185 \times 10^{15}\,\mathrm{sec}^{-1}$, c_0 the velocity of light in vacuum; $n = 2{\cdot}61$ = index of refraction of diamond for $\lambda = 2536{\cdot}5$ A.,

$$Q_x = Q_y = Q_z = |\mathbf{Q}|/\sqrt{3} = 5{\cdot}27 \times 10^5\,\mathrm{cm}^{-1}. \qquad \ldots\ldots(6.38)$$

Substituting (6.37) in (6.3) and using the values of the elastic constants given by Bhagavantam and Bhimasenachar (1946) and used by Smith (1948)

$$c_{11} = 9{\cdot}5 \times 10^{12}\,\mathrm{dyne/cm^2}, \quad c_{12} = 3{\cdot}9 \times 10^{12}\,\mathrm{dyne/cm^2}, \quad c_{44} = 5{\cdot}0 \times 10^{12}\,\mathrm{dyne/cm^2}, \qquad \ldots\ldots(6.39)$$

we find for the frequencies (the experimental values are given in brackets)

$$\nu_{1,2} = 4{\cdot}9\,\mathrm{cm}^{-1}\,(5{\cdot}4\,\mathrm{cm}^{-1}), \quad \nu_3 = 9\,\mathrm{cm}^{-1}\,(8{\cdot}8\,\mathrm{cm}^{-1}). \qquad \ldots\ldots(6.40)$$

(iv) *The Intensity of the Brillouin Components of Diamond*

To calculate the intensities one begins with the summation over l, k, k' of equation (4.17) which reduces the 135 elements $\alpha_{\varrho\sigma,\mu}\begin{pmatrix} l \\ kk' \end{pmatrix}$ of Table 2 to the 27 terms $\alpha_{\varrho\sigma,\mu}\begin{pmatrix} Q \\ j \end{pmatrix}$. Next, the summation over μ, ν, η is performed according to (4.16), (4.17), which again reduces the number of terms to the nine elements of the first order polarizability $\alpha_{\varrho\sigma}\begin{pmatrix} Q \\ j \end{pmatrix}$. Finally, the summation (3.5) and multiplication with the factor $C\begin{pmatrix} Q \\ j \end{pmatrix}$ of (4.20) or (4.21) leads to the intensities.

In order to perform the summation (4.17) it has been assumed that the changes of polarizability $\alpha_{\varrho\sigma,\mu}\begin{pmatrix} l \\ kk' \end{pmatrix}$ of the atom k depend only on the displacements of the first neighbours and of the atom k itself. $(l, \bar{l} = 0, 1, 2, 3, 4)$. Then using Tables 1 and 2, equation (6.19) and the relations

$$\mathbf{r}(\mathrm{O}) = 0, \quad \mathbf{r}(\mathrm{O}') = \tfrac{1}{2}(a, a, a), \quad \mathbf{r}\begin{pmatrix} l \\ kk' \end{pmatrix} = -\mathbf{r}\begin{pmatrix} \bar{l} \\ kk' \end{pmatrix}, \quad \alpha_{\varrho\sigma,\mu}\begin{pmatrix} l \\ kk' \end{pmatrix} = -\alpha_{\varrho\sigma,\mu}\begin{pmatrix} \bar{l} \\ kk' \end{pmatrix},$$

equation (4.17) for elastic vibrations reduces to (a = lattice constant)

$$\alpha_{\varrho\sigma,\mu}\begin{pmatrix} Q \\ j_0 \end{pmatrix} = i2N\left[\alpha^{(0)}_{\varrho\sigma} Q_\mu + 2Q_\mu a\left|\alpha_{\varrho\sigma,\mu}\begin{pmatrix} l \\ \mathrm{O\,O'} \end{pmatrix}\right| + 4\sum_{\nu\eta}\left|\alpha_{\varrho\sigma,\eta}\begin{pmatrix} l \\ kk' \end{pmatrix}\right|\Gamma_{\eta\mu\nu} Q_\nu\right]. \qquad \ldots\ldots(6.41)$$

For the optical vibrations with $\mathbf{Q}.\mathbf{r}\begin{pmatrix} l \\ kk' \end{pmatrix} \ll 1$ and $\mathbf{e}(\mathrm{O}) = -\mathbf{e}(\mathrm{O}')$, $\Delta_\mu\left(kk'\middle|\begin{matrix} Q \\ j_0 \end{matrix}\right) = 2$, (4.18) becomes

$$\alpha_{\varrho\sigma,\mu}\begin{pmatrix} Q \\ j_0 \end{pmatrix} = 16N\left|\alpha_{\varrho\sigma,\mu}\begin{pmatrix} l \\ \mathrm{OO'} \end{pmatrix}\right| \quad (\rho \neq \sigma \neq \mu). \qquad \ldots\ldots(6.42)$$

With the notation of Table 2, the eigen-vectors (6.3) and (6.25) and equation (6.19) the summation over μ, ν, η in (4.16) and (4.17) gives the following $\alpha_{\varrho\sigma}\begin{pmatrix} Q \\ j_\varrho \end{pmatrix}$ for the elastic waves ($M = 2iNQ_\mu/\sqrt{m}$):

longitudinal:

$$\alpha_{11}=\alpha_{22}=\alpha_{33}=M(3\alpha^{(0)}+2aA+4aB)/\sqrt{3}=b,$$
$$\alpha_{12}=\alpha_{21}=\alpha_{13}=\alpha_{31}=\alpha_{23}=\alpha_{32}=4Ma(E+0{\cdot}66D)/\sqrt{3}=e,$$

transverse:

(1) $\alpha_{11}=-\alpha_{22}=2Ma(A-B)/\sqrt{2}=c, \quad \alpha_{33}=0,$
$\alpha_{12}=\alpha_{21}=0, \ \alpha_{13}=\alpha_{31}=-\alpha_{23}=-\alpha_{32}=2Ma(E+0{\cdot}66D)/\sqrt{2}=d,$

(2) $\alpha_{11}=\alpha_{22}=-\tfrac{1}{2}\alpha_{33}=2Ma(A-B)/\sqrt{6}=f,$
$\tfrac{1}{2}\alpha_{12}=\tfrac{1}{2}\alpha_{21}=-\alpha_{13}=-\alpha_{31}=-\alpha_{23}=-\alpha_{32}=2Ma(E+0{\cdot}66D)/\sqrt{6}=g.$

.....(6.43)

For the summation (3.5) the average values of the polarization vectors (3.8) are needed. A convenient pair of unit vector $\mathbf{s}''$ and $\mathbf{s}'$, which fulfil the condition (3.2) and are orthogonal to each other is

$$\mathbf{s}'=\left(\frac{\sqrt{3}+1}{2\sqrt{2}}, \ \frac{\sqrt{3}-1}{2\sqrt{2}}, 0\right), \quad \mathbf{s}''=\left(-\frac{1-\sqrt{3}}{2\sqrt{6}}, \ -\frac{1+\sqrt{3}}{2\sqrt{6}}, \ -\frac{4}{2\sqrt{6}}\right). \quad ...(6.44)$$

Put $\overline{A_\varrho A_\sigma^*}\,\overline{s_\mu s_\nu}+\overline{A_\sigma A_\varrho^*}\,\overline{s_\nu s_\mu}=S_{\varrho\sigma,\mu\nu}$ (for $\rho=\sigma$, $\mu=\nu$ the second term has to be omitted), then

$$\begin{aligned}
&S_{11,11}=0{\cdot}033, \ S_{22,22}=0{\cdot}322, \ S_{33,33}=0{\cdot}167,\\
&\quad S_{12,12}=-0{\cdot}020, \ S_{12,11}=-0{\cdot}244, \ S_{21,22}=-0{\cdot}172,\\
&S_{21,23}=0{\cdot}113, \ S_{11,12}=0{\cdot}005, \ S_{22,23}=-0{\cdot}424,\\
&\quad S_{11,13}=0{\cdot}008, \ S_{22,21}=0{\cdot}077, \ S_{12,13}=-0{\cdot}031,\\
&S_{22,11}=0{\cdot}456, \ S_{33,22}=0{\cdot}345, \ S_{11,33}=0{\cdot}012,\\
&\quad S_{12,31}=-0{\cdot}034, \ S_{21,12}=-0{\cdot}020, \ S_{22,13}=0{\cdot}114,\\
&S_{11,32}=-0{\cdot}038, \ S_{21,33}=-0{\cdot}083, \ S_{11,22}=0{\cdot}024,\\
&\quad S_{22,33}=0{\cdot}156, \ S_{33,11}=0{\cdot}489, \ S_{12,23}=0{\cdot}113.
\end{aligned} \quad .....(6.45)$$

All the other $S_{\varrho\sigma,\mu\nu}$ are zero because they contain the vanishing factor $s_3'=0$.

With these values one obtains according to (3.5) (the factors $(\omega+\omega_{\nu\nu'})^4$ are neglected):

$$\begin{aligned}
I_{(\mathrm{B,l})}&=(0{\cdot}512b^2-0{\cdot}670be+1{\cdot}534e^2)C\begin{pmatrix} Q \\ \mathrm{B,\,l} \end{pmatrix},\\
I_{(\mathrm{B,tr})}&=(0{\cdot}375c^2+1{\cdot}023f^2-0{\cdot}498cd+0{\cdot}182fg+1{\cdot}085d^2\\
&\quad+2{\cdot}449g^2)C\begin{pmatrix} Q \\ \mathrm{B,\,tr} \end{pmatrix}.
\end{aligned} \quad .....(6.46)$$

The indices (B, l) and (B, tr) denote the longitudinal and transverse Brillouin components.

A, B, $(E+0{\cdot}66D)$ and $\alpha^{(0)}$ can be derived from the index of refraction and the elasto-optical constants of diamond, which have been determined by Ramachandran

(1950). The method of derivation will be given in a following paper. The results found are as follows ($R=n^4/32\pi Na$, n = index of refraction, a = lattice constant, N = number of unit cells per cm^3):

$$\left.\begin{aligned} A=Rp_{11}&=-1{\cdot}82\times10^{-16}\,\text{cm}^2, \quad B=Rp_{12}=0{\cdot}53\times10^{-16}\,\text{cm}^2;\\ (E+0{\cdot}66D)&=Rp_{44}=-0{\cdot}71\times10^{-16}\,\text{cm}^2, \quad \frac{\alpha^{(0)}}{a}=\frac{n^2-1}{8\pi Na}=1{\cdot}47\times10^{-16}\,\text{cm}^2, \end{aligned}\right\} \quad \ldots\ldots(6.47)$$

where $p_{11}=-0{\cdot}31$, $p_{12}=0{\cdot}09$, $p_{44}=-0{\cdot}12$, $n=2{\cdot}61$. This yields

$$\left.\begin{aligned} &b=31{\cdot}4\frac{N}{\sqrt{m}}\times10^{-19}, e=-30{\cdot}8\frac{N}{\sqrt{m}}\times10^{-19}, c=-62{\cdot}4\frac{N}{\sqrt{m}}\times10^{-19},\\ &f=-36{\cdot}1\frac{N}{\sqrt{m}}\times10^{-19}, d=-18{\cdot}8\frac{N}{\sqrt{m}}\times10^{-19}, g=-10{\cdot}8\frac{N}{\sqrt{m}}\times10^{-19}. \end{aligned}\right\} \quad \ldots\ldots(6.48)$$

Substitute these values in (6.46) and multiply by

$$C\left(\frac{Q}{\text{B, l}}\right)=\frac{1}{2\pi Nc_0}1{\cdot}75\times10^{-26} \quad \text{and} \quad C\left(\frac{Q}{\text{B, tr}}\right)=\frac{1}{2\pi Nc_0}4{\cdot}75\times10^{-26},$$

hen the intensities at room temperature (300° K.) are

$$I_{(\text{B, l})}=4576\frac{N}{2\pi c_0 m}\times10^{-64}, \quad I_{(\text{B, tr})}=14050\frac{N}{2\pi c_0 m}\times10^{-64}. \quad \ldots\ldots(6.49)$$

The intensity ratio between transverse and longitudinal Brillouin components is

$$I_{(\text{B, tr})}/I_{(\text{B, l})}=3{\cdot}27. \quad \ldots\ldots(6.50)$$

If the phase term $\alpha^{(0)}_{\sigma\sigma}Q_\mu$ in (6.41) were neglected one would obtain the result $I_{(\text{B, tr})}/I_{(\text{B, l})}=6{\cdot}4$ which is in disagreement with experiment, as will be shown.

The only available experimental data are communicated in a paper by Krishnan (1947). He gives two microphotometer records, which are reproduced in Figure 2.

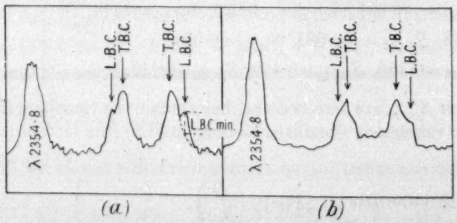

Figure 2. Microphotometer record of Brillouin scattering in diamond for two different orientations. L.B.C. and T.B.C. = longitudinal and transverse components.

Because of the considerable width of the lines a quantitative interpretation of the photometer record is rather difficult. From Figure 2(*a*) it is possible to conclude that the ratio $I_{(\text{B, tr})}/I_{(\text{B, l})}$ lies between the limits

$$2<I_{(\text{B, tr})}/I_{(\text{B, l})}<4. \quad \ldots\ldots(6.51)$$

Figure 2(*b*) does not allow a quantitative measurement of the intensity ratio. Krishnan only points out that the transverse components are much brighter than the longitudinal. In any case, the calculated ratio 3·27 is in good agreement with the experimental result, as given in (6.51).

The intensity of the first order Raman line ($\Delta\nu = 1332\,\mathrm{cm}^{-1}$) depends only on the polarizability derivatives $\alpha_{\varrho\sigma,\mu}(\rho \neq \sigma \neq \mu)$ which cannot be derived from the photo-elastic constants. This different behaviour comes from the different properties of the terms $\mathbf{Q}.\mathbf{r}\begin{pmatrix} l \\ kk' \end{pmatrix}$ and $\Delta_\mu \left(kk' \middle| \begin{matrix} Q \\ j_0 \end{matrix} \right)$ which, according to (4.17) and (4.18), are characteristic for the intensities of the Brillouin components and the optical Raman lines. The sign of $\Delta_\mu \left(kk' \middle| \begin{matrix} Q \\ j_0 \end{matrix} \right)$ and of the polarizability derivative D of Table 2 is independent of l, whereas the sign of $\mathbf{Q}.\mathbf{r}\begin{pmatrix} l \\ kk' \end{pmatrix}$ depends on l in the same way as the polarizability derivatives A, B, E. Hence the products $\alpha_{\varrho\sigma,\mu}\begin{pmatrix} l \\ kk' \end{pmatrix} \Delta\mu \left(kk' \middle| \begin{matrix} Q \\ j_0 \end{matrix} \right)$ cancel in pairs for $\alpha_{\varrho\sigma,\mu}\begin{pmatrix} l \\ kk' \end{pmatrix} = A, B, E$; the products $\alpha_{\varrho\sigma,\mu}\begin{pmatrix} l \\ kk' \end{pmatrix} \mathbf{Q}.\mathbf{r}\begin{pmatrix} l \\ kk' \end{pmatrix}$ cancel for $\alpha_{\varrho\sigma,\mu}\begin{pmatrix} l \\ kk' \end{pmatrix} = D$.

To derive the intensity of the Raman line one can use the fact that in the case treated here ($Q_x = Q_y = Q_z$) the eigen-vectors are the same for the elastic and optical lattice vibrations. The same holds, of course, for the averages $S_{\varrho\sigma,\mu\nu}$. Hence, the expression for the intensity must have the form given by (6.43) and (6.46). The only difference is that only the polarizability derivatives $\alpha_{\varrho\sigma,\mu}\begin{pmatrix} l \\ kk' \end{pmatrix} = D$ with $\rho \neq \sigma$ remain. Consequently A and B, which are of the form $\alpha_{\varrho\varrho,\mu}\begin{pmatrix} l \\ kk' \end{pmatrix}$ must be omitted in (6.43) and instead of the term $2Ma(E + 0{\cdot}66D)$ one has to introduce the term $16ND/\sqrt{m}$ which is characteristic for the optical vibrations (see equation (6.42)). This gives with

$$\left.\begin{aligned} C\begin{pmatrix} Q \\ R \end{pmatrix} &= \frac{1}{2\pi N c_0}\, 4{\cdot}97 \times 10^{-30} \quad \text{from (4.13)}, \\ I_{(R)} &= 0{\cdot}375\, \frac{N}{2\pi N c_0}\, D^2 \times 10^{-26}. \end{aligned}\right\} \quad \ldots\ldots (6.52)$$

From Krishnan's observation that the Raman line at room temperature is at least four times stronger than the total intensity of all Brillouin components, it follows that $D = \alpha_{\varrho\sigma,\mu}(\rho \neq \sigma \neq \mu)$ is at least $0{\cdot}64 \times 10^{-16}\,\mathrm{cm}^2$. This is of the same order of magnitude as the other polarizability derivatives A, B, E and gives a further support to the present theory.

ACKNOWLEDGMENTS

The author wishes to thank Professor M. Born for his continued interest and valuable help in the course of this work; he further wishes to thank Dr. L. M. Yang and Dr. E. Wolf for the useful discussion concerning mathematical details. He is indebted to the British Council for the tenure of a scholarship.

REFERENCES

BHAGAVANTAM, S., and BHIMASENACHAR, J., 1946, *Proc. Roy. Soc.* A, **187**, 381.
BORN, M., 1914, *Ann. Phys., Lpz.*, **44**, 605; 1942, *Rep. Prog. Phys.*, **9**, 294 (London: Physical Society).
BORN, M., and BEGBIE, G. H., 1947, *Proc. Roy. Soc.* A, **89**, 277.
BORN, M., and BRADBURN, M., 1947, *Proc. Roy. Soc.*, A, **188**, 161.
BRILLOUIN, L., 1922, *Ann. Phys., Paris*, **17**, 88.
KRISHNAN, R. S., 1947, *Proc. Indian Acad. Sci.* A, **26**, 399.
LEONTOWITSCH, M., and MANDELSTAMM, S., Jr., 1931, *Phys. Z. Sowjet*, **1**, 317.
MUELLER, H., 1938, *Proc. Roy. Soc.* A, **166**, 425.
PLACZEK, G., 1934, *Handbuch d. Radiologie*, **6**, Pt. 2.
RAMACHANDRAN, G. N., 1950, *Proc. Indian Acad. Sci.* A, **32**, 171.
SMITH, H. M. J., 1948, *Phil. Trans. Roy. Soc.* A, **241**, 105.

Electrical Conductivity of Metals at Low Temperatures: Equilibrium between Electrons and Phonons

BY P. G. KLEMENS

Commonwealth Scientific and Industrial Research Organisation, National Standards Laboratory, Sydney

MS. received 10*th May* 1951

ABSTRACT. The Bloch theory of electrical conductivity of metals assumes that the phonon distribution does not deviate from equilibrium. Peierls has criticized this assumption, showing that in the presence of an electric field a stationary state is achieved only through processes which do not conserve the total wave vector. These can be *Umklapprozesse* involving electrons and a phonon, or phonon–phonon interaction of the type responsible for thermal resistance in dielectric solids. He estimates that if only the latter were to act, strong deviations from Bloch's formula would occur below 50° K. He therefore concludes that the electrical resistance at low temperatures is determined by *Umklapprozesse*.

A more detailed treatment of the statistical equilibrium of phonons and electrons shows that the relaxation times of the important phonons is smaller than estimated by Peierls by a factor of about 100; consequently one would not, as a result of phonon–phonon interactions, expect important deviations from the Bloch theory above 10° K. It is thus unnecessary to consider *Umklapprozesse*. Since *Umklapprozesse* require a special shape of the Fermi surface in wave-vector space, Peierls has concluded from the apparent agreement with Bloch's theory that the Fermi surface has this special shape. Hence it is now shown that this shape is not necessary.

§1. INTRODUCTION

EVER since Peierls (1930, 1932, see also Sommerfeld and Bethe 1933) had pointed out that in the presence of an electric field interactions between phonons and electrons conserving the sum of the wave vectors cannot establish equilibrium, the agreement between Bloch's theory and the observed electrical conductivities at low temperatures has remained unexplained.

In order that equilibrium be obtained, there must be processes which do not conserve the wave vector: these could be *Umklapprozesse* or phonon–phonon processes. The last-mentioned processes are the same as are responsible for the thermal resistance in non-metallic solids. Peierls deduced their effect from the known thermal conductivity of a typical non-metallic solid, NaCl, and came to the conclusion that these processes were sufficient to establish equilibrium at

room temperatures. At low temperatures, however, they would be so rare that the phonon distribution would depart from equilibrium sufficiently to cause a marked increase in the electrical conductivity over that given by Bloch's theory. The Bloch theory would thus hold only to about 50° K.

Since the electrical conductivity seems to agree with Bloch's theory even at lower temperatures, Peierls considered the *Umklapprozesse*. These are interactions between electrons and phonons in which the total wave vector is changed by an inverse lattice vector. The resistance due to these *Umklapprozesse* was estimated, and has the same temperature dependence as the resistance calculated by the Bloch theory. There are, however, two difficulties. Firstly the absolute value of the low-temperature conductivities are related to the high-temperature conductivities in the way predicted by Bloch's theory, while no such estimation is possible for *Umklapprozesse*. Secondly, in order that *Umklapprozesse* can be effective in producing resistance, the energy surface in wave-vector space corresponding to the Fermi energy must come up to the surface of the first Brillouin zone, whereas a number of metals conform to the Bloch theory in spite of having Fermi energy surfaces well inside the first Brillouin zone.

It thus seems probable that Bloch's theory has a wider validity than is conceded in Peierls' argument. It will be shown here that his estimate of the sufficiency of phonon–phonon interactions to maintain the phonon distribution near equilibrium was too pessimistic, and that in fact the Bloch theory is valid at all low temperatures. The two difficulties mentioned above are thus resolved.

§2. RÉSUMÉ OF BLOCH'S AND PEIERLS' THEORIES*

The thermal motion of the lattice destroys its periodicity, causing transitions in the state of the electron gas. Resolving the thermal motion into quantized lattice waves of wave number $\mathbf{q}$ and energy $\hbar\omega$, the change of state due to interaction takes place as discontinuous processes in which an electron of wave number $\mathbf{k}'$ is emitted and an electron $\mathbf{k}$ and a phonon $\mathbf{q}$ are absorbed or vice versa, so that the interference condition

$$\mathbf{k}'=\mathbf{k}+\mathbf{q} \quad \ldots\ldots(1a) \quad \text{or} \quad \mathbf{k}'=\mathbf{k}+\mathbf{q}\pm 2\pi\mathbf{g} \quad \ldots\ldots(1b)$$

is fulfilled. Here $\mathbf{g}$ is a vector of the reciprocal lattice, and has to be included in (1*b*) since we specify an electron by its 'reduced' wave vector only. In addition we require for non-virtual transitions that energy be conserved, i.e.

$$E(\mathbf{k}')=E(\mathbf{k})+\hbar\omega. \quad \ldots\ldots(2)$$

If $N(\mathbf{q})$ is the number of $\mathbf{q}$-phonons and $f(\mathbf{k})$ the average occupation of the electron states about the wave number $\mathbf{k}$, then the rate of change of the electron distribution due to interactions with phonons is given on a simplified model as

$$\begin{aligned}\left.\frac{\partial f}{\partial t}\right]_{\mathrm{p}} = \frac{2C^2G^{-3}}{9M\hbar}\,\frac{\partial}{\partial t}\sum_{\mathbf{q}}\frac{q^2}{\omega}\,\{&\Omega[E(\mathbf{k}+\mathbf{q})-E(\mathbf{k})-\hbar\omega]\\ &\times[\{1-f(\mathbf{k})\}f(\mathbf{k}+\mathbf{q})\{N(\mathbf{q})+1\}-f(\mathbf{k})\{1-f(\mathbf{k}+\mathbf{q})\}N(\mathbf{q})]\\ &+\Omega\{E(\mathbf{k}+\mathbf{q})-E(\mathbf{k})+\hbar\omega\}[\{1-f(\mathbf{k})\}f(\mathbf{k}+\mathbf{q})N(-\mathbf{q})\\ &-f(\mathbf{k})\{1-f(\mathbf{k}+\mathbf{q})\}\{N(-\mathbf{q})+1\}]\},\end{aligned} \quad \ldots\ldots(3)$$

* See Sommerfeld and Bethe (1933).

where C is a coupling constant, G^3 is the number of ions per unit volume and M is the mass of each ion. The resonance factor Ω is defined by

$$\Omega(x) = (2\hbar^2/x^2)(1 - \cos xt/\hbar)$$

and ensures conservation of energy.

Correspondingly the rate of change in the number of phonons through interactions with electrons is

$$\left.\frac{\partial N}{\partial t}\right]_e = \frac{2C^2G^{-3}}{9M\hbar}\frac{q^2}{\omega}\frac{\partial}{\partial t}\Sigma_{\mathbf{k}}\Omega\{E(\mathbf{k}+\mathbf{q}) - E(\mathbf{k}) - \hbar\omega\}$$
$$\times[\{1-f(\mathbf{k})\}f(\mathbf{k}+\mathbf{q})\{N(\mathbf{q})+1\} - f(\mathbf{k})\{1-f(\mathbf{k}+\mathbf{q})\}N(\mathbf{q})]. \quad \ldots\ldots(4)$$

Both (3) and (4) disregard processes (1 *b*), i.e. *Umklapprozesse*, which only occur near the top of an energy band and need special treatment (Peierls 1932).

It is easily verified that $\partial f/\partial t]_p$ and $\partial N/\partial t]_e$ both vanish if we substitute for f and N the equilibrium distributions

$$f_0 = 1/(e^{\epsilon}+1), \quad \mathcal{N} = 1/(e^{x}-1), \quad \ldots\ldots(5)$$

where $\epsilon = (E-\zeta)/\boldsymbol{k}T$, $x = \hbar\omega/\boldsymbol{k}T$ and ζ is the Fermi energy, and if we take account of the conservation of energy. Thus the assembly of fermions and bosons mutually interacting is in equilibrium when each component itself is in equilibrium.

If the total wave vector is conserved in addition to the energy, the following distributions are also stationary if $|\lambda|$ is small

$$\left.\begin{aligned} f_0' &= [\exp\{(E-\zeta+\boldsymbol{\lambda}.\mathbf{k})/\boldsymbol{k}T\}+1]^{-1} \\ &\simeq f_0 + \frac{\boldsymbol{\lambda}.\mathbf{k}}{\boldsymbol{k}T}\frac{\partial f_0}{\partial \epsilon}, \text{ if } |\lambda| \text{ is small} \\ \mathcal{N}' &= [\exp\{(\hbar\omega+\boldsymbol{\lambda}.\mathbf{q})/\boldsymbol{k}T\}-1]^{-1} \\ &\simeq \mathcal{N} + \frac{\boldsymbol{\lambda}.\mathbf{q}}{\boldsymbol{k}T}\frac{\partial \mathcal{N}}{\partial x}, \text{ if } |\lambda| \text{ is small} \end{aligned}\right\} \quad \ldots\ldots(5')$$

where $\boldsymbol{\lambda}$ is a constant vector, and must be the same for f_0' and $\mathcal{N}'$.

Hence, while it is true that an assembly of electrons and phonons in mutual interaction will generally tend to the equilibrium state (5) in the absence of external forces, when all interactions conserve the total wave number of the system $\mathbf{J} = \Sigma_{\mathbf{k}} f(\mathbf{k})\mathbf{k} + \Sigma_{\mathbf{q}} N(\mathbf{q})\mathbf{q}$ the assembly will tend to a quasi-equilibrium given by (5′). Here $\boldsymbol{\lambda}$ is related to $\mathbf{J}$ by

$$\mathbf{J} = \frac{4\pi}{3\boldsymbol{k}T}\boldsymbol{\lambda}\left\{2\int_0^{\infty} k^4\frac{\partial f_0}{\partial \epsilon}dk + 3\int_0^{q_0} q^4\frac{\partial \mathcal{N}}{\partial x}dq\right\}, \quad \ldots\ldots(6)$$

obtained by substituting (5′) into the expression for $\mathbf{J}$ and summing. The fact that true equilibrium cannot be obtained solely by processes conserving the wave vector was first pointed out by Peierls (1930).

Bloch's theory of electrical conduction is based on the assumption that the phonon distribution is in true equilibrium, i.e. $N = \mathcal{N}$, and that all processes conserve the total wave vector. Then the stationary distribution f in the presence of a field F is given by

$$\left.\frac{\partial f}{\partial t}\right]_{\text{field}} = -\frac{eF}{\hbar}\frac{df}{dE}\frac{\partial E}{\partial k_x} = -\left.\frac{\partial f}{\partial t}\right]_p. \quad \ldots\ldots(7)$$

To obtain $\partial f/\partial t]_p$ treat $\mathbf{q}$ as continuous, replace N by $\mathcal{N}$ in (3) and integrate over the angular variation of $\mathbf{q}$. Taking

$$f = f_0 + k_x \chi(E) \qquad \ldots\ldots(8)$$

one obtains the following equation to first order in χ:

$$\int_0^{q_0} q^2\, dq\, \mathcal{N}(q) \left\{ \frac{f_0(E)}{f_0(E+\hbar\omega)} \chi(E+\hbar\omega) \left[1 + \frac{\hbar\omega}{k\, dE/dk} - \frac{q^2}{2k^2} \right] \right.$$
$$+ \frac{f_0(E)}{f_0(E-\hbar\omega)} \exp(\hbar\omega/\boldsymbol{k}T) \left[1 - \frac{\hbar\omega}{k\, dE/dk} - \frac{q^2}{2k^2} \right] \chi(E-\hbar\omega)$$
$$\left. - \left[\frac{f_0(E+\hbar\omega)}{f_0(E)} \exp(\hbar\omega/\boldsymbol{k}T) + \frac{f_0(E-\hbar\omega)}{f_0(E)} \right] \chi(E) \right\} = \frac{9\pi M v e F}{\hbar C^2 \Omega_0} \frac{1}{k} \frac{df_0}{dE} \left(\frac{dE}{dk} \right)^2, \qquad \ldots\ldots(9)$$

where v is the phonon phase velocity, Ω_0 the volume of a unit cell and q_0 the Debye wave number. The solution of (9) gives us $\chi(E)$, hence the electron distribution, and the current

$$I = -\tfrac{2}{3} e \int \frac{dE}{dk} k \chi(E) \frac{4\pi}{(2\pi)^3} k^2 dk, \qquad \ldots\ldots(10)$$

whence the conductivity is found.

If $T \gg \theta$, the Debye temperature, all terms on the left-hand side of (9) cancel except the terms in $q^2/2k^2$, and the solution of (9) is

$$\chi(E) = -\lambda \partial f_0/dE, \qquad \ldots\ldots(11)$$

where

$$\lambda = \frac{M}{\pi^3 \hbar^2} \frac{\bar{k}}{C^2} \left(\overline{\frac{dE}{dk}} \right)^2 \Omega_0 \boldsymbol{k} \theta e F \frac{\theta}{T}, \qquad \ldots\ldots(12)$$

whence the conductivity becomes

$$\sigma = \frac{n_0}{\pi^3} \frac{M}{m} \left(\frac{\bar{k}}{C} \overline{\frac{dE}{dk}} \right)^2 \frac{\boldsymbol{k}\theta}{\hbar \bar{k} a_0} \frac{\theta}{T}. \qquad \ldots\ldots(13)$$

Here n_0 is the number of conduction electrons per atom, a_0 the Bohr radius and the barred quantities $\bar{k}$ etc. refer to the Fermi wave number.

On the other hand if $T \ll \theta$

$$\chi(E) = -\lambda \frac{\partial f_0}{\partial E} + \psi(E), \qquad \ldots\ldots(14)$$

where it can be shown that $\psi(E) \ll \chi(E)$ and

$$\lambda = \frac{9\pi M v e F \bar{k}}{\hbar C^2 \Omega_0 J_5} \left(\overline{\frac{dE}{dk}} \right)^2 \left(\frac{\theta}{T q_0} \right)^5, \qquad \ldots\ldots(12')$$

where $J_n = \int_0^\infty \frac{x^n}{(e^x - 1)^2} dx$ and hence

$$\sigma = \frac{n_0}{4\pi^3 J_5} \frac{M}{m} \left(\frac{\bar{k}}{C} \overline{\frac{dE}{dk}} \right)^2 \frac{\boldsymbol{k}\theta}{\hbar \bar{k} a_0} \left(\frac{\theta}{T} \right)^5. \qquad \ldots\ldots(13')$$

According to Bloch's theory if $T_1 \ll \theta \ll T_2$ from (13) and (13′):

$$\frac{\sigma(T_2)}{\sigma(T_1)} = 497{\cdot}6 \left(\frac{T_1}{\theta} \right)^4 \frac{T_1}{T_2}, \qquad \ldots\ldots(14')$$

and this relation between the conductivity at high and at low temperatures seems well verified by observations.

The temperature dependence can be qualitatively understood as follows: An electron moves in k-space in discontinuous steps due to its interaction with phonons. Consider the action of phonons in a wave number interval q, dq. The rate of change of the distribution function is characterized by a relaxation time τ_q, which is proportional to the time required for an electron to move a given distance over the Fermi surface. The movement can be regarded as a random walk over the Fermi surface and the number of collisions required to move this distance is inversely proportional to the square distance of each step q^2. We have

$$\left.\frac{\partial f}{\partial t}\right]_{dq} \propto \frac{1}{\tau_q} \propto \frac{\text{number of steps per unit time}}{\text{number of steps required}} \qquad \ldots\ldots(15)$$

and since the number of steps per unit time is proportional to $\mathcal{N}(q)\, q^2 dq$, the number of phonons in the interval q, dq, we have

$$\partial f/\partial t]_{dq} \propto \mathcal{N}(q) q^4 dq \qquad \ldots\ldots(16)$$

so that

$$\left.\frac{\partial f}{\partial t}\right] \propto \int \mathcal{N}(q) q^4 dq. \qquad \ldots\ldots(17)$$

Hence if $T \ll \theta$, the resistance is proportional to T^5, while if $T \gg \theta$, it is proportional to T.

We have seen that there are two assumptions in the Bloch theory, i.e. that $N = \mathcal{N}$ and that all processes conserve the total wave vector. These are incompatible, as was already pointed out by Peierls, for the second assumption implies a continuous increase of $\mathbf{J}$ due to the electric field

$$\partial \mathbf{J}/\partial t]_{\text{field}} = e\mathbf{F}n/\hbar, \qquad \ldots\ldots(18)$$

which, in the absence of *Umklapprozesse* (1 *b*), requires that the phonon distribution deviates from equilibrium. Also if the phonon distribution were at equilibrium, the phonon–phonon processes, which are the only other processes capable of producing a stationary state, could not be effective, since $\partial \mathcal{N}/\partial t]_{\text{p}} = 0$ by definition of $\mathcal{N}$.

Hence if we disregard *Umklapprozesse*, we cannot assume that $N = \mathcal{N}$, but must calculate the deviations of the phonon distribution from equilibrium, and then determine the effect of this on the electrical conductivity. This has been done by Peierls in the following way:

The rate of increase of J due to the field (18) is balanced by the rate of decrease due to phonon processes, so that

$$\left.\frac{\partial \mathbf{J}}{\partial t}\right]_{\text{field}} = -\left.\frac{\partial \mathbf{J}}{\partial t}\right]_{\text{p}} = -\left.\frac{\partial \mathbf{J}_{\text{G}}}{\partial t}\right]_{\text{p}}, \qquad \ldots\ldots(19)$$

where $\mathbf{J}_{\text{G}} = \Sigma_{\mathbf{q}} \mathbf{q} N(\mathbf{q})$. Peierls now assumes an overall relaxation time for the decrease of $\mathbf{J}_{\text{G}}$, i.e.

$$\partial J/\partial t]_{\text{p}} = -\mathbf{J}_{\text{G}}/\tau_{\text{G}} \qquad \ldots\ldots(20)$$

and he further assumes that the relaxation time is the same as occurs in the expression for the heat conductivity of a lattice which does not interact with free electrons

$$\kappa_{\text{G}} = \tfrac{1}{3} S v^2 \tau_{\text{G}} \qquad \ldots\ldots(21)$$

since the processes not conserving the wave vector are the same in both cases. Here S is the specific heat per unit volume of the lattice.

Now if

$$f=f_0+\frac{\boldsymbol{\lambda}.\mathbf{k}}{kT}\frac{\partial f_0}{\partial \epsilon} \quad \ldots\ldots(22) \qquad \text{and} \qquad N=\mathcal{N}+\frac{\boldsymbol{\mu}.\mathbf{q}}{kT}\frac{\partial \mathcal{N}}{\partial x} \quad \ldots\ldots(22')$$

then, since $\partial f/\partial t]_p=0$ for $\lambda=\mu$, we can put

$$\frac{\partial f}{\partial t}\Big]_p=\left(\frac{\lambda-\mu}{\lambda_B}\right)\frac{\partial f}{\partial t}\Big\}_p, \quad \ldots\ldots(23)$$

where $\partial f/\partial t\}_p$ is the rate of change of f due to phonons if $N=\mathcal{N}$, and λ_B is the corresponding deviation of the electron distribution. Since the rate of change due to the field is independent of the phonon distribution

$$-\frac{\partial f}{\partial t}\Big]_{\text{field}}=\frac{\partial f}{\partial t}\Big]_p=\left(\frac{\lambda-\mu}{\lambda_B}\right)\frac{\partial f}{\partial t}\Big\}_p=\frac{\partial f}{\partial t}\Big\}_p, \quad \ldots\ldots(23')$$

so that $\lambda=\lambda_B+\mu$. But the electrical conductivity is proportional to λ, whence

$$\sigma=\sigma_B(1+\mu/\lambda_B), \quad \ldots\ldots(24)$$

where σ_B is the conductivity according to the Bloch theory.

Now μ is related to J_G by

$$J_G=\Sigma N(\mathbf{q})\mathbf{q}=\mu\frac{4\pi}{3}\left(\frac{1}{2\pi}\right)^3 q_0^5\frac{1}{kT}\left(\frac{T}{\theta}\right)^5 J_4, \quad \ldots\ldots(25)$$

obtained by substituting (22′) for N, while

$$J_G=eFn\tau_G/\hbar=3en\kappa_G F/S\hbar v^2, \quad \ldots\ldots(26)$$

which is obtained from (19), using (18), (20) and (21). Thus μ can be obtained from the lattice (thermal) conductivity. Similarly λ_B can be obtained from the electrical conductivity using (12) and (13) or (12′) and (13′). In this way Peierls finally obtains for the ratio μ/λ_B, which is indicative of the deviation from Bloch's theory:

$$\mu/\lambda_B=\frac{6\kappa_G e^2 n}{\sigma S v\hbar}\frac{\bar{k}^3}{q_0^4}\left(\frac{\theta}{T}\right)^4\frac{1}{J_4}. \quad \ldots\ldots(27)$$

When $T\gg\theta$, $\mu/\lambda_B\propto\kappa_G$, more generally

$$\mu/\lambda_B\propto\frac{\kappa}{S\sigma}\left(\frac{\theta}{T}\right)^4\frac{1}{J_4}\propto\kappa\left(\frac{\theta}{T}\right)^2\frac{J_5}{J_4^2}, \quad \ldots\ldots(28)$$

and when $T\ll\theta$, $\mu/\lambda_B\propto\kappa(\theta/T)^2$.

Evaluating μ/λ_B numerically from (27), there is an uncertainty about κ_G: the quantity which is required is the thermal conductivity of the lattice, if the lattice did not interact with the free electrons. To get the order of magnitude, Peierls uses the thermal conductivity of a typical dielectric solid, i.e. NaCl. He obtains $\mu/\lambda_B=0{\cdot}21$ at 290° K. But since κ_G increases as the temperature is lowered, Peierls estimates that $\mu/\lambda_B=1$ at about 50° K., and that phonon–phonon interactions are therefore not able to prevent appreciable deviations from the Bloch theory at such low temperatures.

§3. EQUILIBRIUM BETWEEN PHONONS AND ELECTRONS

It is possible to criticize Peierls' argument, since the relaxation time τ_G defined by (20) is not necessarily the same as τ_G defined by (21). Neither equation takes account of the frequency dependence of the relaxation time. Equation (21) should be replaced by

$$\kappa = \tfrac{1}{3}\sum_j \frac{\partial}{\partial T} E(q, T)_j v_j^2 \tau_j(q)\, dq, \qquad \ldots\ldots(29)$$

when $E(q, T)_j\, dq$ is the energy content of modes of wave number q, dq and polarization j; and $\tau_j(q)$ is the effective relaxation time of the (q, j) modes, defined by

$$\frac{\partial N(q,j)}{\partial t}\Big]_p = \frac{\mathcal{N}(q,j) - N(q,j)}{\tau_j(q)}. \qquad \ldots\ldots(30)$$

Since in the presence of a temperature gradient

$$\frac{\partial N}{\partial t}\Big]_p = -\frac{\partial N}{\partial t}\Big]_{\text{drift}} = (\mathbf{v}\,.\,\text{grad}\ T)\frac{d\mathcal{N}}{dT} \qquad \ldots\ldots(31)$$

the relaxation time is simply related to the deviation from equilibrium by

$$N - \mathcal{N} = (\mathbf{v}\,.\,\text{grad}\ T)\frac{\hbar\omega}{\boldsymbol{k}T^2}\frac{\exp(\hbar\omega/\boldsymbol{k}T)}{\{\exp(\hbar\omega/\boldsymbol{k}T)-1\}^2}\tau,$$
$$\propto \tau\, x e^x/(e^x-1)^2. \qquad \ldots\ldots(32)$$

This effective relaxation time depends not only on ω and T, but also on the effective relaxation times (i.e. deviations from equilibrium) of all the other modes, as has been pointed out elsewhere (Klemens 1950, 1951). It is thus clear that to a certain degree τ depends upon the frequency dependence of those processes which cause the deviation from equilibrium. This is an additional reason why one cannot identify τ_G of equations (20) and (21), though, in fact, this will be shown to be less important than the frequency dependence of τ.

In the case of a temperature gradient in a dielectric crystal, when three-phonon processes conserving the wave vector have a negligibly small relaxation time, one can show, as a result of the frequency dependence of $N-\mathcal{N}$ expressed in (32), that for all polarizations

$$\tau_j(q) = \tau_{II}'(\boldsymbol{k}T/\hbar v) \quad \text{for} \quad q \leqslant \boldsymbol{k}T/\hbar v$$
$$= \tau_{II}'(q) \quad \text{for} \quad q \geqslant \boldsymbol{k}T/\hbar v, \qquad \ldots\ldots(33)$$

when $\tau_{II}'(q)$ is the relaxation time of transverse phonons of wave number q due to processes not conserving the total wave vector.

In the case of electrical conductivity, the processes causing the deviation from equilibrium have a different frequency dependence. We obtain from (9), after integrating over all $\boldsymbol{k}$ in a manner outlined by Sommerfeld and Bethe (1933), that the rate of change of the phonon distribution due to interactions with electrons is

$$\frac{\partial N}{\partial t}\Big]_e = \frac{2\hbar C^2 G^{-3}}{9\pi M \boldsymbol{k}T}\frac{\bar{k}^2}{(\overline{dE/dk})^2}\frac{qe^x}{(e^x-1)^2}\frac{(\mathbf{q}\,.\,\mathbf{F})}{F}(\lambda-\mu), \qquad \ldots\ldots(34)$$

so that, since

$$\partial N/\partial t]_e + \partial N/\partial t]_p = 0, \qquad \ldots\ldots(35)$$

we obtain from (30)

$$N - \mathcal{N} = \tau\frac{\partial N}{\partial t}\Big]_e \propto \tau\frac{x^2 e^x}{(e^x-1)^2}. \qquad \ldots\ldots(36)$$

Consequently in the case of electrical conductivity, equation (33) has to be replaced by the following, as is shown in the Appendix:

$$\tau_j(q) = \frac{\boldsymbol{k}T}{\hbar v q}\tau_{\mathrm{II}}'\left(\frac{\boldsymbol{k}T}{\hbar v}\right) \quad \text{for} \quad q \leqslant \boldsymbol{k}T/\hbar v$$

$$= \tau_{\mathrm{II}}'(q) \quad \text{for} \quad q \geqslant \boldsymbol{k}T/\hbar v. \qquad \ldots\ldots(37)$$

Using (22′) for $N-\mathcal{N}$, and substituting into (34), we find, using (36) and dividing both sides by $xe^x/(e^x-1)^2$, that

$$\mu = x\hbar v A\tau(\lambda-\mu) \qquad \ldots\ldots(38)$$

or

$$\mu = \lambda\hbar v A\tau x/(1+\hbar v A\tau x), \qquad \ldots\ldots(38')$$

where

$$A = \frac{2C^2G^{-3}}{9\pi M\hbar v^2}\boldsymbol{k}T\frac{\overline{k^2}}{\overline{(dE/dk)^2}}. \qquad \ldots\ldots(39)$$

Thus μ depends upon frequency, since τ depends upon frequency and $x=\hbar\omega/\boldsymbol{k}T$, while λ, the deviation of the electron distribution, is the same for all phonons. To obtain the deviation from the Bloch theory, we must find λ. As before $\sigma/\sigma_{\mathrm{B}}=\lambda/\lambda_{\mathrm{B}}$. As in (23′) we consider the rate of change of the electron distribution in the case when $\mu=0$ and $\lambda=\lambda_{\mathrm{B}}$, and in the actual case. But since μ depends upon the phonon frequency, we must consider the rate of change of f due to phonons of the wave number interval q, dq, and then integrate.

$$\left.\frac{\partial f}{\partial t}\right]_{\mathrm{p}} = \int\left.\frac{\partial f}{\partial t}\right]_{dq} dq = \int\left\{\frac{\lambda-\mu}{\lambda_{\mathrm{B}}}\frac{\partial f}{\partial t}\right\}_{dq} dq = \int\left\{\frac{\partial f}{\partial t}\right\}_{dq} dq. \qquad \ldots\ldots(40)$$

Now $\partial f/\partial t\}_{dq}$, the rate of change due to phonons q, dq when $\mu=0$, is given by (16). Hence

$$\int\frac{\lambda-\mu}{\lambda_{\mathrm{B}}}\mathcal{N}(q)q^4\,dq = \int\mathcal{N}(q)q^4\,dq, \qquad \ldots\ldots(41)$$

and expressing μ in terms of λ according to (38′)

$$\frac{\sigma_{\mathrm{B}}}{\sigma} = \frac{\lambda_{\mathrm{B}}}{\lambda} = \int_0^\infty\frac{x^4}{e^x-1}[1+\hbar v A\tau x]^{-1}\,dx\Big/\int_0^\infty\frac{x^4\,dx}{e^x-1}. \qquad \ldots\ldots(42)$$

This expresses in general the deviation of the electrical conductivity from the value given by Bloch's theory in terms of τ; this in turn is related to τ_{II}', the relaxation time of phonons due to processes not conserving the wave vector, by (37).

In general $\sigma/\sigma_{\mathrm{B}}$ as calculated by (42) will be smaller than the same quantity given by Peierls' argument, i.e. by (24) and (27). This is because the frequencies most important for the conduction of heat by phonons are not the same as those important for establishing electrical resistance. In general, higher frequencies are important in the latter case, and they have a shorter relaxation time.

§4. THE RANGE OF VALIDITY OF BLOCH'S THEORY

We shall now apply these results to the case treated by Peierls, i.e. we shall find the temperature for which $\sigma/\sigma_{\mathrm{B}}=2$ for the case of gold, assuming the lattice properties of a typical alkali halide, namely KCl.

The thermal resistance of alkali halides in the liquid hydrogen region is due to lattice defects, which scatter phonons according to a fourth-power law. De Haas and Biermasz (1937, 1938) have found that in this region

$$\kappa = 20/0{\cdot}77T \text{ watt/cm/deg.}, \qquad \ldots\ldots(43)$$

whence from (29) with (33) one obtains, as shown by Klemens (1950, 1951),

$$\tau_{\mathrm{II}}' = 3{\cdot}5 \times 10^{-3}(xT)^{-4} \text{ sec.} \qquad \ldots\ldots(44)$$

Put $\tau_{\mathrm{II}}' = \tau_0(xT)^{-4}$ then from (42),

$$\sigma_{\mathrm{B}}/\sigma = \int_0^\infty \frac{x^4}{e^x - 1}[1 + \alpha x^{-3}]^{-1}\, dx/26, \qquad \ldots\ldots(45)$$

where

$$\alpha = \hbar v A \tau_0 T^{-4} = \frac{2C^2G^{-3}}{9\pi Mv} \frac{\bar{k}^2}{(dE/dk)^2} \frac{\boldsymbol{k}\tau_0}{T^3}. \qquad \ldots\ldots(46)$$

Now $\sigma_{\mathrm{B}} = \frac{1}{2}\sigma$ when

$$\int_0^\infty \frac{x^4}{e^x - 1}[1 + \alpha x^{-3}]^{-1}\, dx = 13,$$

i.e. when $\alpha = 105$, as has been found by numerical evaluation.

We thus get for the critical temperature, below which the deviation from Bloch's theory is too large,

$$T_{\mathrm{c}}^3 = \frac{2C^2G^{-3}}{105 \times 9\pi Mv} \boldsymbol{k}\tau_0 \frac{\bar{k}^2}{(dE/dk)^2}. \qquad \ldots\ldots(47)$$

Using (13), we get

$$T_{\mathrm{c}}^3 = \frac{2n_0\bar{k}^3\boldsymbol{k}^2\theta G^{-3}}{9 \times 105\pi^4 m\hbar a_0 v} \tau_0 \left(\frac{\theta}{T\sigma_{\mathrm{T}}}\right). \qquad \ldots\ldots(48)$$

Now for gold $\bar{k} = 1{\cdot}21 \times 10^8\,\mathrm{cm}^{-1}$, $G^3 = 5{\cdot}95 \times 10^{22}\,\mathrm{cm}^{-3}$, $\sigma_{290} = 5{\cdot}76 \times 10^{17}$ E.S.U., $a_0 = 5{\cdot}28 \times 10^{-9}$ cm. (Bohr radius), $v = 2 \times 10^5$ cm/sec., $\theta = 175°$ K. and we take $n_0 = 1$. One then obtains $T_{\mathrm{c}} = 10{\cdot}8°$ K. We have neglected the difference between $\tau_j(q)$ and $\tau_{\mathrm{II}}'(q)$ for $q < \boldsymbol{k}T/\hbar v$; but this difference has very little effect in (42), since the interval $x < 1$ contributes very little to the integral (45).

We have thus seen that the deviations from Bloch's theory due to the finite relaxation time of the phonons are less than estimated by Peierls and become large only at about 11° K. At lower temperatures, however, the size of the specimen will limit the phonon relaxation time (Klemens 1950, 1951), and this will again limit the deviation of the electrical conductivity from Bloch's theory. Thus the deviation of the conductivity from Bloch's theory will only be appreciable, if at all, in a small temperature interval just below 11° K.

It is of course not justified to use the properties of the KCl lattice for a metal, and both Peierls' and the present calculations can be criticized for this reason. Nevertheless the present calculations have shown that in general Peierls' estimate is too pessimistic, and it becomes plausible that the observed agreement between Bloch's theory and observation at low temperatures should be ascribed to interactions amongst the phonons rather than to *Umklapprozesse*. This would resolve the difficulty referred to in the Introduction.

ACKNOWLEDGMENTS

The work described here was started at Oxford, while the author was an Australian National University Research Scholar, and completed in Sydney in the Division of Physics of the Commonwealth Scientific and Industrial Research Organization. The computations were carried out by Miss J. Ward, of the Division of Physics.

APPENDIX

The proof of (37) is very similar to the proof of (33) in the case of thermal conduction (Klemens 1950, 1951): it can be shown quite similarly in the case of electrical conduction that three phonon collisions of the type

$$\omega+\omega_1=\omega_2, \quad \mathbf{q}+\mathbf{q}_1=\mathbf{q}_2 \qquad \ldots\ldots(A\,1)$$

have no appreciable effect on $N(\omega)$ unless $|\omega_1|>|\omega|$ and therefore $|\omega_2|>|\omega$. In that case

$$\left.\frac{\partial N}{\partial t}\right]_p = \sum_1 A_{012}[NN_1(N_2+1)-(N+1)(N_1+1)N_2] \qquad \ldots\ldots(A\,2)$$

and putting $N=\mathcal{N}+n$ etc. the factor in the bracket can be written

$$n(\mathcal{N}_1-\mathcal{N}_2)+\mathcal{N}(n_1-n_2)-(n_1\mathcal{N}_2+n_2\mathcal{N}_1);$$

neglecting n_1-n_2 this is approximately

$$n\frac{\partial \mathcal{N}_1}{\partial \omega_1}\omega-2n_1\mathcal{N}_1. \qquad \ldots\ldots(A\,3)$$

The largest contribution to the rate of change comes from frequencies $\omega_1=\boldsymbol{k}T/\hbar$; thus if $\omega>\boldsymbol{k}T/\hbar$, the three-phonon processes do not contribute appreciably to the rate of change since interactions with $\omega_1<\omega$ are not important. Only when $\omega<\boldsymbol{k}T/\hbar$ will such interactions be important. In this case the ratio of the two terms in (45) becomes

$$n\frac{\partial \mathcal{N}_1}{\partial \omega_1}\frac{\omega}{2n_1\mathcal{N}_1}=\tau\left(\frac{\hbar\omega}{\boldsymbol{k}T}\right)^3\frac{\exp(\hbar\omega/\boldsymbol{k}T)}{\{\exp(\hbar\omega/\boldsymbol{k}T)-1\}^2}\frac{\{\exp(\hbar\omega_1/\boldsymbol{k}T)-1\}}{\tau_1(\hbar\omega_1/\boldsymbol{k}T)^2}\simeq\frac{\tau\omega}{\tau_1\omega_1}, \qquad \ldots\ldots(A\,4)$$

having substituted (36) for n and n_1. Here τ and τ_1 are the effective relaxation times for frequencies ω and ω_1. We now remember that $\omega_1=\boldsymbol{k}T/\hbar$ for maximum effect and obtain the effective relaxation time in terms of τ' and σ_1, where

$$-\frac{n}{\sigma_1}=\sum_1 A_{012}n\frac{\partial \mathcal{N}_1}{\partial \omega_1}\omega, \qquad \ldots\ldots(A\,5)$$

i.e. σ_1 is the relaxation time of the three-phonon processes if all modes are at equilibrium except for ω mode. We then get

$$\tau(\omega)=\frac{\tau'(\omega)[\sigma_1(\omega)+(\boldsymbol{k}T/\hbar\omega)\tau'(\boldsymbol{k}T/\hbar\omega_1)]}{\tau'(\omega)+\sigma_1(\omega)} \qquad \ldots\ldots(A\,6)$$

and in the case of crystals, when $\sigma_1\ll\tau'$, we obtain (37).

REFERENCES

DE HAAS, W. G., and BIERMASZ, TH., 1937, *Physica*, **4**, 752; 1938, *Ibid.*, **5**, 47, 320.

KLEMENS, P. G., 1950, *Thesis* (Oxford University); 1951, *Proc. Roy. Soc.* A, **208**, 108.

PEIERLS, R., 1930, *Ann. Phys., Lpz.*, **4**, 121, **5**, 244; 1932, *Ibid.*, **12**, 154.

SOMMERFELD, A., and BETHE, H., 1933, "Elektronentheorie der Metalle", *Handb. d. Phys.*, 24/2, p. 333.

A Combinatorial Problem in Counting Cosmic Rays

By ERWIN SCHRÖDINGER
Dublin Institute for Advanced Studies

MS. received 1st *August* 1951.

ABSTRACT. The probability is computed that precisely m out of r counters be hit by at least one out of n cosmic particles, each of which has the probability $1/r$ of hitting any particular counter. The estimation of n from given r and m is discussed.

THIS problem was put to me: A tray of r equal counters is exposed to a cosmic-ray shower and hit by $n\,(\geqslant 1)$ rays. A particular ray hits one, and only one, counter and the probability of its hitting any particular counter is $1/r$. What is the probability of precisely m counters going off? Thus m is at least one and at most r or n, whichever is the smaller. The ultimate aim is, of course, to estimate n from the observed m, but this is a second question, to be touched upon at the end.

Let $p(n, m)$ be the probability we want to find. The clue is the recurrence formula

$$p(n+1, m) = \frac{m}{r}\,p(n, m) + \frac{r-m+1}{r}\,p(n, m-1). \qquad \ldots\ldots(1)$$

Indeed, the additional $(n+1)$th ray can produce an m-case either from an m-case by hitting one of the m counters that are already hit, or from an $(m-1)$-case by hitting one of those that are not yet hit; and in no other way. By reflecting and trying one is led to the assumption (which will have to be proved)

$$p(n, m) = b^n{}_m\,\frac{\mu_m(r)}{r^n}, \qquad \ldots\ldots(2)$$

where the b's are constants and

$$\mu_m(x) = x(x-1)(x-2)\ \ldots\ .\ (x-m+1). \qquad \ldots\ldots(3)$$

If we carry (2) into (1) we get

$$b^{n+1}{}_m = m b^n{}_m + b^n{}_{m-1}. \qquad \ldots\ldots(4)$$

Now from common sense $p(1, 1) = 1$, and $p(1, m) = 0$ for $m \neq 1$. Thus (2) is correct for $n = 1$, provided that we take $b^1{}_1 = 1$ and $b^1{}_m = 0$ for $m \neq 1$; it will therefore remain correct for any n, if the b's are successively determined by (4). This can conveniently be done by building up (or rather 'building down') a number triangle, reminiscent of the schoolboy's method for finding the binomial coefficients:

$$\left.\begin{array}{cccccc} 1 & & & & & \\ 1 & 1 & & & & \\ 1 & 3 & 1 & & & \\ 1 & 7 & 6 & 1 & & \\ 1 & 15 & 25 & 10 & 1 & \\ 1 & 31 & 90 & 65 & 15 & 1 \\ \vdots & \vdots & \vdots & \vdots & \vdots & \vdots \end{array}\right\} \qquad \ldots\ldots(5)$$

$n \downarrow$; $\rightarrow m$

(The mth number in any line is obtained on multiplying by m the number above it and adding the latter's left neighbour; empty places are considered to be zero.)

This solves the practical problem. The b-coefficients are familiar to the statistician. The sum of the probabilities (2) for fixed n and $m=1, 2, 3, \ldots . n$ must be unity, and that for any integer r. It follows that the relation

$$x^n = \sum_{m=1}^{n} b^n{}_m \mu_m(x)$$

holds for any integral value of x, and is therefore an identity. In statistics it is mainly used for expressing the 'moments' by the 'factorial moments'. The explicit expression for $b^n{}_m$ is

$$\left.\begin{aligned} b^n{}_m = \sum_{t=0}^{m-1} (-1)^t \frac{(m-t)^n}{t!\,(m-t)!} = \frac{1}{m!} \sum_{t=0}^{m-1} (-1)^t \binom{m}{t} (m-t)^n \\ (n \geqslant 1, \quad 1 \leqslant m \leqslant n). \end{aligned}\right\} \quad \ldots\ldots (6)$$

One easily confirms that it obeys (4) and gives the correct initial $b^1{}_1 = 1$. I hit on (6) in a roundabout way, not worth being reported. It is bound to be contained as a special case in a very complicated formula quoted by Kendall (1948, p. 58, equation (3.20)).

Let us now briefly review the question of *estimating* the number of incident rays n from the observed number m of counters that have gone off (while $r-m$ did not). I believe the only reasonable method of estimation is here as in many other cases that of the 'median'. Let the observed number m be m^*. We would regard as the most likely value of n the one that gives equal probabilities to $m<m^*$ and to $m>m^*$. One must have prepared, from (2), 'for every n' not only the series $p(n, 1)$, $p(n, 2)$, ... $p(n, r)$ (of which the sum is 1), but also the sums

$$\sum_{m=1}^{s} p(n, m) \quad (s = 1, 2, 3, \ldots . r)$$

up to that s for which the sum first exceeds $\frac{1}{2}$. By scanning these tables one will find which n most nearly fulfils the condition of the median. Border cases, and particularly cases with small numbers, are baffling. For example, let $m^* = 1$. We have $p(1, 1) = 1$, $p(2, 1) = 1/r$, $p(2, 2) = (r-1)/r$. Here $n = 1$ fulfils the condition of the median exactly. If r, the total number of counters, is not too small, this is a safe estimate. But if for instance r were only 2, then $n = 2$ gives still a 50 : 50 chance to $m = 1$, and the estimate $n = 1$, though the best, is poor.

The most embarrassing case is $m^* = r$. The median is then reached only in the limit $n \to \infty$. Obviously this case yields no reasonable estimate.

My thanks are due to Professor C. B. A. McCusker of the School of Cosmic Physics who raised this problem.

REFERENCE

KENDALL, M. G., 1948, *The Advanced Theory of Statistics*, Vol. I (London: Charles Griffin).

Observations of the Penetrating Non-Ionizing Component of the Cosmic Radiation

By J. C. BARTON
Birkbeck College, University of London

Communicated by E. P. George; MS. received 1st June 1951

ABSTRACT. An anticoincidence arrangement of Geiger–Müller counters was used to detect that part of the non-ionizing component which is capable of penetrating 10 cm. of lead. Measurements were made at sea level and at an altitude of 3,560 metres. The mean absorption length of the non-ionizing particles was found to be 170 ± 5 gm. cm^{-2} in air, 190 ± 35 gm. cm^{-2} in carbon and 400 ± 25 gm. cm^{-2} in lead. The secondary particles were strongly absorbed in a few centimetres of lead. Studies were made of the angular distribution of the secondaries and of the production of two or more secondary particles in a single process. Less than 0·5% of the non-ionizing particles were found to be associated with extensive air showers, but about 10% appeared to be produced by ionizing particles interacting in the lead above the apparatus.

The angular distribution of the secondary particles produced in carbon was approximately proportional to $\cos\theta$.

The nature of the non-ionizing particles is discussed and it is concluded that the only known particles which could explain the results are high energy neutrons. On this hypothesis, their energy spectrum and intensity at the two altitudes are calculated.

§ 1. INTRODUCTION

At the present time several types of non-ionizing particle are known to be present in the cosmic radiation. These include (i) photons, (ii) thermal energy neutrons, (iii) neutral mesons, (iv) the penetrating non-ionizing component discovered by Jánossy and Rochester (1943), and (v) the particles responsible for the majority of the nuclear disintegrations observed in photographic plates. It is now generally believed that the same particles, high energy neutrons, are responsible for both (iv) and (v), but there has remained a discrepancy between the intensity of neutrons required to account for the two sets of results. Whereas Jánossy and Rochester concluded that the intensity of neutrons at sea level was 0·14% of the total intensity of charged particles, the equivalent figure given by George and Jason (1949) as a result of photographic plate work was 6%. Since, in addition, an alternative explanation for the stars, in terms of unstable neutral particles, had been put forward (Perkins 1947), it seemed important to repeat and extend the measurements of Jánossy and Rochester. The present work has been carried out for this purpose and, more generally, to obtain further information about the non-ionizing component.

§ 2. EXPERIMENTAL METHOD

It was shown in a series of experiments by Jánossy and Rossi (1940) and Rossi *et al.* (1940 b) that the only satisfactory method of measuring the non-ionizing component with Geiger–Müller counters would be to use an efficient anticoincidence arrangement. This was first achieved by Jánossy and Rochester (1943). The general arrangement of the present apparatus, Figure 1, is rather

similar to that used by the latter workers, although the geometry is slightly different.

The apparatus consisted of a counter telescope B, C, D, surrounded on all sides except underneath by a screen of anticoincidence counters A. When the telescope recorded a threefold coincidence without any of the anti-coincidence counters being discharged, the event was interpreted as being caused by a neutral particle entering the apparatus and producing a secondary ionizing particle in the material at *b*. This type of event is usually referred to as an anticoincidence. The question of spurious events will be discussed later. It is useful to note here that any effects due to photons were greatly reduced by the lead screening *a*, which had a thickness of 10 cm. on top and 5 cm. at the sides.

The Geiger–Müller counters used in this work were of the normal copper foil cathode–glass envelope type. The counters in the anticoincidence screen were used with univibrator circuits which were designed to reduce the dead time of the counters (Simpson 1944). This enabled the ' blocking ' time of the apparatus

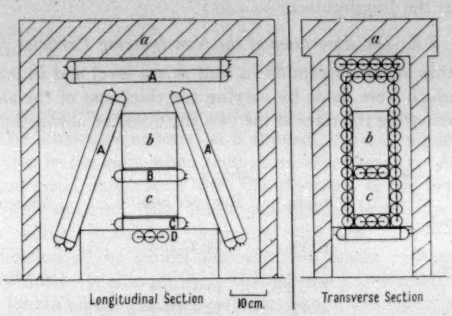

Figure 1. Arrangement of counters.

(cf. Jánossy and Rochester 1943), i.e. the time during which the apparatus was made insensitive to the recording of true coincidences, to be less than 1%.

Most of the circuits used were of a conventional type and will not be described. The actual anticoincidence circuit was derived from that used by Hodson (1948). An additional stage was added to avoid troubles arising from the fact that a univibrator circuit is insensitive to a pulse for a short period after returning to its stable state.

Three separate sets of observations were made. The first and third were carried out, during the periods January to June 1949 and December 1949 to February 1951, on the roof of the tower of the University of London Senate House, at a height of 90 metres above sea level. The second set of experiments was carried out from July to September 1949 in the Sphinx observatory of the Scientific Station, Jungfraujoch, at a height of 3,560 metres above sea level. For both the sea-level and high-altitude measurements the apparatus was set up in a hut which had a roof of light material. In neither situation was there any large amount of material screening the apparatus at angles greater than 20° to the horizontal.

§ 3. EXPERIMENTAL RESULTS

3.1. *General Remarks*

Most of this experimental work has consisted of measuring the anti-coincidence rates $-A+B+C+D$ as a function of the thickness of material at a, b and c. The value of the telescope coincidence rate $B+C+D$ will not normally be quoted; it is sufficient to note that, with 10 cm. of lead at a and no absorber at b or c, this counting rate was 1,050 per hour at sea level and 2,100 per hour at the Jungfraujoch.

Two corrections have been made to the results for the anticoincidence rates. Firstly, variations in the barometric pressure are assumed to have changed the rates by $-0{\cdot}65\%$ per millibar. This figure was obtained from the measured absorption of the radiation in air. Secondly, allowance has been made for those counts which were due to the leakage of mesons through the anticoincidence screen. The method of determining this residual background rate will be discussed later. It was about 7% of the maximum anticoincidence rate at sea level and 3% at the Jungfraujoch.

3.2. *The Absorption of the Non-Ionizing Particles*

Measurements of the absorption in lead at sea level and in lead and carbon at the Jungfraujoch were made by varying the thickness of the absorber a. In addition, by comparing the rates at the two altitudes the absorption in air can be calculated.

Table 1

	a (cm.)	Rate per hour	Absorption length
Jungfraujoch			
b=15 cm. paraffin wax	10 Pb	$18{\cdot}3\pm0{\cdot}4$	
	17·5 Pb	$14{\cdot}4\pm0{\cdot}4$	400 ± 40 gm/cm² Pb
c=0	25 Pb	$12{\cdot}7\pm0{\cdot}4$	
	10 Pb+ 36 C	$15{\cdot}1\pm0{\cdot}5$	190 ± 35 gm/cm² C
b=7·5 cm. C	10 Pb	$15{\cdot}3\pm0{\cdot}4$	
c=0	25 Pb	$10{\cdot}3\pm0{\cdot}5$	430 ± 60 gm/cm² Pb
b=15 cm. paraffin wax	10 Pb	$5{\cdot}1\pm0{\cdot}3$	
c=4·1 cm. Pb	25 Pb	$3{\cdot}3\pm0{\cdot}3$	380 ± 100 gm/cm² Pb
Sea Level			
b=5 cm. Pb	10 Pb	$2{\cdot}05\pm0{\cdot}10$	
c=0	20 Pb	$1{\cdot}75\pm0{\cdot}09$	700 ± 200 gm/cm² Pb
	30 Pb	$1{\cdot}53\pm0{\cdot}09$	
b=0·9 cm. Pb	10 Pb	$2{\cdot}13\pm0{\cdot}15$	
c=0	20 Pb	$1{\cdot}32\pm0{\cdot}14$	300 ± 50 gm/cm² Pb
	30 Pb	$1{\cdot}21\pm0{\cdot}12$	

Corrected results for the absorption in lead and carbon are given in Table 1. The values for the absorption length have been calculated on the assumption of exponential absorption. It is seen from the Table that the absorption in lead could be the same at the two altitudes and is not markedly dependent on the nature

of the materials at *b* and *c*. The mean values for the absorption lengths of the non-ionizing particles are found to be 400 ± 25 gm/cm² in lead, and 190 ± 35 gm/cm² in carbon.

In these experiments the area of the absorber was always sufficient to cover the solid angle defined by the counter telescope BCD. This means that the geometric conditions were satisfactory provided that the non-ionizing particle always produced an ionizing particle which maintained roughly the same direction.

The corrected results which are relevant to the absorption in air are presented in Table 2.

Table 2. ($a = 10$ cm. Pb)

b (cm.)	*c* (cm.)	Rate/hr. at sea level	Rate/hr. at Jungfraujoch	Ratio
15 paraffin wax	0	$2{\cdot}47 \pm 0{\cdot}10$	$18{\cdot}3 \pm 0{\cdot}4$	$7{\cdot}4 \pm 0{\cdot}3$
7·5 C	0	$2{\cdot}14 \pm 0{\cdot}15$	$15{\cdot}3 \pm 0{\cdot}4$	$7{\cdot}2 \pm 0{\cdot}5$
5 Pb	0	$2{\cdot}00 \pm 0{\cdot}10$	$15{\cdot}0 \pm 0{\cdot}8$	$7{\cdot}5 \pm 0{\cdot}6$
0	0	$1{\cdot}00 \pm 0{\cdot}07$	$7{\cdot}9 \pm 0{\cdot}5$	$7{\cdot}9 \pm 0{\cdot}9$
15 paraffin wax	0·9 Pb	$1{\cdot}05 \pm 0{\cdot}09$	$10{\cdot}0 \pm 0{\cdot}5$	$9{\cdot}5 \pm 1{\cdot}0$
15 paraffin wax	2·2 Pb	$0{\cdot}76 \pm 0{\cdot}06$	$7{\cdot}9 \pm 0{\cdot}3$	$10{\cdot}4 \pm 0{\cdot}9$
7·5 C	2·2 Pb	$0{\cdot}59 \pm 0{\cdot}08$	$6{\cdot}1 \pm 0{\cdot}3$	$10{\cdot}3 \pm 1{\cdot}4$

The last column gives the ratio of the rates at the two altitudes for various values of *b* and *c*. The particular material at *b* appears to be unimportant but there is a slight increase in the ratio when there is an absorber at *c*. Again assuming exponential absorption and noting that the thickness of air between the two stations was 340 gm/cm², the mean absorption length in air becomes 170 ± 2 gm/cm² with $c = 0$, and 147 ± 4 gm/cm² with $c \neq 0$.

The classification of the results into the two classes $c = 0$ and $c \neq 0$, is the simplest possible one. It is more likely that there is a systematic dependence of the absorption length on the thickness of material at *c*, but the data are much too scanty to establish this. Clearly the case $c \neq 0$ means that the apparatus was only detecting the more energetic particles.

The errors given above are the statistical standard deviations. An estimate of the experimental error is less certain. For although the same apparatus, including mostly the same counters, was used, there is the possibility that the geometrical arrangements were not exactly the same. From the observed ratio of meson rates, as compared with the results of Rossi *et al.* (1940 a), this error cannot have been greater than a few per cent. Therefore, allowing for the experimental error, the final value for the absorption length for *all* the non-ionizing particles is 170 ± 5 gm/cm².

3.3. *Production and Absorption of the Secondary Particles*

Table 3 gives the anticoincidence rates for various materials at *b* and different thicknesses of lead at *c*. The masses of the lead, carbon and carbon content of the paraffin wax at *b* were identical. The carbon and lead were used in the form of layers spread out to occupy the same volume as the paraffin wax, thus minimizing any geometric effect due to change in position of the producer material. In each case the thickness was sufficiently small for the absorption of the primaries to be neglected. It is seen from Table 3 that equal masses of carbon and lead are about equally effective in producing secondaries and that

the hydrogen present in the paraffin wax makes a significant contribution to the anticoincidence rates.

The comparatively high counting rates when no material was placed at b need to be discussed. It seems possible to explain them in terms of the matter present in the walls of the counters, supports, etc. It is estimated that the average mass of matter between the active volume of the anticoincidence counters and the top bank of the telescope was several grammes per square centimetre. Also the geometric conditions were favourable for recording any event which occurs, for example,

Table 3

a (cm. Pb)	b (cm.)	c (cm.) 0	0·9 cm. Pb.	2·2 cm. Pb.	4·1 cm. Pb.
Sea Level					
10	15 par. wax.	$2{\cdot}47\pm0{\cdot}10$	$1{\cdot}05\pm0{\cdot}09$	$0{\cdot}76\pm0{\cdot}05$	$0{\cdot}35\pm0{\cdot}07$
10	7·5 C	$2{\cdot}13\pm0{\cdot}14$	—	$0{\cdot}53\pm0{\cdot}08$	—
10	0·9 Pb	$2{\cdot}13\pm0{\cdot}15$	—	$0{\cdot}42\pm0{\cdot}08$	—
10	0	$1{\cdot}02\pm0{\cdot}07$	$0{\cdot}38\pm0{\cdot}07$	$0{\cdot}23\pm0{\cdot}05$	$0{\cdot}14\pm0{\cdot}06$
Jungfraujoch					
10	15 par. wax.	$18{\cdot}3\pm0{\cdot}4$	$10{\cdot}3\pm0{\cdot}5$	$7{\cdot}9\pm0{\cdot}3$	$5{\cdot}1\pm0{\cdot}3$
10	7·5 C	$15{\cdot}3\pm0{\cdot}4$	—	$6{\cdot}1\pm0{\cdot}3$	$3{\cdot}7\pm0{\cdot}3$
10	0	$7{\cdot}9\pm0{\cdot}5$	—	$2{\cdot}3\pm0{\cdot}3$	$1{\cdot}6\pm0{\cdot}2$
25	15 par. wax.	$12{\cdot}7\pm0{\cdot}5$	—	—	$3{\cdot}3\pm0{\cdot}3$

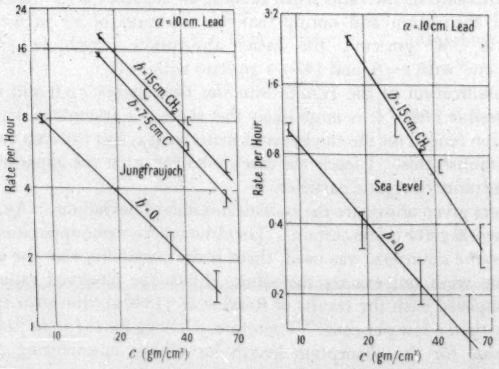

Figure 2. Absorption of secondaries.

in the glass of the top bank of telescope counters. Further measurements were made at thicknesses of c greater than those shown in Table 3. From the appreciably constant rates which were recorded it was concluded that this residual background was due to a leakage of mesons through the anticoincidence screen; in this way it was possible to estimate the value of the necessary correction, as mentioned in § 3.1.

It is obvious from Table 3 that the secondary particles are strongly absorbed in a few centimetres of lead. The results are shown graphically in Figure 2, where the

thickness of absorber has been converted into the equivalent mass of lead. In doing this, allowance has been made for the finite amount of material in the telescope even when $c=0$ and for self-absorption in the producer layer b. The absorption is seen to be similar in all cases but is rather greater at sea level. This corresponds to the greater absorption in the air of the more energetic primaries, an effect which was noted in the previous section.

3.4. *Multiplicity of the Secondary Particles*

During part of the sea-level experiments, an additional circuit indicated whether the centre counter of the trays B or C was discharged simultaneously with either of the outer two counters of the same tray. Anticoincidences in which this occurred will be referred to as multiple events; the results, given as a fraction of the total number of anticoincidences, are shown in Table 4.

Table 4. ($a=10$ cm. Pb)

c (cm. Pb)	b (cm.)	Multiples in B	Multiples in C	Total (%)
0	15 paraffin wax	11/374	6/219	$3{\cdot}8\pm0{\cdot}7$
	0	7/153	6/45	
0·9	15 paraffin wax	5/133	1/109	$1{\cdot}9\pm0{\cdot}7$
	0	1/91	0/41	
2·2	15 paraffin wax	4/120	2/106	$3{\cdot}0\pm0{\cdot}9$
	0	3/65	1/46	
4·1	15 paraffin wax	0/150	1/45	$1{\cdot}1\pm0{\cdot}5$
	0	2/160	1/11	

The proportion of multiple events does not appear to depend on which tray is subdivided nor on whether $b=0$ or 15 cm. paraffin wax. It is possible that there are rather less multiple events for large values of c. The average ratio from all the experiments is $2{\cdot}7\pm0{\cdot}4\%$.

The possibility that this result can be explained in terms of knock-on electrons has to be considered before the multiplicity can be regarded as a genuine effect. Indeed, when the anticoincidence counters were switched off and the telescope recorded fast mesons, the measured 'multiplicity' was 2·8%. The similarity between these figures must, however, be accidental. For it can be shown that any particle which is absorbed as easily as the secondaries in these experiments cannot knock on an electron with sufficient energy to penetrate the walls of the counters.

It therefore seems that the multiplicity is a genuine effect. From the fact that the effect did not depend on the amount of material at b it can be concluded that two or more secondaries are produced simultaneously and not in successive collisions of the non-ionizing particles.

The measured multiplicity of 2·7% can be only a fraction of the true multiplicity, as the geometrical conditions for recording two particles, without discharging any of the anticoincidence counters, are very stringent. It seems likely that more than one secondary particle is produced in at least 10% of the interactions of the non-ionizing particles, and that the proportion of multiple events might well be still higher.

3.5. *Association of the Non-Ionizing Particles with Extensive Air Showers*

During some of the experiments at the Jungfraujoch an attempt was made to determine whether any of the anticoincidence events were accompanied by extensive showers. Two trays of counters, each having an area of 700 cm², were placed in the same horizontal plane as the anticoincidence set and distant 2·5 metres from it and each other.

It was found that out of 1,220 anticoincidences, with various values of *a*, *b* and *c*, none were accompanied by the simultaneous discharge of both the extensive trays. In the same period the expected number of accidental coincidences was 0·2.

It can therefore be concluded that less than 0·5% of the non-ionizing particles are part of extensive air showers with a density greater than one particle per 1,000 cm². This conclusion would not apply to dense penetrating showers which, by discharging the anticoincidence screen, would prevent the detection of any non-ionizing particles accompanying them.

3.6. *Local Production of the Non-Ionizing Particles*

An experiment was carried out at the Jungfraujoch to determine whether any of the non-ionizing particles were produced by ionizing particles interacting in the absorber *a*. For this purpose an additional tray of counters was placed above *a*. It was found that $10 \pm 2{\cdot}5\%$ of the anticoincidences occurred simultaneously with the discharge of this tray of counters. In these experiments *a* was varied from 10 to 30 cm. of lead, but there was no marked dependence on this thickness. A similar effect, of roughly the same relative magnitude, was subsequently found to occur at sea level.

It seems necessary to interpret these results as evidence for the local production of a fraction of the non-ionizing particles. A possible alternative explanation, in terms of the simultaneous arrival of ionizing and non-ionizing particles, is rendered unlikely by the negative result of the extensive shower experiment.

3.7. *Measurement of the Angular Distribution*

The counter assembly was modified for this experiment and is shown in Figure 3. The entire counter assembly was so mounted that it could be rotated inside the fixed lead screen *a*. The axis of rotation was approximately the same as the axis of the counter B and pointed E–W.

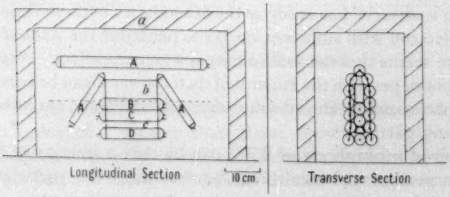

Figure 3. Angular distribution apparatus.

At sea level, the telescope counting rate B + C + D was about 400 per hour; the angular distribution for all the ionizing particles was found to agree, except at large angles, with the expected $\cos^2\theta$ law. The results for the anticoincidence

rates are presented in Table 5. Neither the coincidence nor the anticoincidence rates showed any marked N–S asymmetry.

It may at first sight seem surprising that this much smaller apparatus should give anticoincidence counting rates comparable with those obtained previously. There are two reasons for this: firstly, the minimum amount of material in the telescope is about 25% less than before, because there is no longer a supporting framework of wood and tin-plate; secondly, the geometric conditions are more favourable for the detection of the secondary particles.

Table 5. ($a=5$ cm. Pb, $b=5$ cm. C)

θ (deg.)	0	30	60	90
$c=0$	$2{\cdot}22\pm0{\cdot}08$	$1{\cdot}89\pm0{\cdot}07$	$1{\cdot}29\pm0{\cdot}06$	$0{\cdot}86\pm0{\cdot}05$
$c=1{\cdot}9$ cm.Pb	$0{\cdot}40\pm0{\cdot}03$	$0{\cdot}32\pm0{\cdot}025$	$0{\cdot}21\pm0{\cdot}02$	$0{\cdot}09\pm0{\cdot}01$

If it is assumed that the angular distribution of the secondaries is given by $\cos^n\theta$, then the required value of n, for values of θ between 0 and 60°, is $1{\cdot}0\pm0{\cdot}2$. The distribution does not seem to depend greatly on the thickness of absorber in the telescope at c, except that there is a larger proportion of low energy particles at directions close to the horizontal. It is unlikely that the secondaries maintain the direction of the non-ionizing primaries, so that the value of n for the latter must be greater than 1·0.

§ 4. DISCUSSION

4.1. *Nature of the Non-Ionizing Particles*

Despite the comparatively high intensity of photons present in the cosmic radiation, it is easily seen that they cannot be responsible for the present results. In particular, the measured ratio of the absorption in lead and carbon (Table 1) was about one to two, whereas the absorption of photons is at least ten times greater in lead than in carbon. Many of the other results also serve to show that the photon hypothesis is untenable.

Any contribution from high energy neutrinos, which may have been produced during the decay of mesons, is extremely unlikely, as the interaction cross section is thought to be exceedingly small.

Recently the existence of neutral mesons in the cosmic radiation has been established (Carlson *et al.* 1950), but their lifetime is extremely short. The apparatus used in the present experiments is incapable of detecting any particle whose lifetime is insufficient for it to pass through the anticoincidence counters. Thus it would be necessary to postulate a second and more stable type of neutral meson.

The neutral V-particles of high mass which have recently been found in penetrating showers are believed to have a lifetime just sufficient for them to be detected by this apparatus (Armenteros *et al.* 1951), but their occurrence in showers means that the anticoincidence arrangement will invariably discriminate against them.

A comparison of the results with those to be expected if the particles were neutrons can be made with the help of results obtained from accelerator work on their behaviour. In particular it is possible to compare the absorption with the cross sections given by Fox *et al.* (1950) for 280 Mev. neutrons. The work of DeJuren and Moyer (1951) has shown that the absorption is constant for neutron

energies between 180 and 280 MEV. In making this comparison it is important to note that in the cosmic-ray experiments the conditions are those which nuclear physicists specify as ' bad geometry '. This means that the comparison must be made with the *inelastic* cross sections, as the elastic collisions will have little effect on the measured absorption ranges.

The comparison is set out in Table 6, which shows that the absorption of the cosmic-ray non-ionizing particles is slightly less than that expected for neutrons of a few hundred MEV., and that the dependence on atomic number is similar.

In view of this relatively close agreement it seems worth while to consider whether the other experimental results are consistent with the neutron hypothesis. Firstly it can be concluded from the results on the absorption of the secondaries, which would now be identified as protons, that the necessary neutron energies are greater than 100 MEV. That these neutrons should sometimes produce more than one secondary in a single interaction is not improbable. The local production of the non-ionizing particles would be explained as the nuclear interaction of high energy protons leading to the ejection of neutrons.

Table 6. Comparison of Cross Sections (expressed in barns)

	Carbon	Air	Lead
180 to 280 MEV. neutrons	$0{\cdot}14 \pm 0{\cdot}01$	$0{\cdot}16 \pm 0{\cdot}01$	$1{\cdot}43 \pm 0{\cdot}08$
Cosmic-ray particles	$0{\cdot}11 \pm 0{\cdot}02$	$0{\cdot}140 \pm 0{\cdot}005$	$0{\cdot}87 \pm 0{\cdot}06$

It is now usual to assume that the primary protons of the cosmic radiation are not absorbed catastrophically but give rise to a number of high energy nucleons, which in turn can make further collisions. This picture has been developed theoretically in some detail, particularly by Messel (1951). The particles observed in the present experiments can reasonably be interpreted as the lower energy neutrons and protons which are produced in these nucleon cascades. This view is supported by the experimental results on the local production of the non-ionizing particles. Similarly the results for the angular distribution show that most of the neutrons must have been produced within a few interaction lengths of the apparatus, since even an isotropic production at high altitudes would give rise to a sharply collimated distribution at sea level. The complicated nature of the events occurring in the nucleon cascades may explain the slight difference between the absorption of the non-ionizing particles and neutrons which is shown in Table 6.

As the neutron hypothesis appears capable of explaining most of the observed effects, it will be developed more quantitatively in the next sub-section.

4.2. *The Energy Spectrum and Intensity of High Energy Neutrons*

On the assumption that the secondary particles are protons it is possible to convert the range spectra of Figure 2 to integral energy spectra. In the case of the paraffin wax–carbon difference the process occurring is the simple (n, p) one, where it is known that, owing to the influence of exchange forces, the proton usually acquires nearly all or else very little of the neutron's energy. In the former case there is a strong correlation between the direction of the neutron before collision and of the proton afterwards. Thus the proton spectrum should correspond directly to the neutron spectrum. If it is assumed that the differential energy spectrum is of the form $N(E)\,dE = E^{-\gamma-1}\,dE$, then the value of γ obtained is $1{\cdot}0 \pm 0{\cdot}5$.

Similarly, the spectrum for all the secondary particles from paraffin wax is given by $\gamma = 1{\cdot}6 \pm 0{\cdot}1$. It is possible that these two spectra are really the same, although it would not be surprising if the energy spectrum of the particles ejected from carbon nuclei was rather steeper.

In estimating the neutron intensity it is more satisfactory to use the results for the paraffin wax–carbon difference. The measured value for this difference at the Jungfraujoch was $3{\cdot}0 \pm 0{\cdot}6$ per hour. After correcting for the absorption in the 10 cm. of lead at a above the apparatus, this becomes $4{\cdot}0 \pm 0{\cdot}8$.

The important constants of the apparatus are : area of producer layer $b = 150\,\text{cm}^2$, thickness of $b = 12\,\text{gm/cm}^2$ of paraffin wax, composition of wax $(CH_2)_n$ mean solid angle subtended by telescope at b, $\Omega = 0{\cdot}12$ steradians.

It will be assumed that the angular distribution at the Jungfraujoch is not very different from that measured at sea level. The partial (n, p) cross-section, $\sigma(\theta)$, can be found from the results of Hadley *et al.* (1949) and Kelly *et al.* (1950). Values were interpolated to correspond to a mean energy of about 200 Mev. for the cosmic-ray neutrons.

Then the total counting rate becomes $\int_0^{\pi/2} I(\theta)\, 2\pi \sin\theta\, N\, \Omega\, \sigma(\theta)\, d\theta$. This can be integrated numerically and equated to the measured anticoincidence rate. In this way it is found that the vertical intensity of neutrons must be 14 cm^{-2} sterad^{-1} hour^{-1}. The ratio of penetrating non-ionizing to the total ionizing radiation at an altitude of 3,560 metres is therefore 11%. The equivalent figure at sea level is found to be 4·5%.

The absolute accuracy of these estimates is not very good, chiefly because the standard deviation is 20%. There is a further uncertainty of about 10% in assessing the geometrical constants of the apparatus. For these reasons it has not seemed necessary to take account of the energy spectrum and the variation of the cross section with energy.

4.3. *Comparison with other Measurements of the Intensity*

The only comparable measurements which have been made with an anticoincidence arrangement are those of Jánossy and Rochester (1943). Their results are compared with those of the present experiment in Figure 4; the rates given by

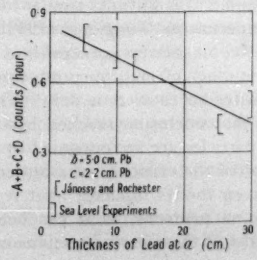

Figure 4. Comparison with previous results.

Jánossy and Rochester have been multiplied by a normalizing factor of 1·5, which was obtained from the ratio of the telescope counting rates in the two experiments. The agreement is seen to be satisfactory, despite somewhat different geometrical

arrangements. However, Jánossy and Rochester estimated that the intensity of non-ionizing particles at sea level was not greater than 0·14%, which is only one thirtieth of the value calculated above. The difference can be accounted for as follows: (i) Jánossy and Rochester always had 2·2 cm. of lead at *c* which, as shown in Table 3, reduces the rates to about one quarter; (ii) they used 5 cm. of lead at *b*; again because of the strong absorption of the secondaries, not more than one third of this would be effective; (iii) they assumed on theoretical grounds that the collision length in lead for the non-ionizing radiation was 10 cm.; the absorption length is now found to be 35 cm. and it is unlikely that there will be more than one high energy secondary produced in this distance. These corrections bring the two sets of results into good agreement.

Estimates of the intensity of particles producing stars, which are also assumed to be neutrons, have been made by George and Jason (1949). Working in terms of the integrated intensity, their results give values of 11% and 3·5% at the same two altitudes. The agreement here is rather better than would be expected as it is now known that about one-sixth of the stars are due to ionizing particles (Brown *et al.* 1949). On the other hand the mean energy for the smallest size star detected is larger, about 150 MeV. (Brown *et al.* 1949). These two corrections will apply in opposite directions, which may be responsible for the final close agreement. It is satisfactory that the ratio for the two altitudes agrees with that found here in the case $c \neq 0$, i.e. the higher energy neutrons.

From similar observations Page (1950) concluded that the intensity of the star producing radiation was only about one half of that given by George and Jason. The difference is a result of assuming that the collision length for star production is half the absorption length, on the grounds that the latter corresponds to a cross section which is only one-half of the geometric area of the nucleus. The Berkeley results have now shown that although the total absorption cross section for neutrons of 270 MeV. is roughly geometric, about 50% of the collisions cause only elastic scattering (DeJuren 1950). Hence the cross section for star production is half the geometric one, and the assumption made by Page is incorrect for the moderate energy neutrons which produce most of the cosmic-ray stars.

Another estimate of the intensity has been made by Tongiorgi (1949 b) from measurements on low energy neutrons. It was concluded that the flux of high energy neutrons was 20% and 5% at altitudes similar to those used in the present experiments. In other experiments Tongiorgi (1949 a) has found that about 2% of the particles in extensive air showers are capable of producing slow neutrons. Compared with the total number of neutron-producing particles, however, the number occurring in extensive air showers is only 0·03%. Hence this result is not in disagreement with the conclusion reached here: namely, that less than 0·5% of the non-ionizing particles are accompanied by extensive air showers.

Rogozinski (1948) reported the existence of a horizontal neutral component. No absolute value was given for its intensity, but it seems possible that the observed effects were due to neutrons, as it has been found in the present experiments (§ 3.7) that many of these have directions making large angles to the vertical.

4.4. *Production of High Energy Secondaries*

The results of § 3.5 enable the relative number of secondaries from hydrogen and carbon to be compared directly. For the high altitude results the corrected rates were carbon $9{\cdot}4 \pm 0{\cdot}7$ per hour, paraffin wax – carbon $3{\cdot}0 \pm 0{\cdot}6$ per hour.

Hence it follows from the composition of the paraffin wax that the cross section for the ejection of a fast ionizing particle from carbon is about six times the (n, p) cross section. Substituting the known value of the latter, it is found that the partial cross section for the forward ejection of a high energy secondary from carbon is 120 ± 40 millibarns per sterad. This value is comparable to the total absorption cross section for neutrons by carbon, and may therefore seem surprisingly high. It is, however, confirmed by the work of Hadley and York (1950) who found that the partial cross section for the forward knock-on of secondaries from carbon by 90 MEV. neutrons was about 100 millibarns per sterad. They also showed that, for light nuclei, the angular distribution of the secondaries was strongly peaked in the forward direction, so that the total cross section remains reasonably small.

The emission from cosmic-ray stars of protons with an energy too great to be explained on the evaporation theory is well known. Detailed results referring to the stars observed in nuclear plates exposed at mountain altitudes have been given by Brown *et al.* (1949) and Bernardini *et al.* (1950). Their results are expressed in rather different forms, but indicate that the mean number of high energy secondaries per star is between 0·5 and 1·0. In about 20% of the stars more than one fast secondary is produced, in agreement with the results obtained here from the multiplicity experiments.

§ 5. CONCLUSIONS

1. The mean absorption lengths of that part of the non-ionizing component capable of penetrating more than 10 cm. of lead are 170 ± 5 gm/cm² in air, 190 ± 35 gm/cm² in carbon and 400 ± 25 gm/cm² in lead.

2. The average range of the secondary particles produced by the non-ionizing component is about 30 gm/cm² of lead.

3. The number of secondary particles produced in equal masses of different materials is roughly constant.

4. Two or more secondary particles are produced simultaneously in more than 10% of the interactions of the non-ionizing particles.

5. The angular distribution of the secondary particles produced in carbon is approximately proportional to $\cos\theta$.

6. Less than 0·5% of the non-ionizing particles at 3,560 metres are part of extensive air showers with a density greater than one particle per 1,000 cm².

7. About 10% of the non-ionizing particles are produced by ionizing particles in the lead above the apparatus.

8. All the experimental results are consistent with the hypothesis that the majority of the non-ionizing particles are neutrons, and are inconsistent with the behaviour of any other known particles.

9. The differential energy spectrum of the neutrons is given by $E^{-\gamma-1}$ where $\gamma = 1{\cdot}0 \pm 0{\cdot}5$ in the energy range $100 < E < 250$ MEV.

10. The vertical intensity of neutrons with energy greater than 100 MEV. is 11% of that of the total ionizing radiation at a height of 3,560 metres, and 4·5% at sea level.

ACKNOWLEDGMENTS

I should like to thank Professor J. D. Bernal for providing the opportunity to carry out this work. I am grateful to the authorities of the Hochalpine Forschungsstation, Jungfraujoch and of the London University Senate House,

for their assistance during the course of the experiments. Mr. J. A. Gay gave valuable help in obtaining the results at high altitude. I am indebted to Dr. E. P. George for much encouragement and many valuable discussions throughout the whole of the work.

REFERENCES

ARMENTEROS, R., BARKER, K. H., BUTLER, C. C., CACHON, A., and CHAPMAN, A. H, 1951, *Nature, Lond.*, **167**, 501.
BERNARDINI, G., CORTINI, G., and MANFREDINI, A., 1950, *Phys. Rev.*, **79**, 952.
BROWN, R. H., CAMERINI, U., FOWLER, P. H., HEITLER, H., KING, D. T., and POWELL, C. F., 1949, *Phil. Mag.*, **40**, 862.
CARLSON, A. G., HOOPER, J. E., and KING, D. T., 1950, *Phil. Mag.*, **41**, 701.
DEJUREN, J., 1950, *Phys. Rev.*, **80**, 27.
DEJUREN, J., and MOYER, B. J., 1951, *Phys. Rev.*, **81**, 919.
FOX, R., LEITH, C., WOUTERS, L., and MACKENZIE, K. R., 1950, *Phys. Rev.*, **80**, 23.
GEORGE, E. P., and JASON, A. C., 1949, *Cosmic Radiation* (London : Butterworth's Scientific Publications), p. 31.
HADLEY, J., KELLY, E., LEITH, C., SEGRÉ, E., WIEGAND, C., and YORK, H. F., 1949, *Phys. Rev.*, **75**, 351.
HADLEY, J., and YORK, H., 1950, *Phys. Rev.*, **80**, 345.
HODSON, A. L., 1948, *J. Sci. Inst.*, **25**, 11.
JÁNOSSY, L., and ROCHESTER, G. D., 1943, *Proc. Roy. Soc.* A, **181**, 399; 1944, *Ibid.*, **183**, 186.
JÁNOSSY, L., and ROSSI, B., 1940, *Proc. Roy. Soc.* A, **175**, 88.
KELLY, E., LEITH, C., SEGRÈ, E., and WIEGAND, C., 1950, *Phys. Rev.*, **79**, 96.
MESSEL, H., 1951, *Comm. Dublin Inst. Adv. Studies*, A, no. 7.
PAGE, N., 1950, *Proc. Phys. Soc.* A, **63**, 250.
PERKINS, D. H., 1947, *Nature, Lond.*, **160**, 707.
ROGOZINSKI, A., 1948, *C. R. Acad. Sci., Paris*, **227**, 628.
ROSSI, B., HILBERRY, N., and HOAG, J. B., 1940 a, *Phys. Rev.*, **57**, 461.
ROSSI, B., JÁNOSSY, L., ROCHESTER, G. D., and BOUND, M., 1940 b, *Phys. Rev.*, **58**, 761.
SIMPSON, J. A., 1944, *Phys. Rev.*, **66**, 39.
TONGIORGI, V. C., 1949 a, *Phys. Rev.*, **75**, 1532; 1949 b, *Ibid.*, **76**, 517.

LETTERS TO THE EDITOR

The Long-Wave Limit of Infra-Red Photoconductivity in PbSe

Published measurements on the spectral distribution of photoconductivity in PbSe (Roth 1938, Blackwell *et al.* 1947, Moss and Chasmar 1948, Starkiewicz 1948, Milner and Watts 1949) indicate that the long wavelength 'limit' is not greater than, and is possibly identical with, that of PbTe. The 'limit', as measured, indicates a 50% drop in sensitivity at about 5·0μ when the cell is at a temperature of 90° K. We have now established that the 'limit' of photoconductivity in PbSe is in fact at a significantly longer wavelength than that of PbTe provided the layers are prepared in a suitable manner.

Recent work by R. V. Jones and his colleagues (Paul, Jones and Jones 1951) has shown that certain single crystals of PbS are relatively transparent beyond 3μ, a sharp absorption edge occurring at this wavelength. This observation has been confirmed by us and in addition the absorption spectra of PbSe and PbTe crystals grown in this laboratory (Lawson 1951) have also been measured over the temperature range 20° to 600° K. This work will be reported in another publication. It is found that the position of the absorption edges in PbS and PbTe is in good agreement with the observed limits of photoconductivity. For PbSe, however, the absorption edge occurs at about 4·7μ at room temperature and 6·7μ at liquid oxygen temperature. These figures indicate that the long-wave photoconductive limit of PbSe has been set in the past at much too low a value. This has now been confirmed by direct measurement. The photoconductivity of a PbSe photo-diode consisting of a PbSe p-type crystal and a tungsten cat's whisker, has been studied. The

long-wave limits, defined as above, are found to be at 4·7μ and 6·8μ at room temperature and 90° K. respectively. These values are in good agreement with the absorption spectra. In addition it has recently proved possible to make photoconductive layers of PbSe with long wavelength limits (50% down from maximum) at 4·8μ at room temperature and 7·1μ at 90° K. The spectral sensitivity curve for such a layer is shown in the Figure. The

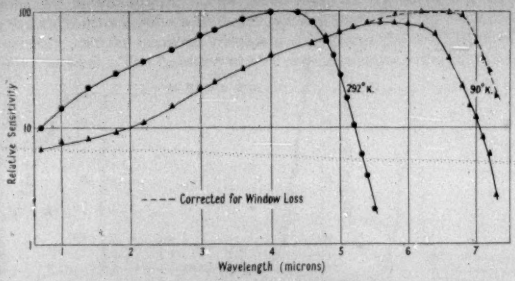

Spectral response of lead selenide cell.

technique of layer sensitization has not, as yet, been studied in any detail and PbSe cells produced up to the present are of relatively low sensitivity. There is no obvious reason why this deficiency should not be overcome and, if so, a cooled PbSe cell should be very valuable for infra-red spectroscopy in the 5–7μ region.

We should like to acknowledge our indebtedness to Messrs. A. S. Young and D. A. H. Brown, of this Establishment, for providing the sapphire windows and electronic equipment used in the above measurements.

This letter is published by permission of the Chief Scientist, Ministry of Supply.

Note added in proof. A later cell with a periclase window gave 'limit' at 8·1μ at 20° K.

Telecommunications Research Establishment,
Great Malvern, Worcs.
20th August 1951.

A. F. Gibson.
W. D. Lawson.
T. S. Moss.

Blackwell, D. E., Simpson, O., and Sutherland, G. B. B. M., 1947, *Nature, Lond.*, **160**, 793,
Lawson, W. D., 1951, *J. Appl. Phys.*, in the press.
Milner, C. J., and Watts, B. N., 1949, *Nature, Lond.*, **163**, 322.
Moss, T. S., and Chasmar, R. P., 1948, *Nature, Lond.*, **161**, 244.
Paul, W., Jones, D. A., and Jones, R. V., 1951, *Proc. Phys. Soc.* B, **64**, 528.
Roth, L., 1938, *Dissertation*, Erlangen.
Starkiewicz, J., 1948, *Nature, Lond.*, **161**, 481.

Angular Distributions of the Neutron Groups from the Reaction $^{12}C(d,n)^{13}N$

Using the same technique as described in our previous communication (El-Bedewi, Middleton and Tai 1951), we have observed, at a bombarding energy of 8 Mev., three neutron groups from the reaction $^{12}C(d, n)^{13}N$ which correspond to the transitions to the ground state and two excited states of ^{13}N at $2{\cdot}38 \pm 0{\cdot}05$ Mev. and $3{\cdot}53 \pm 0{\cdot}05$ Mev. respectively. The angular distributions of these groups, plotted in the centre-of-mass system, together with the theoretical curves calculated by Newns (private communication) on a deuteron stripping theory similar to that proposed by Butler (1950) are shown in Figures 1, 2 and 3.

For the first and second excited states the best agreement between the theoretical and the observed angular distributions was achieved by assuming the angular momentum of the absorbed proton l_p equal to 0 and 2 respectively. It follows that the first excited state of ^{13}N must have spin $\frac{1}{2}$ and even parity and the second excited state has spin 5/2 or 3/2 and even parity. Apart from the parity of the second excited state, which is in contradiction to

that given by Hornyak, Lauritsen, Morrison and Fowler (1950), the results agree with previous predictions (Hornyak *et al.* 1950, Goldhaber and Williamson 1951).

For the ground state the general appearance of the angular distribution suggests $l_p=2$, but this interpretation would involve an excessively large radius of interaction to be

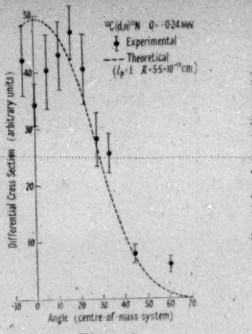

Figure 1.

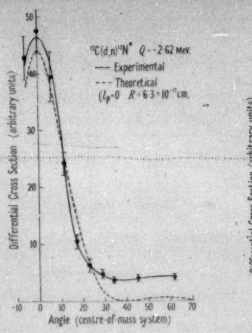

Figure 2.

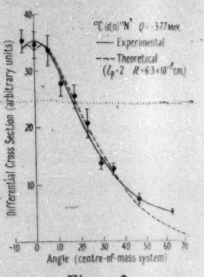

Figure 3.

used in the theoretical calculation. Fair agreement was obtained, as shown in Figure 1, by assuming $l_p=1$, which would indicate this state to be $P_{3/2}$ or $P_{1/2}$ state. This agrees with the prediction of $P_{1/2}$ state from Mayer's model (Mayer 1950) and also with the results obtained for the mirror nucleus ^{13}C, recently reported by Rotblat (1951).

Nuclear Physics Research Laboratories,
University of Liverpool.
13th August 1951.

F. A. El-Bedewi.
R. Middleton.
C. T. Tai.

El-Bedewi, F. A., Middleton, R., and Tai, C. T., 1951, *Proc. Phys. Soc.* A, **64**, 756.
Butler, S. T., 1950, *Phys. Rev.*, **80**, 1095.
Goldhaber, G., and Williamson, R. M., 1951, *Phys. Rev.*, **82**, 495.
Hornyak, W. F., Lauritsen, T., Morrison, P., and Fowler, W. A., 1950, *Rev. Mod. Phys.*, 22, 291.
Mayer, M. G., 1950, *Phys. Rev.*, **78**, 16.
Rotblat, J., 1951, *Nature, Lond.*, **167**, 1027.

The Reaction $^{12}C(\gamma, 3\alpha)$ and a 16·9 Mev. Level of ^{8}Be Emitting Alpha-Particles

The stars formed in a nuclear emulsion by the $^{12}C(\gamma, 3\alpha)$ reaction have already been studied for gamma-ray energies up to 25 Mev. (Goward, Telegdi and Wilkins 1950, Wilkins and Goward 1951). The purpose of this letter is to report a study of the reaction using Ilford E1 and C2 emulsions (200 microns thick) exposed to 70 Mev. bremsstrahlung. The $^{12}C(\gamma, 3\alpha)$ stars were first selected from the considerable variety of stars observed (many of which are as yet unidentified) on the basis of appearance combined with a momentum balance criterion (Goward and Wilkins 1950). 180 stars selected in this way proved to be sufficient to determine the variation of the $^{12}C(\gamma, 3\alpha)$ cross section as a function of gamma-ray energy, E_γ, up to $E_\gamma \simeq 40$ Mev. A second maximum in the cross section appears at $E_\gamma \simeq 27$ Mev., of approximately three-quarters the amplitude of the maximum already known to exist at 18·5 Mev. At 23·5 Mev. and 33 Mev. the cross section falls to half the value at 27 Mev.

Further analysis of the selected stars also reveals a $(16{\cdot}9 \pm 0{\cdot}3)$ Mev. excited level of ^{8}Be, which decays by emitting two alpha-particles and whose existence has not been reported

previously. This level may be shown to play a predominant part in the formation of the stars at $E_\gamma \geqslant 26$ MEV. For each star (with $E_\gamma \geqslant 26$ MEV.), three values were calculated for the energy E^* released when an assumed intermediate ^{8}Be nucleus disintegrates into two alpha-particles. For eight of the stars an E^* value $\sim 0{\cdot}1$ MEV. was obtained, indicating probable transition through the ground state of ^{8}Be; the remaining 52 yielded the E^* histogram shown in the Figure. The curve fitted to the histogram was calculated by assuming that all 52 stars involve a 16·9 MEV. excited level of ^{8}Be, of apparent width 1·0 MEV. at half maximum, and the excellent fit obtained indicates the predominance of transitions through this new level. The estimate of 16·9 MEV. excitation energy is unlikely to be more

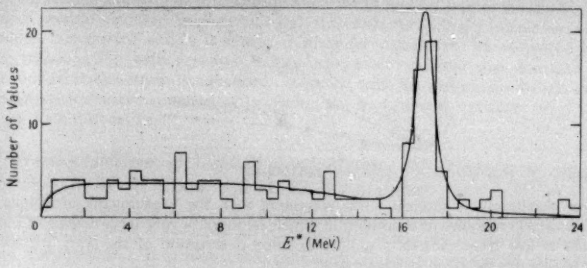

than 0·3 MEV. in error, and allowance for limitations of energy resolution (arising particularly from straggling) enables the real width at half maximum to be estimated as less than 0·8 MEV. The nearest levels of ^{8}Be already known lie at 17·6 MEV. and 18·1 MEV. excitation (Hornyak *et al.* 1950), but neither of these levels emits alpha-particles.

The 60 stars with $E_\gamma \geqslant 26$ MEV. hardly provide a sufficient basis for detailed figures of the proportions in which the various ^{8}Be levels occur. Eight stars probably involve the ground state, and all the remaining 52 are consistent with either the 3 MEV. or 16·9 MEV. excited levels (roughly in the proportion 5 : 47), but other levels are not definitely excluded.

We are indebted to Dr. H. C. Pollock for irradiating our emulsions at the General Electric Co., Schenectady, U.S.A., where Dr. A. M. Gurewitsch is carrying out experiments similar to that reported here.

Atomic Energy Research Establishment,
Harwell, Didcot, Berks.
27th August 1951.

J. J. WILKINS.
F. K. GOWARD.

GOWARD, F. K., TELEGDI, V. L., and WILKINS, J. J., 1950, *Proc. Phys. Soc.* A, **63**, 402.
GOWARD, F. K., and WILKINS, J. J., 1950, *Proc. Phys. Soc.* A, **63**, 662.
HORNYAK, W. F., LAURITSEN, T., MORRISON, P., and FOWLER, W. A., 1950, *Rev. Mod. Phys.*, **22**, 291.
WILKINS, J. J., and GOWARD, F. K., 1951, *Proc. Phys. Soc.* A, **64**, 201.

The Thermal Conductivity of Cadmium in a Magnetic Field at Low Temperatures

In the course of measurements of the thermal conductivity of a number of metals (Au, Mo, Rh, U, Cd) at low temperatures the effect of a magnetic field was investigated. While in the other metals this produced only a very small decrease in the thermal conductivity, in the case of cadmium the effect was very marked even in the relatively small fields used. The specimen was a rod cast from H.S. cadmium (Lab. No. 10,547) whose impurity content was less than 1 in 10^6.

The graph shows the relation between the ratio R_H/R_0 and H, where R_H is the thermal resistance at a given temperature in a field H and R_0 is the thermal resistance at this temperature in zero field. For H=3,800 gauss, when the field was transverse to the temperature gradient, the thermal resistance increased five times at 4·4° K. and over seven

times at 2·2° K. As can be seen from the graph, the effect of a longitudinal field was very much smaller. Except for the lowest fields the relation is approximately linear and there is no sign of any saturation in the highest fields used.

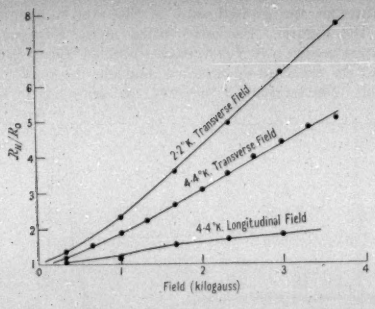

These results are of interest when compared with the experiments of Milner (1937) on the electrical resistance of cadmium, in which he found a very large change of resistivity with field at low temperatures. A more detailed description of the work together with further results will be given at a later date.

Clarendon Laboratory,
Oxford.
31st August 1951.

K. Mendelssohn.
H. M. Rosenberg.

Milner, C. J., 1937, *Proc. Roy. Soc.* A, **160**, 207.

CONTENTS FOR SECTION B

PAGE

Dr. W. H. Hall and Dr. G. K. Williamson. The Diffraction Pattern of Cold Worked Metals: I—The Nature of Extinction 937
Dr. W. H. Hall and Dr. G. K. Williamson. The Diffraction Pattern of Cold Worked Metals: II—Changes in Integrated Intensity 946
Mr. J. F. Nicholas. Outer Brillouin Zones for Face-Centred and Body-Centred Cubic Lattices 953
Dr. G. Liebmann and Miss E. M. Grad. Imaging Properties of a Series of Magnetic Electron Lenses 956
Dr. G. Liebmann. The Symmetrical Magnetic Electron Microscope Objective Lens with Lowest Spherical Aberration 972
Dr. J. R. Greening. The Photographic Action of X-Rays 977
Dr. C. A. Hogarth and Mr. J. W. Granville. A Study of Rectification Effects at Surfaces of Germanium and Lead Sulphide 992
Dr. K. W. Hillier. A Vibrating Cantilever Method for the Investigation of the Dynamic Elasticity of High Polymers 998
Dr. R. L. Drew. A Simplified Shearing Interferometer 1005
Letters to the Editor:
Dr. D. G. Dhavale. An Unusual Kind of Fringe System 1011
Mr. M. E. Haine and Dr. G. Liebmann: Dr. P. A. Lindsay. Certain Properties of Electrostatic Fields encountered in Electron Lenses . . 1012
Dr. L. Riddiford. The Acceleration of Electrons to Energies above 10^9 ev. 1013
Dr. H. K. Henisch. Thermo-Electric Measurements on Semiconductors . 1014
Reviews of Books 1015
Contents for Section A 1018
Abstracts for Section A 1018

ABSTRACTS FOR SECTION B

The Diffraction Pattern of Cold Worked Metals : I—The Nature of Extinction, by W. H. HALL and G. K. WILLIAMSON.

ABSTRACT. The influence of crystal perfection on extinction is briefly discussed and the possible corrections given. Experimental results for chemically produced copper and annealed aluminium filings have been obtained with a Geiger counter spectrometer using monochromatic radiation. The intensity measurements, and for copper the experimentally determined particle size, were inconsistent with the views that primary extinction occurred, but could be interpreted wholly in terms of secondary extinction, the corrected f values agreeing within $\pm 2\%$ with accepted values. Evidence to show that annealed metals contain residual lattice strain is advanced, in accord with the dislocation theory, and it is suggested that secondary extinction will predominate over primary extinction in all crystals containing such dislocations.

The Diffraction Pattern of Cold Worked Metals : II—Changes in Integrated Intensity, by W. H. HALL and G. K. WILLIAMSON.

ABSTRACT. Measurements have been made, using a Geiger counter spectrometer, of the changes produced by cold work on the integrated intensities in the Debye–Scherrer spectrum of aluminium. It is shown that cold work reduces the integrated intensity of all reflections, this decrease being exactly compensated by a rise in the diffuse background scatter, so that the total reflected intensity is unchanged. These results are at variance with those of previous workers, but the discrepancy can be readily explained by the absence of a correction for extinction in previous work. Brief reference is made to measurements of line width and it is shown that the results support the dislocation theory of plastic deformation.

Outer Brillouin Zones for Face-Centred and Body-Centred Cubic Lattices, by J. F. NICHOLAS.

ABSTRACT. In order to resolve some inconsistencies in the literature on the second Brillouin zones of cubic lattices, the shapes of these zones have been recalculated. The results, together with descriptions of the third and fourth zones, are given.

Imaging Properties of a Series of Magnetic Electron Lenses, by G. LIEBMANN and E. M. GRAD.

ABSTRACT. The paraxial lens data and the more important first order lens aberrations were determined for a series of symmetrical magnetic lenses of equal lens diameter D but variable air gap width S for a wide range of lens excitations. The range of gap widths covered was $S/D=0{\cdot}2$ to $S/D=2$. The field distribution within the lenses was measured to a high degree of accuracy with a resistance network analogue, and the lens data were then obtained through numerical trajectory tracing. The results are represented as a series of graphs. These results are representative of the most common magnetic electron lenses, and should have useful applications in lens design. An approximate formula for the focal length is $f \simeq 50(DS)^{1/2}V_r/(NI)^2$. A few design examples are discussed.

The Symmetrical Magnetic Electron Microscope Objective Lens with Lowest Spherical Aberration, by G. LIEBMANN.

ABSTRACT. Using results recently published it is shown that each of the investigated symmetrical magnetic lenses has an optimum value of the lens excitation parameter, for which the spherical aberration constant is smallest. Taking account of the dependence of the maximum obtainable axial field strength H_0 on the maximum field strength H_p in the pole piece gap, one finds that there is an optimum design of electron microscope objective lens of conventional type which gives a lowest value of spherical aberration and highest resolving power. A modification of this optimum lens as adapted for practical use is described.

The Photographic Action of X-Rays, by J. R. GREENING.

ABSTRACT. The variation of photographic blackening with intensity, exposure, the thickness of material round the film, the angle of incidence and the wavelength of x-rays, are examined theoretically and, with one exception, experimentally. A detailed theoretical investigation is made of the energy absorption in the silver bromide grains, consideration being given to the energy lost by scatter and fluorescence and to the electron interchange between the silver bromide grains and the surrounding gelatine and other material. It is concluded that for the majority of emulsions there will be no variation of blackening with x-ray intensity and that the photographic density will be proportional to the exposure at low densities. At very short wavelengths the blackening is critically dependent upon the thickness of material round the emulsion. Photographic density decreases with increase of angle of incidence of x-rays, the maximum decrease observed being about 17%. Within the wavelength range examined experimentally (0·020 to 0·354 A.) the photographic density was approximately proportional to the energy absorbed by the silver bromide. The density per röntgen varied by a factor of 42 in this range. The variation of density per röntgen with wavelength and angle of incidence limits the applications of photographic methods of x-ray measurement. Methods by which emulsion manufacturers can reduce these variations are suggested.

A Study of Rectification Effects at Surfaces of Germanium and Lead Sulphide, by C. A. HOGARTH and J. W. GRANVILLE.

ABSTRACT. Previously reported results of polishing and chemically etching the surfaces of germanium crystals are confirmed. The effects of vacuum heat treatment are investigated and it is found that treatment of this kind at temperatures between 500 and 900° C. can improve the rectification characteristics considerably. The treatment does not spoil the optical quality of a polished surface and in this connection may provide an advantage over chemical etching. Similar effects are obtained with deficit-conducting lead sulphide. Modifications to the surface structures of the crystals by various treatments are investigated by electron diffraction.

A Vibrating Cantilever Method for the Investigation of the Dynamic Elasticity of High Polymers, by K. W. HILLIER.

ABSTRACT. A method is described for obtaining dynamic values of Young's modulus at low frequencies (20 c/s. to 100 c/s.) by using the forced resonance of a vibrating cantilever. Provision has been made for keeping the apparatus at a constant temperature and a few measurements of the dynamic modulus are given for polythene at 30° C. and 40° C. The theory of the vibrations of a cantilever including viscous internal damping is discussed. The results continue previous work carried out at higher frequencies by a different method and indicate the continuity of the dynamic modulus–frequency relation between 20 kc/s. and 20 c/s. for polythene. 'Static' measurements have also been carried out and agree with those published earlier. Even at the lowest frequency the dynamic modulus is still three times the 'static' value, and it is concluded that lower frequencies should be investigated.

A Simplified Shearing Interferometer, by R. L. DREW.

ABSTRACT. A simple new design of interferometer based on the wave-front shearing principle is described and illustrations given of its application to the solution of a variety of 'through-type' and autostigmatic testing problems.

Figure 2. (×½)

Figure 3. (×½)

Figure 4. (×½)

[Tracks have been retouched for clearer reproduction.]

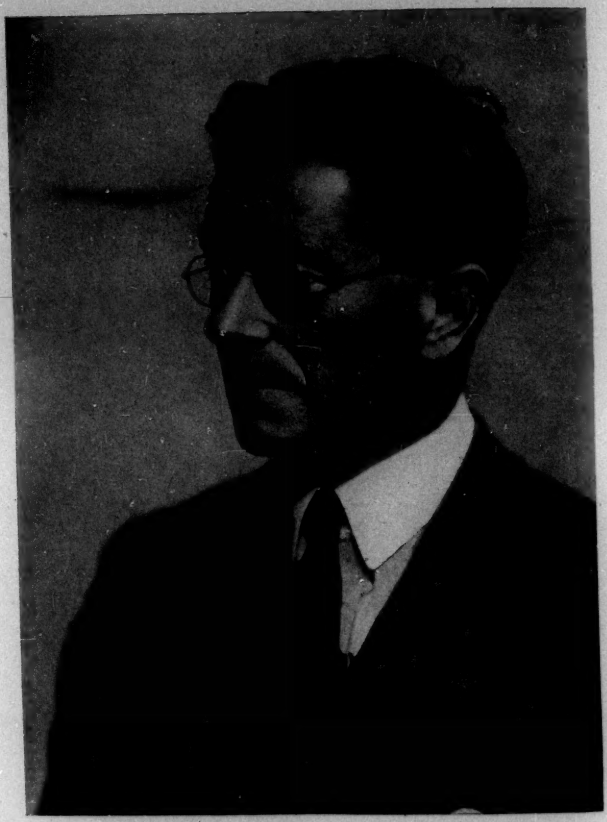

PROFESSOR S. CHAPMAN, M.A., D.SC., F.R.S.,
President of the Physical Society 1949–1950.

(*Note*—Prof. Chapman's Presidential Address is published in the October 1951 *Proceedings*, Section B, page 833.)